CHARACTERIZING THE ROLE OF *C. ELEGANS* DSH-2 IN ASYMMETRIC CELL DIVISION AND EMBRYONIC DEVELOPMENT

by

Sam C. H. Lee
B.Sc, University of British Columbia 2003

THESIS SUBMITTED IN PARTIAL FULFILLMENT OF
THE REQUIREMENTS FOR THE DEGREE OF

MASTER OF SCIENCE

In the
Department of
Molecular Biology and Biochemistry

SIMON FRASER UNIVERSITY

Fall 2005

APPROVAL

Name: **Sam C. H. Lee**

Degree: **Master of Science**

Title of Thesis: **Characterizing the role of *C. elegans* DSH-2 in asymmetric cell division and embryonic development**

Examining Committee:

Chair: **Dr. David Baillie**
Professor, Department of Molecular Biology and Biochemistry

Dr. Nancy Hawkins, Senior Supervisor
Assistant Professor, Department of Molecular Biology and Biochemistry

---

Dr. Esther Verheyen, Committee Member
Associate Professor, Department of Molecular Biology and Biochemistry

---

Dr. Nicholas Harden, Committee Member
Associate Professor, Department of Molecular Biology and Biochemistry

---

Dr. Michel Leroux, Internal Examiner
Associate Professor, Department of Molecular Biology and Biochemistry

Date Defended/Approved: December 5, 2005

ABSTRACT

In *C. elegans,* a Dishevelled homolog, *dsh-2,* is required for asymmetric cell division in the lineage that generates the PHA neuron. Using cell-specific GFP reporters, I have identified additional cells that are either lost or duplicated in *dsh-2* mutants, indicating that *dsh-2* may be required for cell fate specification or the regulation of additional cell divisions. Loss of *dsh-2* function also disrupts ventral enclosure, a morphogenetic process in which hypodermal cells migrate over the surface of the embryo and fuse on the ventral side. Using hypodermal- and neural-specific promoters to control *dsh-2* expression, I have evidence suggesting that *dsh-2* function may be required in both cell types during ventral enclosure. Dishevelled is a component of both the Wnt and planar cell polarity (PCP) pathways. I have undertaken a domains analysis of DSH-2 that suggests the domain necessary for PCP is required for both asymmetric cell division and ventral enclosure.

Keywords: *C. elegans*, developmental genetics, cell differentiation, neuroblasts, asymmetric cell division, Wnt genes, planar cell polarity genes, dishevelled, cellular signal transduction, morphogenesis.

DEDICATION

To my Grandma, who shows me there is more to life than just living.

ACKNOWLEDGEMENTS

I want to sincerely thank my senior supervisor Nancy Hawkins. Over the past two years, her tireless patience and unparalleled enthusiasm has transformed me from a dishevelled undergrad to a purposeful grad student. Everything she has taught me about science and research, nothing I do can justly repay her.

Also, I must thank Chris Beh for his unlimited support and guidance. My "unofficial co-supervisor" influenced me tremendously without him having to intentionally do so. I also deeply appreciate the generosity of Michel Leroux and David Baillie for making their equipment available to me. Without their help a large part of my research would not have been possible. I would also like to thank my collaborators Tim Walston and Jeff Hardin at the University of Wisconsin, Madison for kindly providing reagents as well as sharing unpublished experimental data. Their help was instrumental in both the experiment and writing stages of my thesis.

Thank you to past and present members of the Hawkins/Beh lab for instilling so much fun and life into the lab. I want to especially thank Minna, Sandra, and Amy for keeping me focused and sane. To members of the MBB department, thank you all for making my two years of Master studies at SFU a terrific experience.

To my Family and Connie, thank you for the unconditional support, love, and care. Having you guys made me proud; now, I will do everything in my power to, in turn, make you proud of me.

TABLE OF CONTENTS

LIST OF FIGURES

LIST OF TABLES

CHAPTER 1 INTRODUCTION

1.1 Asymmetric cell division

Asymmetric cell division is a process where a mother cell divides to give two daughters that adopt distinct cell fates (reviewed in Hawkins and Garriga, 1998; Figure 1). Division asymmetry can be generated by extrinsic signals that act on either the mother cell or one of the daughter cells. Also, interactions between the two daughter cells could lead to different cell fates. On the other hand, intrinsic mechanisms can also lead to asymmetric divisions. Cell fate determinants could be preferentially segregated into one of the daughter cells. The daughter that inherited the cell fate determinant could thereby adopt a cell fate that is developmentally distinct from the other daughter. In another scenario, the mitotic spindle could be pushed toward one side of the cell, and the daughter cells would differ in size. The bigger cell may inherit more cell fate determinants than the smaller cell, leading to different developmental fates.

Asymmetric cell divisions are the primary means of generating cellular diversity in multicellular organisms (reviewed in Knoblich, 2001). We use *Caenorhabditis elegans* as a model organism to elucidate the underlying mechanisms that regulate asymmetric cell division. *C. elegans* is an ideal system for these studies due to its short life cycle, ease of maintenance, and amenability to genetic manipulation and analysis. Also, since the entire cell lineage of *C. elegans* has been determined and is found to be invariant, cell divisions can be studied at the resolution of single cells.

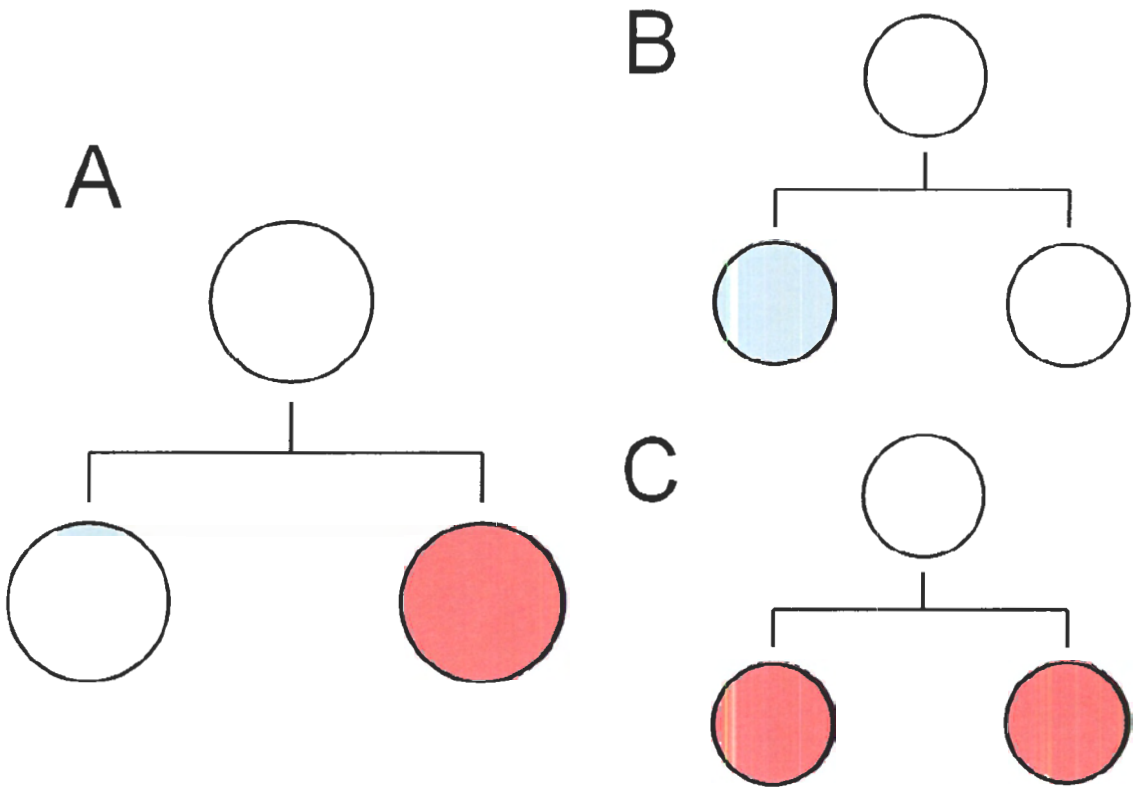

Figure 1 Asymmetric cell division.

During asymmetric cell division, a mother cell generates two daughter cells that adopt different cell fates (A). In mutants where this process is disrupted, the division becomes symmetric, and the two daughter cells adopt the same cell fate (B or C).

1.2 Early cell divisions in *C. elegans* embryos

In *C. elegans*, asymmetric cell division is observed during the first mitosis when the one-celled zygote divides to generate a larger anterior AB blastomere and a smaller posterior P_1 blastomere. Genetic screens for aberrant anterior-posterior polarity of the zygote led to the isolation of "partitioning-defective" or *par* mutants (reviewed by Nance, 2005). Since polarity is lost in *par* mutant zygotes, the first division becomes symmetric. The protein PAR-3, PAR-6, and PKC-3 preferentially associate with the anterior cortex, while PAR-1 and PAR-2 strictly localize to the posterior. The localization patterns of PAR proteins dictate the inheritance of cell fate determinants in the AB and P_1 blastomeres (Bowerman et al., 1997; Schubert et al., 2000).

In addition to preferentially segregating cell fate determinants, PAR proteins also play a role in the posterior displacement of the mitotic spindle. LET-99, a DEP domain-containing protein, is localized in a narrow band just posterior to the future cleavage furrow. The protein becomes uniformly localized at the cortex in *par-2* or *par-3*, causing defects in the posterior displacement of the mitotic spindle (Tsou et al., 2002).

In addition to the PAR proteins, other signalling molecules also regulate asymmetric cell divisions in the early embryo. After the first zygotic division, P_1 subsequently divides to produce two blastomeres called P_2 and EMS. EMS then divides asymmetrically to produce the E and MS cell, and the Wnt signalling pathway has been shown to regulate this asymmetric cell division.

1.3 Wnt signalling regulates early embryonic divisions

The canonical Wnt pathway regulates the stabilization of the intracellular protein β-catenin (reviewed by Nusse, 2005). In absence of a Wnt ligand, the GSK-3β/APC/Axin destruction complex targets β-catenin for degradation. Before secretion, Wnt proteins are subjected to post-translational modifications by the Porcupine protein. Once secreted, the Wnt ligand can interact with seven-pass transmembrane proteins of the Frizzled family. Upon ligand/receptor interaction, a signal is transduced to Dishevelled (Dsh) proteins. This leads to the inhibition of the GSK-3β/APC/Axin destruction complex and in turn causes β-catenin to accumulate in the cytoplasm. β-catenin then translocates into the nucleus and regulates transcription by binding the Tcf/Lef transcription factors.

Wnt signalling genes have been shown to regulate the asymmetric division of EMS (reviewed in Thorpe et al., 2000; Figure 2). In the four-celled embryo, the ventral blastomere EMS divides asymmetrically to generate two daughters with distinct developmental fates: the E cell goes on to make endoderm and the MS cell generates mesoderm. This asymmetric division requires a polarization signal specifically from the posterior blastomere P_2. If the EMS blastomere was isolated and cultured, it would divide to produce two MS daughters. EMS would divide correctly if it was cultured next to the P_2 but not any one of the other two blastomeres (Goldstein, 1992). In a genetic screen for mutants with EMS division defects, a class of mutants called *mom* (more-mesoderm) were isolated. In *mom-1/porcupine*, *mom-2/wnt*, and *mom-5/frizzled* mutants, both daughters generated from the EMS division adopt the MS-like fate (Thorpe et al., 1997). *mom-2* function is required in the P_2 cell, confirming that a Wnt ligand from P_2 induces endodermal fate.

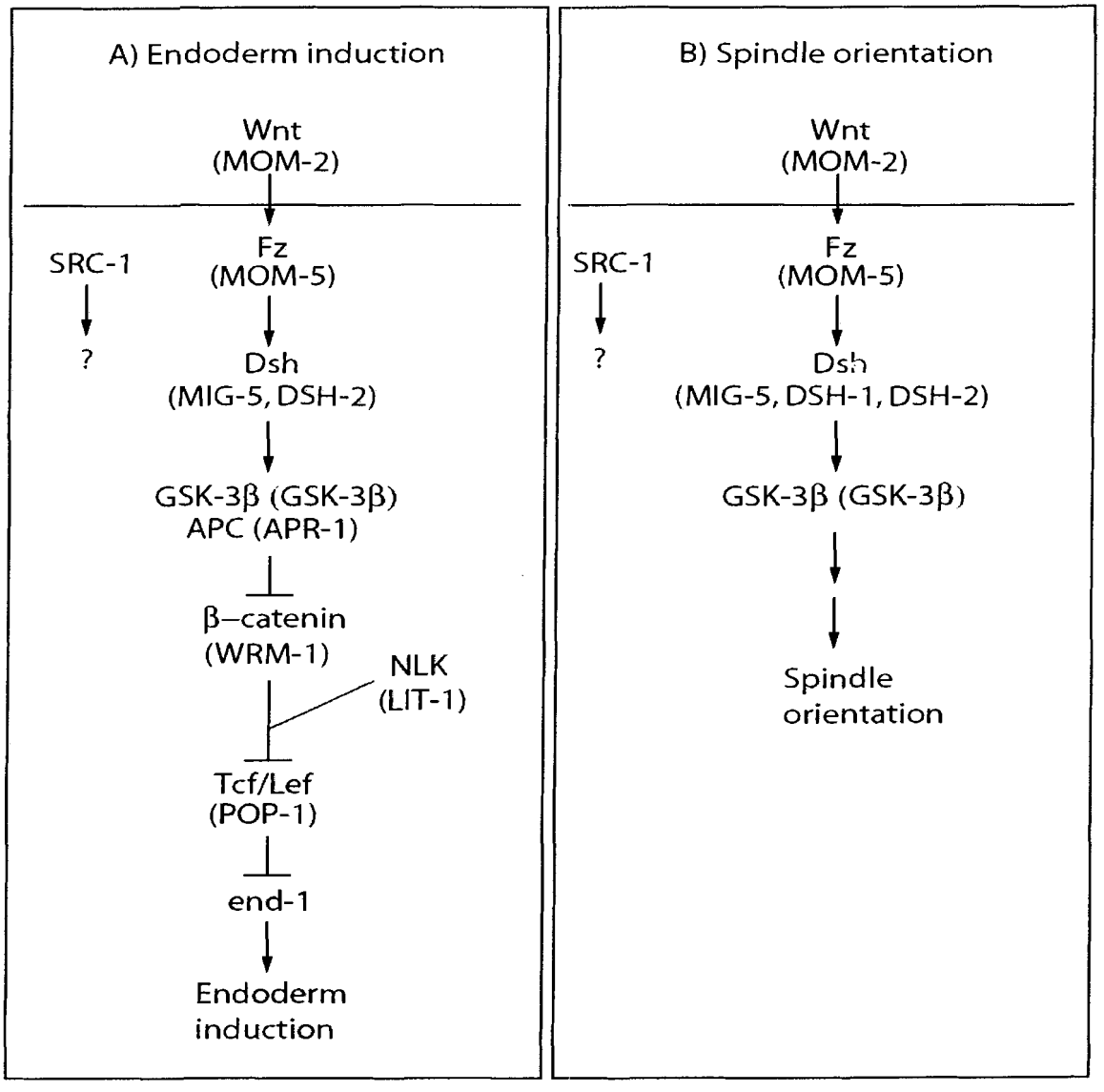

Figure 2 Wnt signalling regulates EMS division.

MIG-5 and DSH-2 function with the SRC-1 kinase to induce the E cell fate. All three Dsh proteins also have minor roles in spindle orientation. (Adapted from Walston et al., 2005, with permission from J. Hardin.)

How does Wnt signalling polarize the EMS cell for asymmetric cell division? Mutants of *pop-1*, the *C. elegans* homolog for the TCF/LEF transcription factor, also results in symmetric division of the EMS. However, as opposed to the *mom* mutants, *pop-1* mutants have no mesoderm and an excess of endoderm (Lin et al., 1995). The MS cell normally contains higher levels of the POP-1 protein than the E cell. POP-1 may induce mesodermal fate by suppressing endoderm-specific genes such as *end-1* in the MS cell (Calvo et al., 2001). To induce endoderm fate, Wnt signalling acts to reduce the amount of POP-1 protein in E (Thorpe et al., 1997). This Wnt-induced reduction of POP-1 level in E is mediated by SGG-1/GSK-3 β and WRM-1/β-catenin (Rocheleau et al., 1997; Schlesinger et al., 1999). APR-1/Adenomatous polyposis coli (APC) also acts on WRM-1 to regulate POP-1 levels (Rocheleau et al., 1997). Furthermore, the MAPK pathway converges on POP-1 in a parallel pathway to specify the E cell fate. MOM-4/MAPK functions to increase the protein level of LIT-1/Nemo-like kinase in the E nucleus, in turn causing increased nuclear export of POP-1 (Lo et al, 2004).

In addition to inducing divisional asymmetry, the Wnt signal from P2 to EMS also controls the orientation of the EMS mitotic spindle. After the EMS is born, the nucleus and centrioles are aligned in the left-right axis. Upon induction from P_2, the two structures rotate to adopt an anterior-posterior orientation. MOM-1, MOM-5, and SGG-1 are required for spindle positioning while WRM-1, APR-1, and POP-1 are not (Thorpe et al., 1997; Rocheleau et al., 1997; Schlesinger et al., 1999).

Recently, a role for Dishevelled (Dsh) proteins in endoderm specification and EMS mitotic spindle positioning was uncovered. There are three Dsh homologs in *C.*

elegans: *dsh-1*, *dsh-2*, and *mig-5*. Reducing function of *dsh-2* or *mig-5* (individually or together) weakly disrupts EMS mitotic spindle positioning but does not disrupt endoderm specification (Walston et al., 2004). A tyrosine kinase called SRC-1 has been proposed to act in parallel to the Wnt pathway to regulate division of the EMS cell. Similar to reducing *dsh-2* and *mig-5* function, loss of *src-1* function leads to defects in EMS mitotic spindle orientation but none in endoderm induction (Bei et al., 2002). Strikingly, when the functions of *dsh-2*, *mig-5*, and *src-1* were all reduced by RNAi, endoderm was never induced (Walston et al., 2004), indicating that Dishevelled proteins act redundantly with SRC-1 to regulate endoderm specification.

1.4 Wnt signalling also regulates post-embryonic development

In addition to embryogenesis, Wnt signalling also has a role in post-embryonic development in *C. elegans*. The T cell is born during embryogenesis but divides asymmetrically post-embryonically. The posterior daughter generates the phasmid socket cells while the anterior daughter gives rise to primarily hypodermis (Sulston and Horvitz, 1977). LIN-44/Wnt, LIN-17/Frizzled, LIT-1/Nlk, and POP-1/Tcf all regulate the T cell division (Herman, 2001; Rocheleau et al., 1999). In wildtype, the anterior daughter has higher levels of POP-1 than the posterior daughter. When zygotic *pop-1* function is reduced by RNAi, the posterior daughter of the T cell is often transformed into a second anterior daughter-like cell (Herman, 2001). In *lin-44/wnt* or *lin-17/frizzled* mutants, POP-1 levels are higher in the posterior instead of the anterior daughter (Herman, 2001).

The migration of the Q neuroblast descendants is also regulated by Wnt signalling. Before hatching, the Q neuroblast divides to give a left daughter QL and a right daughter QR. QL and its descendants migrate posteriorly toward the tail, whereas

the descendants of QR migrate anteriorly toward the head. In *egl-20/wnt* mutants, descendants from both QL and QR migrate to the anterior (Whanbgo and Kenyon, 1999). EGL-20 promotes posterior migration of the QL neuroblast and its descendants by activating the expression of the homeobox gene *mab-5* (Maloof et al., 1999). LIN-17/Frizzled, BAR-1/β-catenin, PRY-1/Axin, and POP-1 are also involved in this pathway to modulate *mab-5* expression (Harris et al., 1996; Herman, 2001).

A third post-embryonic process that is regulated by Wnt signalling is gonadogenesis. In L1 animals, the primordial gonad consists of four cells: Z1, Z2, Z3, and Z4. Z2 and Z3 produce all germline cells, whereas Z1 and Z4 subsequently divide to generate all the somatic gonad cells (described below). In a hermaphrodite, starting at the early L2 larval stage, the anterior and posterior gonad arms elongate ventrally along the anterior/posterior axis of the animal. During the L3 larval stage, both gonad arms first migrate dorsally and then toward each other to form the U-shaped goand. Migration is halted as the tips of the gonad arms meet at the middle of the animal. The somatic gonad cells called the distal tip cells (DTCs) initiates and guides the elongation of the gonad arms (Hedgecock et al., 1987). As the gonad develops, another somatic gonad cell called the anchor cell (AC) is important for signalling to the underlying vulval precursor cells to adopt vulval cell fates (Kimble 1981; Newman et al., 1995).

The DTC and AC are generated late in the L1 stage from the Z1 and Z4 precursor cells (Figure 3). The two precursor cells undergo an identical pattern of cell divisions. Both Z1 and Z4 divide in the proximal/distal axis, and their distal daughters become DTCs. However, lateral inhibition signalling causes one of the proximal daughters to become an AC while the other becomes the ventral uterine (VU) cell (Seydoux and

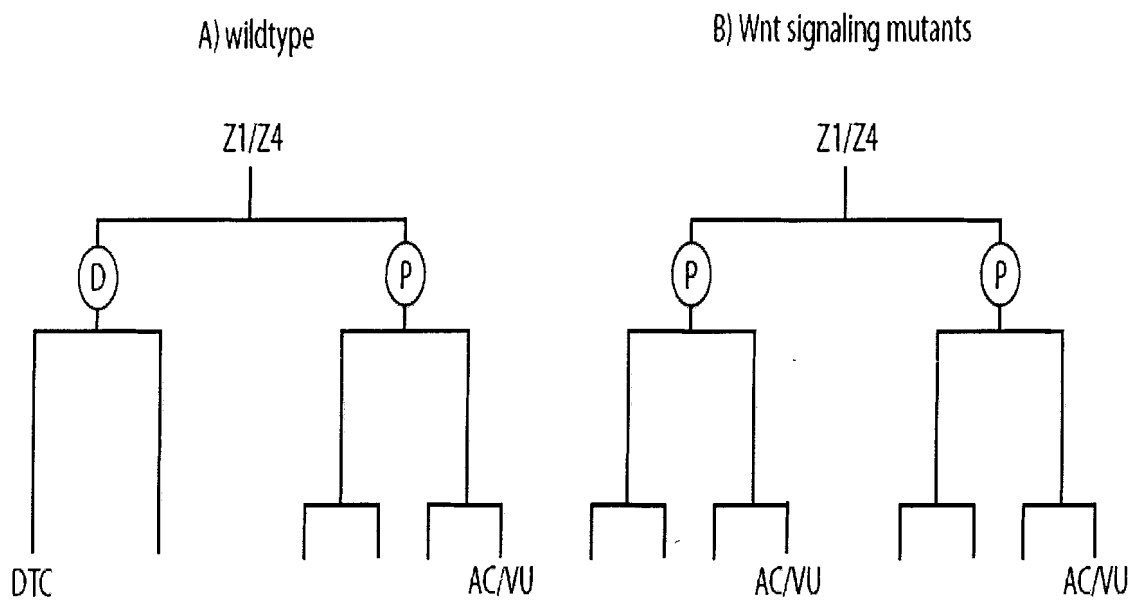

Figure 3 Wnt signalling regulates asymmetric division of the Z1/Z4 cells.

In wildtype, both Z1 and Z4 (Z1/Z4) divide asymmetrically to generate a distal (D) and a proximal (P) daughter cell. Both of the distal daughters generate the distal tip cells. One of the proximal daughters generates the anchor cell while the other generates the ventral uterine cell. In Wnt signalling mutants, Z1/Z4 divides symmetrically to produce two proximal daughter-like cells. As a result, the anchor cell and ventral uterine cell are duplicated while distal tip cells are lost.

Greenwald, 1989). Therefore, in a wildtype animal, two DTCs are produced whereas only one AC is generated.

Wnt signalling pathway has been shown to regulate the asymmetric division of the Z1/Z4 cells. In the Z1/Z4 division, POP-1 specifies the distal cell fate. In wildtype, the proximal daughters of Z1/Z4 have higher POP-1 levels than the distal daughters. When zygotic *pop-1* function is lacking, the Z1/Z4 divisions become symmetric, resulting in DTC losses and AC/VU duplications. The same phenotypes are also observed in *lin-17/frizzled* mutants (Siegfried and Kimble, 2002). Reducing *wmr-1* or *lit-1* function by RNAi causes the Z1/Z4 daughters to divide symmetrically by reversing or abolishing POP-1 asymmetry (Sternberg and Horvitz, 1988; Siegfried and Kimble, 2002; Siegfried and Kimble, 2004). Recently, a fourth β-catenin called SYS-1 has been identified in *C. elegans*. Analysis using a DTC-specific YFP (yellow) and an AC-specific CFP (cyan) marker showed that extra ACs were generated at the expense of DTCs in the same mutant animal (Kidd et al., 2005).

1.5 PHA lineage

Our lab has evidence that Wnt signalling also regulates asymmetric neuroblast divisions. Specifically, we focus on the divisions that generate the PHA sensory neuron in the tail. The PHA lineage is shown in Figure 4. At 180 minutes of embryogenesis, the ABpl/rpppa neuroblast divides asymmetrically to generate distinct anterior and posterior daughter cells. The anterior daughter subsequently divides to generate 5 neurons, one of which is PHA. The posterior daughter generates a phasmid sheath (support) cell, a hypodermal cell, and a cell that undergoes apoptosis.

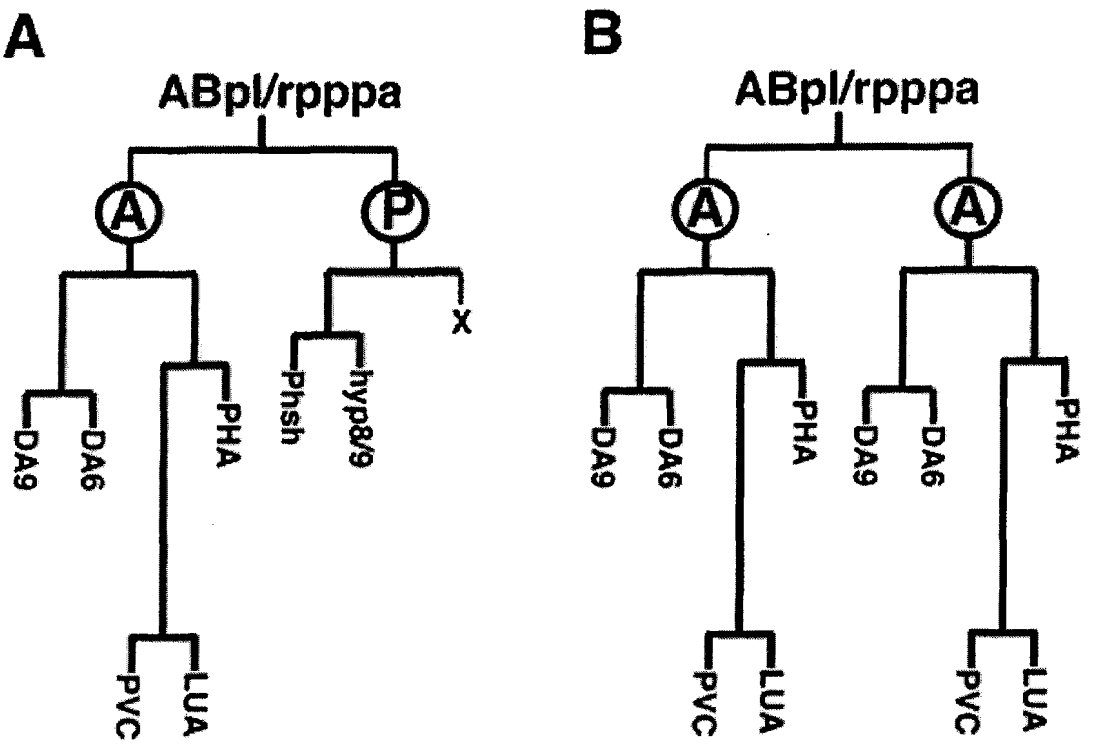

Figure 4 *dsh-2* regulates an asymmetric cell division in the PHA lineage.

A) The PHA lineage in wildtype. At 180 minutes during embryogenesis, the ABpl/rpppa neuroblast divides asymmetrically to generate distinct anterior and posterior daughter cells. The anterior daughter generates five neurons, including PHA. The posterior daughter produces non-neuronal cells. B) In *dsh-2* mutants, the posterior daughter is often transformed into a second anterior daughter-like cell. As a result, neurons are often duplicated and the non-neuronal cells are lost. (Figure reproduced from Hawkins et al., 2005, with permission from N. Hawkins.)

A recent paper by Hawkins et al. (2005) showed that cell signalling regulates the generation of the PHA neuron. The PHA neuron can be easily identified by using the PHA-specific GFP reporter *flp-15::gfp*. In animals where function of the Dishevelled homolog *dsh-2* is reduced, PHA neuronal duplications are frequently observed. PHA is duplicated 3% of the time in homozygous *dsh-2* mutants that have maternal but lack zygotic *dsh-2* function (M+ Z-). These animals are viable but partially sterile (Chang et al., 2005; Hawkins et al., 2005). Embryos produced by these homozygous mutants lack both maternal and zygotic *dsh-2* function (M- Z-), and 70-80% fail to hatch due to defects in a morphological process called ventral enclosure (T. Walston and J. Hardin, personal communication; described below). In these mutants, PHA is duplicated at a frequency of 22% (Figure 5). GFP reporters for cells lineally-related to PHA were also examined in *dsh-2* mutants. The PVC neuron was often duplicated, whereas the phasmid sheath cell, hyp8/9 cell, and the cell that undergoes apoptosis were often missing. These observations are consistent with a division defect of the ABpl/rpppa neuroblast (Figure 4). Reducing *mom-5/frizzled* function through RNAi also resulted in PHA neuronal duplications. Furthermore, MOM-5 appears to function upstream of *dsh-2.* In wildtype animals, the DSH-2 protein is localized to the plasma membrane. In *mom-5* mutants however, DSH-2 localization at the cortex is greatly reduced, and the DSH-2 protein often forms cytoplasmic puncta.

1.6 Ventral enclosure

Ventral enclosure is a morphogenetic process that occurs between 310-350 minutes of embryogenesis (Labouesse, 1997; Podbilewicz and Whilte, 1994; reviewed by Simske and Hardin, 2001). Preceding ventral enclosure, two rows of dorsal hypodermal

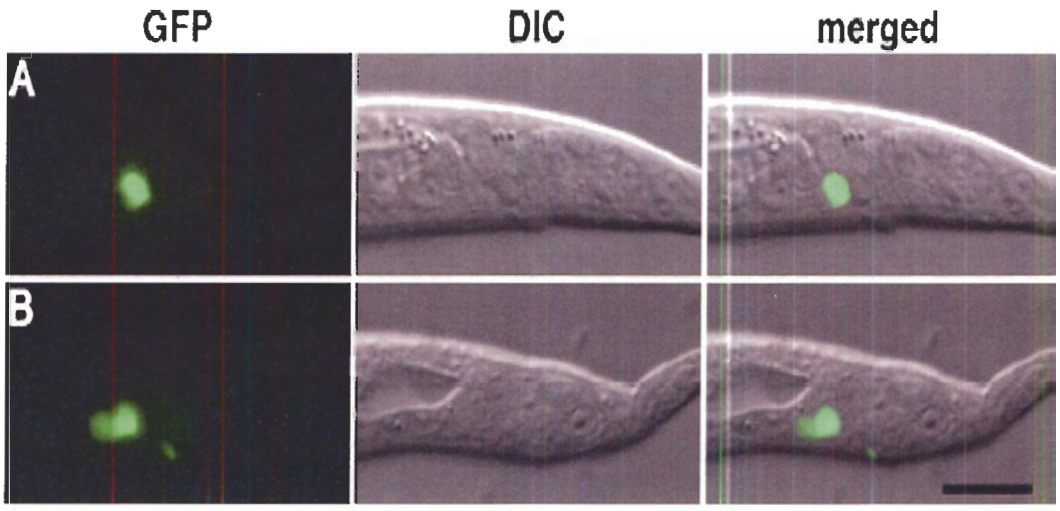

Figure 5 PHA duplications in *dsh-2* mutants.

In panel A, a single neuron in the tail expresses the PHA-specific marker *flp-15::gfp*. In *dsh-2* mutants, two PHA-like cells often express *flp-15::gfp*. (Figure reproduced from Hawkins et al., 2005, with permission from N. Hawkins.)

cells undergo cell shape changes and intercalate. Ventral enclosure begins when the anterior-most hypodermal cells, called leading cells, extend actin-rich filopodia to migrate around the lateral sides of the embryo (Williams-Masson et al., 1997; Figure 6). Then, the posterior hypodermal cells become wedge-shaped and also migrate toward the ventral side by accumulating actin at the migrating front. A ventral pocket is formed as the hypodermal cells from both the left and the right side approach the ventral midline. Eventually, the hypodermal cells meet and fuse with their contralateral partners at the ventral midline. Once the embryo is encased in hypodermis, actin filaments are aligned circumferentially in the dorsal and ventral hypodermis. Contractile forces from these filaments subsequently cause the worm to elongate in the anterior-posterior axis (Priess and Hirsh, 1986).

Many proteins are required for proper migration of the hypodermal cells. HMP-1/α-catenin, HMP-2/ β-catenin, and HMR-1/cadherin localize to adherens junctions of the migrating hypodermis (Costa et al., 1998). In *hmr-1* mutants, leading cells fail to form adherens junctions and ventral enclosure is severely affected (Raich et al., 1999). Another protein found at adherens junctions of the embryonic hypodermis is DLG-1, the *C. elegans* Discs-large homolog. In *Drosophila*, the Discs-Large protein localizes at septate junctions and regulates epithelial cell polarity (Woods and Bryant, 1991; Woods et al., 1996). In *C. elegans dlg-1* mutants, adherens junctions fail to form in the hypodermis and ventral enclosure is aborted (Bossinger et al., 2001). Inositol 1, 4, 5-triphophate (IP_3) signaling is also important during ventral enclosure. Mutation in the *C. elegans* gene *itr-1*, which encodes an IP_3 receptor, leads to hypodermal cells with fewer filopodia and

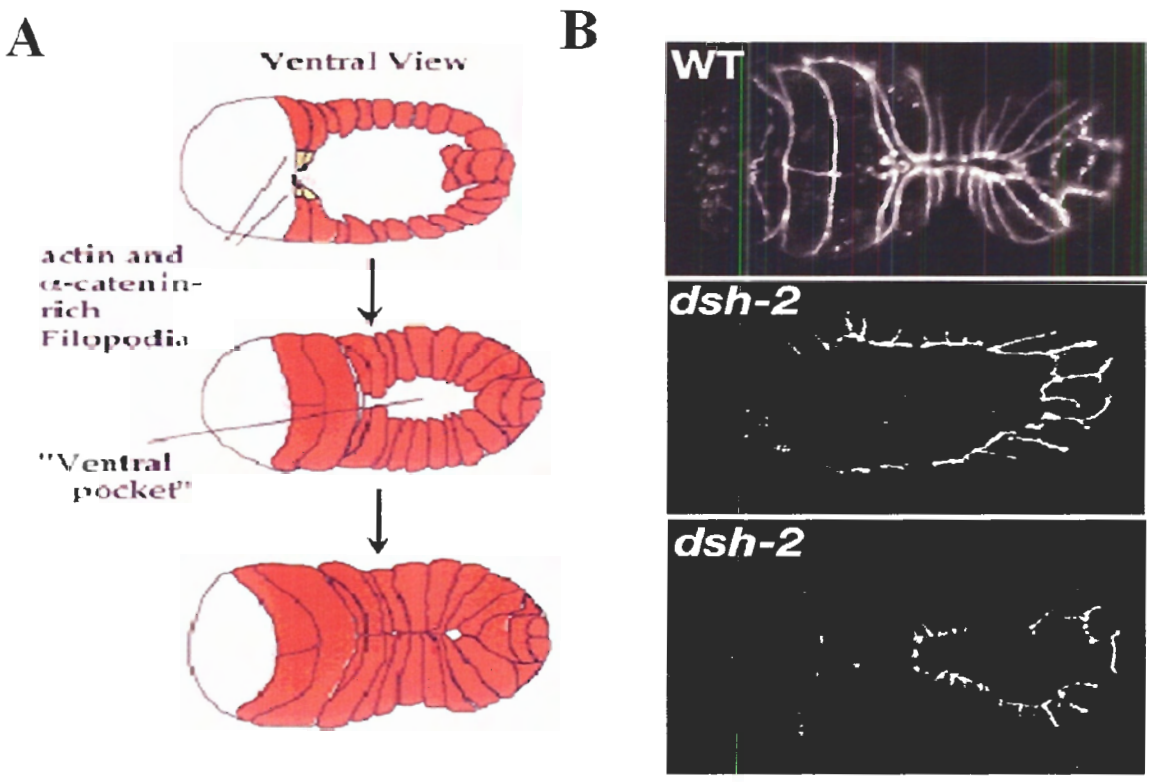

Figure 6 Ventral enclosure is defective in *dsh-2* mutants.

A) Schematic of ventral enclosure. Hypodermal cells are in red, and the filopodia-rich leader cells are in yellow. B) AJM-1::GFP in wildtype and *dsh-2* (M- Z-) mutants. AJM-1::GFP is expressed specifically in the hypodermal cells during ventral enclosure. In wildtype, at about 350 minutes of embryogenesis, the hypodermal cells meet at the ventral midline to close the ventral pocket. In *dsh-2* (M- Z-) mutants, ventral pockets are frequently unsealed. As the embryo elongates, cells are expelled through the ventral hole, resulting in embryonic lethality. (Images from Simske and Hardin, 2001, and provided by J. Hardin, used with permission from J. Hardin.)

the cells fail to migrate (Thomas-Virnig et al., 2004). In *Xenopus*, IP_3 signalling also governs filopodia dynamics during neuronal outgrowth (Takei et al., 1998).

APR-1/APC also regulates epithelial morphogenesis. The APR-1 protein is localized to the plasma membrane in migrating hypodermal cells, similar to where HMR-1, HMP-1, and HMP-2 are localized (Hoier et al., 2000). In *apr-1* mutant embryos, hypodermal cells fail to migrate during ventral enclosure and also during elongation, and both phenotypes are observed in *hmr-1*, *hmp-1*, and *hmp-2* mutants. However, APR-1 has additional roles that are independent of adherens junction proteins, as defects in dorsal intercalation and organization of the lateral hypodermal cells are only observed in mutants of *apr-1* but not of *hmr-1*, *hmp-1*, or *hmp-2*.

Non-hypodermal cells are also important for ventral enclosure. During ventral enclosure, migration of the hypodermal cells requires proper organization of the underlying neuroblasts. Variable abnormal morphology (*vab*) mutant embryos have defects in gastrulation and ventral enclosure, leading to morphological defects in hatched animals. *vab-1* encodes the only Ephrin receptor in *C. elegans*, and *vab-2* encodes an Ephrin ligand. *vab-1* and *vab-2* mutant embryos exhibit high lethality due to defects in ventral enclosure. VAB-1 and VAB-2 are expressed in non-overlapping subsets of neuroblasts. In *vab-1* mutants, the population of neuroblasts expressing VAB-2 spreads out and becomes disorganized (Chin-Sang et al., 1999; George et al., 1998).

As mentioned above, *dsh-2* (M- Z-) mutants exhibit high embryonic lethality due to defects in ventral enclosure. Hypodermal cells often fail to migrate, resulting in large ventral holes (T. Walston and J. Hardin, personal communication). As mutant embryos attempt to elongate, internal cells are expelled though the ventral hole, causing high

embryonic lethality. However, it is unclear where *dsh-2* function is required for proper ventral enclosure. *dsh-2* may function to organize the substrate of neuroblasts for the overlying hypodermal cells to migrate over. Therefore, ventral enclosure defects are a secondary consequence of prior defects in asymmetric neuroblast divisions. On the other hand, *dsh-2* function may be required directly in the migrating hypodermal cells. Hence, ventral enclosure defects are independent of defects in asymmetric neuroblast divisions.

1.7 Dishevelled proteins

Dishevelled (Dsh/Dvl) proteins are members of three distinct signalling pathways: the canonical Wnt signalling pathway, non-canonical or planar cell polarity (PCP) pathway, and a Wnt/Ca^{2+} pathway (reviewed by Habas and Dawid, 2005; Figure 7). In *Drosophila*, a null allele of *dsh* causes defects in segment polarity. In wildtype, the ventral cuticle alternates between a denticle belt and naked cuticle. In *dsh* null mutants, only denticle belts are formed. This process is regulated by a canonical Wnt pathway as Porcupine, Wingless/Wnt, Zeste-white 3/GSK-3β, and Armadillo/β-catenin are all involved in dictating segment polarity (Siegfried et al., 1992; Siegfried et al., 1994; van den Heuvel et al., 1989). However, viable alleles of *dsh* show defects in PCP signalling, leading to polarity defects in various cell types. For instance, *dsh* polarizes cells in the pupal wing. The *Drosophila* wing consists of wing cells that are arranged in the distal-proximal plane. Each cell projects a single distally-pointing hair at the cell's distal edge. In *dsh* mutants, the hair is projected centrally relative to the distal edge, the hair no longer points distally, and wing cells often project multiple hairs (Krasnow et al., 1995; Wong and Adler, 1993). Other PCP proteins also involved in the polarization of a wing cell include Frizzled, Flamingo/Cadherin, Diego, Van Gogh/Stabismus, and Prickle

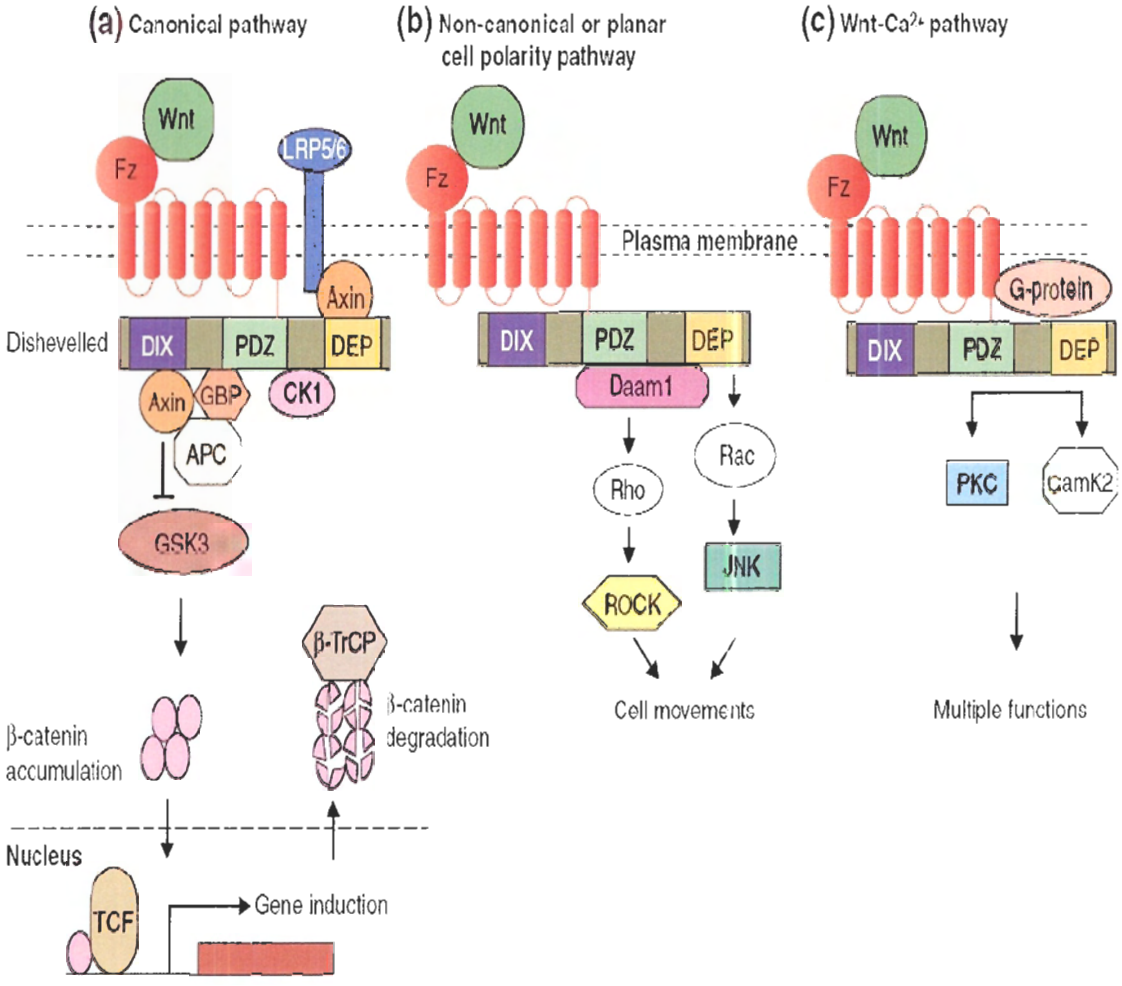

Figure 7 Dishevelled can participate in three distinct signalling pathways.

A) The canonical Wnt signalling pathway. Dishevelled is activated to inhibit the β-catenin destruction complex. β-catenin accumulates in the cytoplasm and translocates to the nucleus to regulate transcription. The DIX domain is important for Dsh to transduce signals in this pathway. B) The non-canonical or planar cell polarity (PCP) pathway. Dishevelled activates the Rho/Rac GTPases to regulate cell polarity during development. The DEP domain of Dsh is required for PCP signalling. C) The Wnt/Ca^{2+} signalling pathway. Dishevelled activates PKC and CamK2 to regulate multiple processes during vertebrate development. The DEP domain of Dsh is also important for this pathway. (Reproduced from from Habas and Dawid, 2005, used with permission from R. Habas, I. Dawid, and Journal of Biology.)

(Axelrod, 2001; Bastock et al., 2003; Feiguin et al., 2001; Shimada et al., 2001). Functions of these proteins lead to cell polarization by dictating the asymmetric localization of the other PCP proteins. For instance, Frizzled co-localizes asymmetrically with Dsh at the distal edge of a dividing pupal wing cell. Prickle functions to inhibit Dsh localization at the proximal edge. In absence of Prickle function, polarity in wing cells is lost due to Dsh and Fz localizing to both the proximal and distal edges (Tree et al., 2002).

The PCP pathway also signals through Dsh to polarize dividing neuroblasts in the *Drosophila* peripheral nervous system (Figure 8). The pI primary sensory organ precursor cell divides asymmetrically to generate an anterior and a posterior daughter called pIIb and pIIa, respectively. The cell fate determinant Numb is preferentially localized to the anterior cortex of the pI precursor cell prior to division (Rhyu et al., 1994). The mitotic spindle then rotates and aligns along the anterior-posterior axis, and subsequent division causes Numb to preferentially segregate into the pIIb anterior daughter (Roegiers et al., 2001). Two protein complexes consisting of PAR-6/atypical protein kinase C (aPKC)/Bazooka and Discs-large/Partner of Inscuteable (Pins) regulate both the asymmetric localization of cell fate determinants and the orientation of the pI mitotic spindle (Bellaiche et al., 2001b; Kuchinke et al., 1998; Petronczki and Knoblich 2001; Wodarz et al., 2000). Mitotic spindle orientation also involves Frizzled and Dsh (Bellaiche et al., 2001a; Gho and Schweisguth, 1998). Both proteins are localized at the posterior cortex of the pI cell, and Dsh regulates spindle polarity by excluding Pins from the posterior domains of pI (Bellaiche et al., 2004).

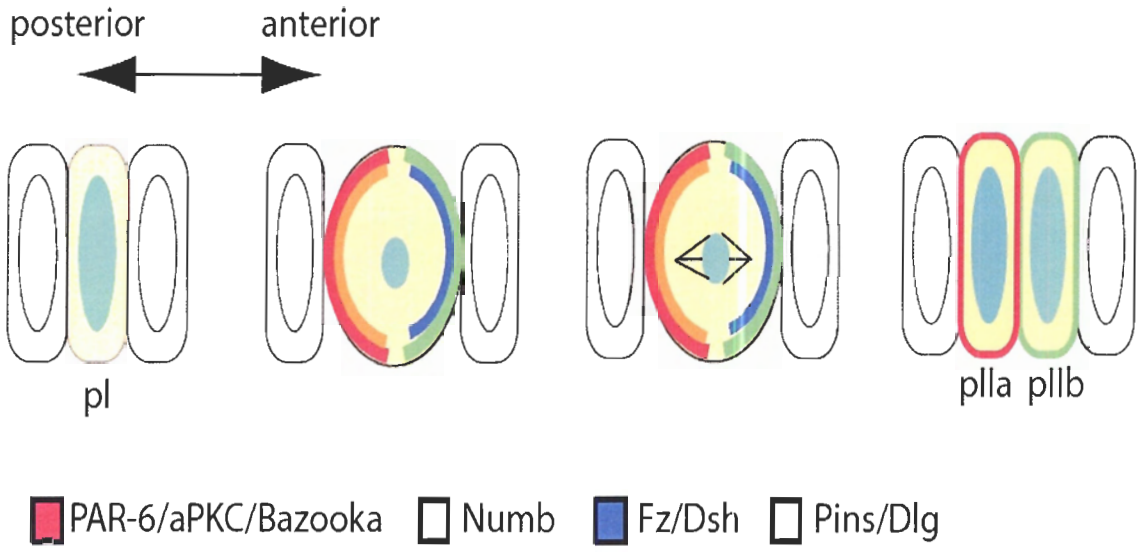

Figure 8 Asymmetric neuroblast division in *Drosophila* peripheral nervous system.

The pI neuroblast divides asymmetrically to generate the posterior daughter pIIa and the anterior daughter pIIb. During the division, the cell fate determinant Numb is preferentially localized to the anterior cortex, and the mitotic spindle becomes oriented along the anterior-posterior axis. The protein complexes PAR-6/aPKC/Bazooka and Pins/Dlg regulate the asymmetric localization of Numb as well as orientation of the mitotic spindle. Fz and Dsh also regulate mitotic spindle orientation and, to a lesser degree, the unequal segregation of Numb. (Figure adpated from M. Roh, M.Sc thesis, with permission from M. Roh.)

Dsh proteins in vertebrates participate in a PCP signalling pathway to regulate a developmental process called convergent extension (CE) (reviewed by Wallingford et al., 2002). During this process, mesodermal cells migrate mediolaterally to align at the midline. Intercalation between the cells would elongate the embryo along the anterior-posterior axis. In *Xenopus*, Xdsh functions with other PCP signalling proteins, such as Frizzled, Strabismus, Prickle, and JNK, to regulate CE. (Darken at al., 2002; Ewald et al., 2004; Medina et al., 2000; Sokol, 1996; Takeuchi et al., 2003; Wallingford et al., 2000, Yamanaka et al., 2002). In zebrafish, Dsh also regulates CE via a PCP-like pathway, and this regulation involves Strabismus and RhoA (Jessen et al., 2002; Matsui et al., 2004). However, unlike the *Drosophila* PCP pathway, Wnt ligands are involved in zebrafish PCP signalling (Carreira-Barbosa et al., 2003; Heisenberg et al, 2000).

In addition, vertebrate Dsh also activates the canonical Wnt and Wnt/Ca2+ signalling pathways. *Xenopus* XDsh functions in a canonical Wnt signalling pathway with homologs of Wnt, β-catenin, and GSK-3β to induce dorsal cell fate in the embryo (Larabell et al., 1997; Moon et al., 1997; Pierce and Kimelman, 1995). Xdsh also participates in a Wnt/Ca^{2+} signalling pathway. This pathway regulates various developmental processes such as ventral cell fate induction and heart development (reviewed in Kuhl et al., 2000). Xdsh can activate effectors of the Wnt/Ca^{2+} pathway such as PKC, Ca^{2+} flux, and calcium/calmodulin-dependent kinase II *in vivo* (Sheldahl et al., 2003).

1.8 Domains of Dsh and specific signalling capabilities

Three domains are evolutionarily conserved in Dsh proteins (reviewed in Wharton, 2003). The DIX domain is the most N-terminal domain in Dsh proteins. The domain consists of approximately 80 amino acids that are conserved in Dishevelled and Axin proteins. The middle domain PDZ is termed after Post Synaptic Density 95, Discs-large, and Zonula occludens-1. The most C-terminal domain is termed DEP for Dishevelled, egl-10, and pleckstrin. Each of the three domains has been implicated to have different functions. The PDZ domain is important for protein-protein interactions (Hung and Sheng, 2002), and the PDZ domain of mouse Dvl1 has been shown *in vitro* to directly bind the receptor Frizzled (Wong et al., 2003). The PDZ domain of Dsh proteins has been tested for its requirement in different signalling pathways. However, results varied depending on the developmental contexts under which the experiments were performed. Thus, instead of conferring signalling specificity, the PDZ domain has been proposed to have a more general role of protein stabilization. Unlike the PDZ domain, the DIX and DEP domains have been shown to be preferentially required for different signalling pathways.

The DIX domain is important for transducing Wnt signals. *Drosophila* Dsh lacking the DIX domain (ΔDIX) was unable to stabilize β-catenin when expressed in cell culture (Yanagawa et al., 1995). However, since the DEP domain is intact in ΔDIX Dsh, the truncated protein was able to rescue eye PCP defects in dsh^{1} mutants (Boutros et al., 1998). Expressing just the DIX domain in wildtype flies produces dominant negative Wnt but not PCP phenotypes, indicating that the DIX domain is sufficient to activate Wnt signalling (Axelrod et al., 1998). In *Xenopus*, Wnt signalling regulates dorsal axis

formation (Larabell et al., 1997; Moon et al., 1997; Pierce and Kimelman, 1995). When a Xdsh deletion construct lacking the DEP domain (ΔDEP) was expressed in wildtype, an ectopic dorsal axis was formed. However, when a ΔDIX Xdsh truncation was expressed, ectopic axis was not induced (Rothbacher et al., 2000; Tada and Smith, 2000), suggesting that the DIX but not DEP domain is important for activating the Wnt pathway. ΔDIX Xdsh also reduces the ability to accumulate β-catenin when expressed in cell culture (Capelluto et al, 2002). The DIX domain also affects the localization Dsh proteins. The DIX domain of mammalian Dvl2 is necessary and sufficient to target the protein to vesicular structures that resemble actin stress fibers (Capelluto et al, 2002).

Conversely, the DEP domain is required for PCP signalling. The original mutant allele of *dsh,* called dsh^1, was isolated in *Drosophila*. This allele is a point mutation in the DEP domain and has defects specifically in PCP signalling (Boutros et al., 1998; Krasnow et al., 1995). Expressing the ΔDIX Dsh truncation rescues the PCP defects in the eye and wing of dsh^1 mutants (Axelrod et al., 1998; Boutros et al., 1998). Expression of just the DEP domain alone in wildtype causes a dominant negative polarity phenotype that is similar to the dsh^1 mutation (Axelrod et al., 1998). In *Xenopus*, expression of ΔDEP Xdsh in wildtype can function in Wnt signalling as it induces secondary axis formation (Rothbacher et al., 2000), suggesting that the DEP is required for PCP but not Wnt signalling. Moreover, overexpression of the DEP domain alone is sufficient to rescue CE defects in *wnt11* mutants, but causes ectopic CE phenotypes in wildtype animals (Heisenberg et al., 2000). The Formin homology protein Daam1 forms a complex with Xdsh and Rho to control CE, and the DEP domain of Xdsh is required for its interaction with Daam (Habas et al., 2001). Membrane association of *Drosophila* and

Xenopus Dsh proteins has been shown to be a hallmark of PCP signalling, and the DEP domain is essential for membrane localization of Dsh proteins (Axelrod et al, 1998; Park et al., 2005; Rothbacher et al., 2000; Wong and Zheng, 2000).

1.9 Experimental approach

In this study, we further characterized the role of *dsh-2* in asymmetric cell division and embryonic development. In addition to the PHA lineage, preliminary results suggest other asymmetric cell divisions to be defective in *dsh-2* mutants. Using various cell-specific GFP markers, many cells were found to be either lost or duplicated in *dsh-2* mutants, indicating potential defects in asymmetric division. Loss of *dsh-2* function also leads to high embryonic lethality due to defects in ventral enclosure, a morphogenetic process where hypodermal cells migrate over neuroblasts. By specifically expressing *dsh-2* in either neuroblasts or the hypodermis, we found that *dsh-2* function may be required in both cell types for ventral enclosure. Dsh proteins can transduce signal from either the canonical Wnt or PCP pathway. By expressing *dsh-2* deletion constructs, the DEP domain appears to be essential for both processes, suggesting DSH-2 participates in a PCP-like pathway during development.

CHAPTER 2 MATERIALS AND METHODS

2.1 Strains and alleles

Methods for culturing, handling, and genetic manipulation of *C. elegans* were performed as described in Brenner, 1974. Worms were cultured in petri plates with nematode growth media (NGM) streaked with *Escherichia coli* strain *OP50*. All experiments were performed at 20°C unless otherwise stated. *C. elegans* animals described as wildtype were the Bristol strain N2. The following mutations were obtained from the *C. elegans* Genetics Center unless otherwise noted:

Linkage group (LG) I: gpa-16(it143) (Rose and Kemphues, 1998)

LG II: dsh-2(ez25) (Chang et al., 2005; obtained from D. Zarkower), *dsh-2(or302)* (Hawkins et al., 2005), *mIn1[mIs14 dpy-10(e128)]* (Edgley and Riddle, 2001), *mnC1 [dpy-10(e128) unc-52(e444)]* (Edgley and Riddle, 2001), *gpb-1(pk44)* (Zwaal et al., 1996), *vab-1(dx31)* (George et al., 1998)

LG IV: ced-3(n717) (Ellis and Horvitz, 1986), *vab-2(e96)* (Chin-Sang et al., 1999)

LG X: unc-2(e55) (Brenner, 1974)

The following strains carrying cell-specific GFP reporters were obtained from the *C. elegans* Genetics Centre unless otherwise noted:

LG I: zdIs5[mec-4::gfp] (Clark et al., 2003)

LG III: gmIs12[srb-6::gfp] (Hawkins et al., 2005)

LG V: qIs19[lag-2::gfp] (Siegfried and Kimble, 2002), *oyIs14[sra-6::gfp]* (Sarafi-Reinach et al., 2001)

LG X: otIs138[ser-2prom3::gfp] (Tsalik et al., 2003), *kyIs104[str-1::gfp]* (Troemel et al., 1997)

Unknown LG: gmIs18[ceh-23::gfp] (Withee et al., 2004), *hdIs26[odr-2::cfp, sra-6::dsRed2]* (Hutter, 2003; obtained from H. Hutter), *juIs14[acr-2::gfp]* (Hallam et al., 2000), *kyIs128[str-3::gfp]* (Peckol et al., 1999), *syIs50[cdh-3::gfp]* (Siegfried and Kimble, 2002), *ynIs22[flp-8::gfp]* (Li et al., 1999)

Extrachromosomal: adEx1296[gcy-32::gfp] (Yu et al., 1997)

2.2 Constructing strains carrying a cell-specific GFP marker and *dsh-2*

Strains containing *dsh-2(or302)* or *dsh-2(ez25)* and integrated cell-specific GFP reporters were all constructed using a common strategy (Appendix 7). For simplicity, only the strategy to generate strains with *dsh-2(or302)* will be discussed. Since *dsh-2* mutants are maternal effect lethal, the *dsh-2* mutation is maintained over the balancer *mIn1[mIs14 dpy-10(e128)]* (Edgley and Riddle, 2001). It is a convenient balancer for several reasons. *mIs14* is an integrated array that expresses GFP in the pharynx as well as embryonic gut cells, allowing the animals that carry the balancer to be easily identified under an epi-fluorescence dissecting microscope. In addition, the recessive mutation *dpy-10(e128)* on the balancer chromosome allows *mIn1[mIs14 dpy-10(e128)]* homozygotes to be phenotypically distinguishable from heterozygotes.

Most of the GFP markers obtained were integrated arrays. Thus, N2 males were first crossed with hermaphrodites carrying a specific integrated array (*In[prom::gfp]*), and *+/In[prom::gfp]* F1 males were then mated with *dsh-2(or302)/mIn1[mIs14 dpy-10(e128)]* hermaphrodites. Males expressing *+/mIn1; +/In[prom::gfp]* were selected and mated with *+/dsh-2(or302); +/In[prom::gfp]* sibling hermaphrodites. In the next generation, 10-12 hermaphrodites carrying *mIn1* and *In[prom::gfp]* were cloned. Progeny were then examined for the presence of *dsh-2(or302)*. Since many homozygous *dsh-2* mutants have gonadogenesis defects, they could be easily identified under a dissecting microscope by clear patches in the gonadal arms (Chang et al., 2005; Hawkins et al., 2005). Therefore, from plates containing *dsh-2* homozygotes, animals expressing the cell-specific GFP reporter and pharyngeal GFP would be of the genotype *dsh-2(or302)/mIn1; +/In[prom::gfp]*. These progeny were then cloned to homozygose the *In[prom::gfp]* chromosome. For the extrachromosomal array *adEx1296*, the same scheme was employed with the exception that the marker was not homozygosed.

2.3 Molecular biololgy

2.3.1 DNA gel electrophoresis

Unless otherwise noted, all DNA gel electrophoresis were performed on 0.8% agarose gels made with 0.5x TBE (45 mM M Tris-borate, 1 mM EDTA) and 25 μg/mL ethidium bromide.

2.3.2 DNA transformations

All ligation reactions were transformed into electrocompetent *Escherichia coli DH5α* (F- ϕ80*lac*ZΔM15 Δ(*lac*ZYA-*arg*F)U169 *deo*R *rec*A1 *end*A1 *hsd*R17(r_k-, m_k+)

*pho*A *sup*E44 *thi*-1 *gyr*A96 *rel*A1 λ-)) cells. The electrocompetent cells were prepared by harvesting a *DH5α* culture at log-phase ($O.D._{600}$ 0.6-0.8), washing twice with ice-cold 10% glycerol, and aliquoting 100 μL into tubes, and frozen at -80°C indefinitely. 0.5-1 μL of the ligation reaction was directly electroporated into 50 μL of *DH5α* cells in a 1 mm electroporatable cuvette using an electroporator (BioRad Micropulsor). 500 μL of LB broth was added immediately to the suspension and the cells were allowed to recover at 37°C for 30 minutes. 100-400 μL of the solution was then plated onto LB plates containing ampicillin at 100 μg/mL. Transformants were selected and the correct subclones were confirmed by diagnostic restriction enzyme digests.

2.3.3 Construction of the *unc-119-dsh-2::gfp* plasmid

This construct was previously generated in the lab by Amy Leung (Figure 9). Briefly, the 1.2 kb *unc-119p* fragment was subcloned into the HindIII/PstI restriction sites of the promoter-less GFP vector pPD95.77 to generate pAL5. Next, the 2.2 kb *dsh-2* cDNA was PCR-amplified from the cDNA clone yk433c8 using the forward primer dsh79 (5'-GATCCTGCAGATGACAGATTCCCCTTCACC-3') and the reverse primer dsh80 (5'-CGATCCCGGGCAATTATCAATGTTAAACTGTGG-3'), with the underlined sequences being Pst I and Xma I sites, respectively. The PCR product was then purified, digested, and subcloned in-frame into pAL5 between the *unc-119* promoter and GFP to generate pNH136, which is the *unc-119-dsh-2::gfp* plasmid.

2.3.4 Constructing the *lin-26p-dsh-2::gfp* construct

To construct the *lin-26p-dsh-2::gfp* plasmid, a plasmid called pML433 (generous gift from M. Labouesse) containing a fragment of the *lin-26* promoter was used. This

plasmid contains 4 kb of genomic sequence upstream of the *lin-26* ATG start site. This promoter fragment has been shown to express GFP in the major hypodermal cells during mid-embryogenesis (Landmann et al., 2004). A nuclear localization signal (NLS) is present in this plasmid. Since the DSH-2 protein functions outside of the nucleus, the NLS fragment needed to be removed from the construct. Since the NLS is only 40 base pairs long and flanked by two KpnI restriction sites, pML433 was digested with KpnI and the resulting DNA fragments were separated by gel electrophoresis. The larger portion of pML433 was isolated by gel extraction and subsequently re-ligated to generate the plasmid pSL3.

A 2.2 kb *dsh-2* cDNA was inserted in-frame into pSL3 between the *lin-26* promoter and the GFP coding sequence. The *dsh-2* cDNA sequence was PCR-amplified using the cDNA clone yk433c8 as template and the *Pfu Ultra* DNA Polymerase Kit (Stratagene). The forward primer dsh81 (5'-GATGATATCATGACAGATTCCCCTT CACCAATT-3') and the reverse primer dsh82 (5'-GATGATATCGCATTATCA ATGTTAAACTGTGGATG-3') were used, with EcoRV restriction sequences underlined. PCR reactions were in a final volume of 50 μL, consisting of 2.5 units of polymerase, 0.2 μM of each primer, and 0.2 mM dinucleotide triphosphate. The cycling conditions were: 1 cycle of 94°C for 2 minute; 30 cycles of 94°C for 30 seconds, 55°C for 30 seconds, 72°C for 2 minutes and 30 seconds; and 1 cycle of 72°C for 10 minutes. The PCR product was purified using the Sigma PCR Clean-up Kit, digested with EcoRV, and subcloned into the unique MscI site between the *lin-26* promoter and GFP coding sequence in pSL3 to generate pSL2K-R1 (Figure 9), which is the *lin-26p-dsh-2::gfp* construct.

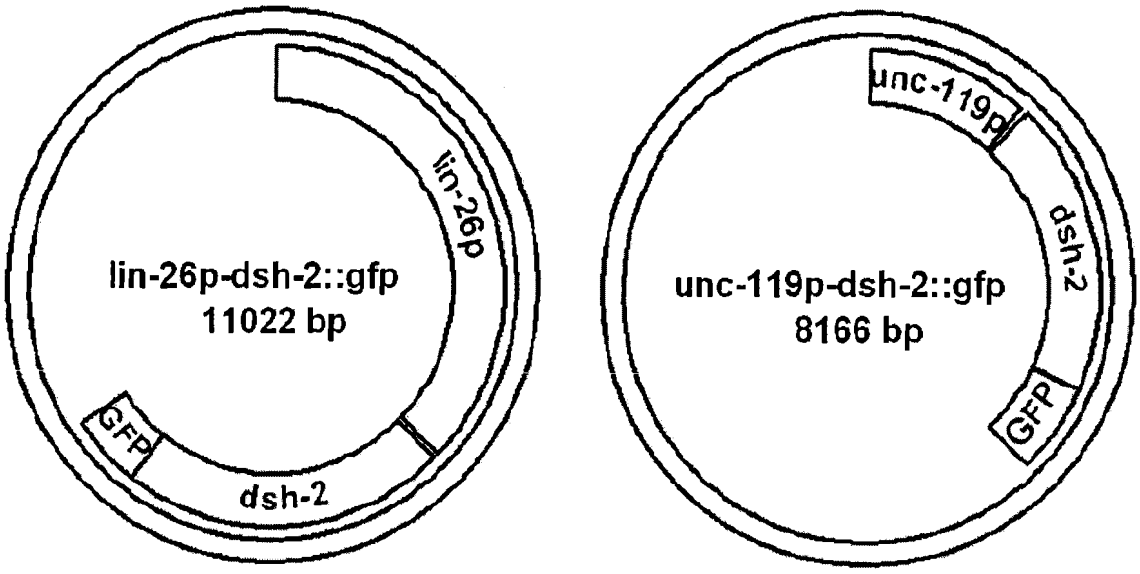

Figure 9 The *lin-26p-dsh-2::gfp* and *unc-119p-dsh-2::gfp* constructs.

dsh-2 cDNA was placed under control of either a 4 kb *lin-26* promoter or a 1.2 kb *unc-119* promoter. See Materials and Methods for details of construction.

2.3.5 Stitching PCR to generate *F25B3.3p-dsh-2::gfp*

Stitching PCR has been previously described by O. Hobert (Hobert, 2002; Figure 10.). The Long Expand PCR Polymerase Kit (Roche) was used for all stitching PCR reactions. All reactions were in a final volume of 25 μL, consisting of 2.8 units of DNA polymerase, 2.5 μL of Buffer 1, 0.6 μM of each primer, 0.2 mM dinucleotide triphosphate. For PCR #1, 2.5 μL of N2 worm lysate was used as template, and the forward primer st-F25-dsh.A (5-CTGAGCTTTCCACGTAGTTATCAAA-3') and reverse primer st-F25-dsh.B (5'-CAATTGGTGAAGGGGAATCTGTCATCG TCGTCGTCGTCGATGCCGTC-3') were used, with the underlined sequence being the reverse complement of the forward primer in PCR #2 (see below). The cycling conditions were: 1 cycle of 94°C for 1 minute; 10 cycles of 94°C for 10 seconds, 65°C for 30 seconds, 68°C for 2 minutes; 25 cycles of 94°C for 15 seconds, 65 °C for 30 seconds, 68°C for 2 minutes (plus 20 seconds per cycle); and 1 cycle of 68°C for 7 minutes.

In PCR #2, 5μL of diluted Pvu I-digested pSL2K-R1 (*lin-26p-dsh-2::gfp*) was used as template, and the forward primer st-F25-dsh.C (5'-ATGACAGATTCCCCTTC ACCAATTG-3') and reverse primer D primer (5'-AAGGGCCCGTACGGCCGACT AGTAGG-3') were used. The cycling conditions for PCR #2 were: 1 cycle of 94°C for 1 minute; 10 cycles of 94°C for 10 seconds, 65°C for 30 seconds, 68°C for 3 minutes 30 seconds; 25 cycles of 94°C for 15 seconds, 65 for 30 seconds, 68°C for 3 minutes 30 seconds (plus 20 seconds per cycle); and 1 cycle of 68°C for 7 minutes.

For the fusion PCR, 1.25 μL each of products from PCR #1 and 2 were used as template. The forward primer st-F25-dsh.A* (5'-CAAATCCTCCAAGGGTAACG

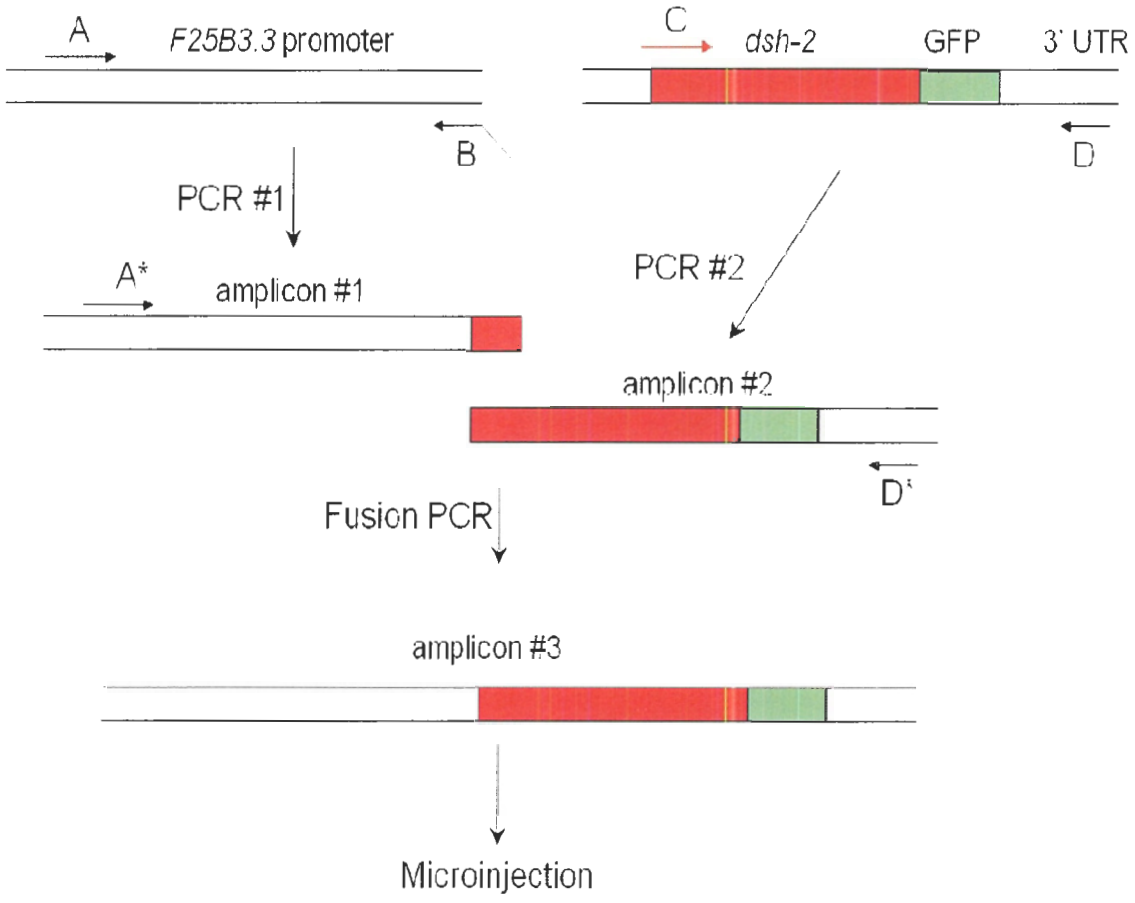

Figure 10 Stitching PCR was used to generate *F25B3.3p-dsh-2::gfp*.

PCR #1 amplifies the *F25B3.3* promoter fragment from genomic DNA using primers A and B. PCR #2 amplifies the *dsh-2::gfp* coding sequence using primers C and D using the plasmid *lin-26p-dsh-2::gfp* as template. Primer B has a 25 bp overhang to the 5' end of *dsh-2::gfp*, allowing the 3'-ends of products from PCR #1 to form complementary base pairs with the 5'-ends of products from PCR #2. In the fusion PCR, the nested primers A* and D* are used.

TACC-3') (sequence generously provided by I. Chin-Sang) and the reverse primer D* primer (5'-GGAAACAGTTATGTTTGGTATATTGGG-3') were used. Cycling conditions were: 1 cycle of 94°C for 1 minute; 10 cycles of 94°C for 10 seconds, 65°C for 30 seconds, 68°C for 3 minutes 30 seconds; 25 cycles of 94°C for 15 seconds, 65 for 30 seconds, 68°C for 4 minutes (plus 20 seconds per cycle); and 1 cycle of 68°C for 7 minutes. Product from the fusion PCR was visualized on an agarose gel and the concentration of the fusion PCR product quantified by comparing band intensity with the 1 kb DNA ladder. PCR products from two independent fusion PCR reactions were pooled and injected into worms at the specified concentrations.

2.4 Germline Transformation

Prior to injection, all plasmids were purified using either the QIAgen Plasmid Miniprep columns or the Sigma GeneElute Plasmid Miniprep Kit. The plasmid was further purified using a PEG precipitation protocol. 100 µL of plasmd DNA was combined with 400 µL of TE and mixed thoroughly with 200 µL of PEG solution (30% PEG8000, 1.6 M NaCl). After an overnight incubation at 4°C, the mixture was spun down at 13K rpm for 20 minutes, also at 4°C. The supernatant was removed and the pellet resuspended in 200 µL TE. Following a phenol-chloroform extraction, the plasmid was then resuspended in 100 µL of ddH_2O. Concentration of the plasmid was quantified by measuring its photoabsorbance at 260 nm using a spectrophotometer. For injecting *F25B3.3p-dsh-2::gfp*, the stitching PCR products were resolved on an agarose gel and quantified with reference to the 1 kb DNA ladder (New England BioLabs).

All constructs were injected into *dsh-2(or302)/mIn1[mIs14 dpy-10(e128)]* hermaphrodites using standard techniques (Mello et al., 1991). See Table 1for a list of transgenic strains generated. For injections, an injection mix was created consisting of the plasmid of interest and the respective co-injection markers. For the majority of injections, the co-injection markers pRF4 (*Rol-6(su1006)* and pNH3B (*srb-6::gfp*) were each injected at 30-50 ng/μL. For injections of *F25B3.3p-dsh-2::gfp* at 20 ng/μL and ΔDIX *dsh-2::gfp* at 10 ng/μL, *srb-6::gfp* was replaced with the plasmid *dpy-30p::dsRed* as a co-injection marker and injected at 40-50 ng/μL. For a subset of injections with the *dsh-2* deletion constructs, genomic DNA was co-injected as junk DNA at 20 ng/μL. This increases the complexity of the extrachromosomal arrays and enhances embryonic expression of the injected plasmids (Kelly et al., 1997).

The injection mix was injected into the syncytium gonad of young adult hermaphrodites. Four to five injected hermaphrodites were placed onto a seeded NGM plate and allowed to lay eggs. The injected animals were transferred every 24 hours onto another seeded plate. F1 transgenic animals were identified by the presence of co-injection markers, and two to three transgenic F1 *dsh-2(or302)/mIn1* animals were placed onto a seeded NGM plate ("F1 plate") and allowed to produce F2 progeny. On average, about 10% of all F1 transgenic animals will produce transgenic F2s. For every F1 plate that produces F2 transgenic animals, six to seven transgenic *dsh-2(or302)/mIn1* F2s were cloned and allowed to self-fertilize. Transgenic F3 animals from one of the F2 plates were then selected as the founders for the respective transgenic line.

Table 1 Transgenic lines generated.

Construct injected (conc.)	Co-injection marker (conc.)	Arrays generated
unc-119p-dsh-2::gfp (5 ng/ul)	*srb-6::gfp* (50 ng/ul), *Rol-6* (50 ng/ul)	*hkEx17-19*
unc-119p-dsh-2::gfp (20 ng/ul)	*srb-6::gfp* (50 ng/ul), *Rol-6* (50 ng/ul)	*hkEx20-22*
lin-26p-dsh-2::gfp (5 ng/ul)	*srb-6::gfp* (50 ng/ul), *Rol-6* (50 ng/ul)	*hkEx23-26*
lin-26p-dsh-2::gfp (20 ng/ul)	*srb-6::gfp* (50 ng/ul), *Rol-6* (50 ng/ul)	*hkEx27-28*
unc-119p-dsh-2::gfp (100 ng/ul)	*srb-6::gfp* (50 ng/ul), *Rol-6* (50 ng/ul)	*hkEx29*
unc-119p-dsh-2::gfp (50 ng/ul)	*srb-6::gfp* (50 ng/ul), *Rol-6* (50 ng/ul)	*hkEx30-31*
ΔDIX *dsh-2::gfp* (0.5 ng/ul)	*srb-6::gfp* (50 ng/ul), *Rol-6* (50 ng/ul)	*hkEx32-34*
ΔDIX *dsh-2::gfp* (0.5 ng/ul)	*srb-6::gfp* (30 ng/ul), *Rol-6* (30 ng/ul), genomic DNA (20 ng/ul)	*hkEx35-37*
Δ*EP *dsh-2::gfp* (0.5 ng/ul)	*srb-6::gfp* (30 ng/ul), *Rol-6* (30 ng/ul), genomic DNA (20 ng/ul)	*hkEx38-40*
ΔDIX *dsh-2::gfp* (2.5 ng/ul)	*srb-6::gfp* (30 ng/ul), *Rol-6* (30 ng/ul), genomic DNA (20 ng/ul)	*hkEx52-53*
Δ*EP *dsh-2::gfp* (2.5 ng/ul)	*srb-6::gfp* (30 ng/ul), *Rol-6* (30 ng/ul), genomic DNA (20 ng/ul)	*hkEx54-62*
F25B3.3p-dsh-2::gfp (20 ng/ul)	*srb-6::gfp* (25 ng/ul), *Rol-6* (25 ng/ul), *dpy-30p::dsRed* (40 ng/ul)	*hkEx63-65*
F25B3.3p-dsh-2::gfp (50 ng/ul)	*Rol-6* (30 ng/ul)	*hkEx77-83*
ΔDIX *dsh-2::gfp* (10 ng/ul)	*Rol-6 (30 ng/ul), dpy-30::dsRed* (50 ng/ul), genomic DNA (20 ng/ul)	*hkEx84-86*

2.5 Integration of extrachromosomal arrays

Before integration, all extrachromosomal lines were crossed out of the *dsh-2(or302)* genetic background into N2 animals. The integration protocol was generously provided by members of the Baillie lab. Mixed-stage worms on NGM plates were placed faced up and lid off into the Torrex 150D X-ray Inspection System and irradiated at the following settings: 1500 rads, 135 seconds, five mA, and 145 KV. After an hour of recovery time, 20 to 25 transgenic adult hermaphrodites (P0) were individually selected onto separate large plates seeded with *E. coli* strain *HB101*. The P0 animals were allowed to lay eggs (F1s) for 24 hours before being removed from the plates, and the F1s were allowed to mature and produce F2 progeny. 10 to 12 F2s from each P0 plate were then cloned onto individual NGM plates. Integrated lines were obtained by identifying F2 animals in which 100% of the progeny inherited the co-injection markers. See Table 2 for a list of integrated lines generated.

2.5.1 Backcrossing integrated strains after X-ray irradiation

A general schematic is shown in Appendix 9. For the first backcross, N2 males were mated with hermaphrodites homozygous for the integrated array (*In[Rol]*). Since the *Rol-6* plasmid was included as a co-injection marker, animals that carry the integrated array could be identified by the roller phenotype. Therefore, +/*In* roller males were selected for the next backcross. However, roller males do not mate well. To facilitate mating, they were mated with *unc-2* hermaphrodites. These hermaphrodites are fertile but move very sluggishly, increasing the chance for roller males to copulate. +/*In; +/unc-2* cross progeny Roller hermaphrodites were selected and again mated with N2 males if

Table 2 Integrated arrays generated.

Original extrachromosomal array	Construct injected (conc.)	Integrated array
hkEx25	*lin-26p-dsh-2::gfp* (5 ng/ul)	*hkIs1-4*
hkEx22	*unc-119p-dsh-2::gfp* (20 ng/ul)	*hkIs5-9*
hkEx27	*lin-26p-dsh-2::gfp* (20 ng/ul)	*hkIs10-17*
hkEx32	ΔDIX *dsh-2::gfp* (0.5 ng/ul)	*hkIs18-21*
hkEx36	ΔDIX *dsh-2::gfp* (0.5 ng/ul)	*hkIs22-23*
hkEx39	Δ*EP *dsh-2::gfp* (0.5 ng/ul)	*hkIs24-28*

additional backcrosses were performed. In the last backcross, cross progeny +/*In* Roller hermaphrodites were selected and allowed to self-fertilize to homozygose the integrated array.

2.5.2 Crossing *dsh-2(or302)* into integrated arrays

Transgenic animals carrying the *unc-119p-dsh-2::gfp* or *lin-26p-dsh-2::gfp* integrated arrays were backcrossed 4 to 6 times before *dsh-2(or302)* was crossed in. Transgenics carrying the ΔDIX or Δ*EP integrated arrays were backcrossed at least twice before crossing in *dsh-2(or302)*.

A common scheme (Appendix 10) was used to construct strains carrying integrated arrays and *dsh-2(or302)*. N2 males were crossed with hermaphrodites carrying an integrated array (*In[Rol]*), and F1 Roller males were selected and crossed with *dsh-2(or302)/mIn1[mIs14 dpy-10(e128)]* hermaphrodites. Simultaneously, crosses between N2 males and *dsh-2(or302)/mIn1[mIs14 dpy-10(e128)]* hermaphrodites were also set up, and F1 +/*mIn1* males expressing pharyngeal GFP from were selected and mated with +/*In*; +/*dsh-2(or302*) hermaphrodites from the concurrent cross. In the next generation, roller hermaphrodites that express pharyngeal GFP are of the genotype +/*In*; + or *dsh-2(or302)/mIn1[mIs14 dpy-10(e128)]*. About 10 of these hermaphrodites were cloned onto separate plates and allowed to produce self-progeny. Homozygous *dsh-2(or302)* mutants were determined by the presence of clear patches in the gonad due to gonadogenesis defects. From a plate that segregated homozygous *dsh-2(or302)* mutants, +/*In; dsh-2(or302)/mIn1[mIs14 dpy-10(e128)]* hermaphrodites were selected and allowed to self-fertilize to homozygose the integrated array.

2.6 Worm lysis for PCR reaction

Six to eight adult worms were placed in 12-16 μL of worm lysis solution (60 μg/mL proteinase K, 10 mM Tris pH 8.2, 50 mM KCl, 2.5 mM $MgCl_2$, 0.5% Tween 20, 0.05% gelatin) in the cap of a PCR tube. The tube was then spun at 13K rpm for 2 minutes and then placed at -80°C for 15 minutes. Once thawed, the lysis solution containing the worms was incubated in a PCR machine at 60°C for 1 hour and then 95°C for 15 minutes. 2.5 μL of worm lysate was then used as template in PCR reactions.

2.6.1 Genotyping *ced-3(n717)* mutants

This method of detecting the *ced-3(n717)* mutation was courtesy of S. Cordes and G. Garriga at the University of California, Berkeley. The *ced-3(n717)* mutation is a dimorphism that changes from the wildtype N2 sequence of GCNGC to GC-GC. The restriction enzyme Fnu4H I specifically recognizes the sequence in N2 but not the *ced-3(n717)* mutation. Therefore, to molecularly identify the *ced-3(n717)* mutation, a PCR-restriction digest method was employed.

The primers used were n717-F (5'-TCGGATTGGTTTGAAAGTGG-3') and n717-R (5'-ACAGACGGCTTGAATGAACC-3'). PCR reactions were performed in a final volume of 25 μL consisting 1.5 mM $MgCl_2$, 0.2 mM dinucleotide triphosphates, 0.2 μM of each primer, 2.5 μL of worm lysate, and 1 unit of Taq polymerase. The cycling conditions were: 95°C for 2 minutes, 36 cycles of 95°C for 40 seconds, 58 °C for 40 seconds, 72 °C for 40 seconds, and then 72 °C for 10 minutes. If N2 worm lysate was used as template, the PCR would generate a product of 319 bp in size. Conversely, if worm lysate from *ced-3(n717)* mutants was used as template, a fragment of 318 bp would

be generated. The PCR products were then digested with Fnu4H I, and the digested products were visualized on a 1.8% agarose gel with ethidium bromide. The N2 PCR product would be digested by the enzyme, yielding two fragments of 198 and 121 bp on the agarose gel. The PCR products from *ced-3(n717)* homozygotes lack the restriction enzyme cut site and thus would not be cut, giving a single band at 318 bp on the gel. *ced-3(n717)* heterozygotes would generate a mixture of the two PCR products, and three bands of sized 318, 198, and 121 bp would be observed.

2.7 Immunohistological Methods

2.7.1 General embryo fixation protocol

Embryos for antibody staining were fixed using the modified Ruvkun protocol (Finney and Ruvkun, 1990). To collect embryos, gravid hermaphrodites were washed off and treated with a hypochlorite solution (0.8 M NaOH, 0.125% sodium hypochlorite). This solution dissolves adult tissues and leaves embryos intact. The embryos were then fixed in 1% paraformaldehyde containing 80 mM KCl, 20mM NaCl, 2 mM EGTA, 0.5 mM spermidine HCl, 0.2 mM spermine, 0.5% β-mercaptoethanol, 15 mM PIPES pH 7.4, with 1/5 volume of 90% MeOH; 10% 0.05 M EGTA for 15-20 minutes. Fixed embryos were then frozen rapidly in liquid nitrogen for 1 minute and then stored in -80°C for future use.

Tubes of embryos were thawed in tap water and the embryos fixed for an additional 20 minutes at room temperature. The embryos were then washed twice in Tris-Triton buffer (100 mM Tris-Cl pH 7.4, 1% Triton X-100, 1 mM EDTA), two to three times with 1mL PBST-B (1X PBS, 0.1% BSA, 0.5% Triton X-100, 0.05% azide, 1 mM

EDTA), and blocked for 1 hour in 1mL PBST-A (1X PBS, 1% BSA, 0.5% Triton X-100, 0.05% azide, 1 mM EDTA). Embryos were incubated with primary antibodies in PBST-A overnight. The next day, embryos were washed with 1mL of PBST-B, 15-30 minutes per wash. After 3-5 washes, embryos were incubated with secondary antibodies in PBST-A overnight. Similarly, the embryos were washed 3-5 times with 1 mL of PBST-B, 15-30 minutes each. In the last wash, 4',6-diamidino-2-phenylindole (DAPI) was added to a final volume concentration of 1 μg/mL. To view the stained embryos, they were mounted on 2% agarose pads in an equal amount of DABCO (0.1 g/mL DABCO in 1x PBS and 90% glycerine) to prevent photo-bleaching. A coverslip was placed on top and sealed with clear nailpolish.

2.7.2 Antibodies used

Anti-DSH-2 antibodies (made by N. Hawkins) were generated by immunizing rats with the C-terminal region of the DSH-2 protein. Antibody dilutions were anti-DSH-2 (rat, 1:500; Hawkins et al., 2005), anti-GFP (chick, 1:200, Chemicon), anti-LIN-26 (rabbit, 1:2000; Labouesse and Horvitz, 1996), MH27 (mouse, 1:500; Francis and Waterston, 1991), Cy3 conjugated anti-rat secondary antibody (1:1000, Jackson Laboratories), Cy3 conjugated anti-rabbit secondary antibody (1:1000, Jackson Laboratories), FITC conjugated anti-chick secondary antibody (1:500, Jackson Laboratories).

2.8 Microscopy

Worms were immobilized in 3 μL of 100mM sodium azide and then mounted on 2% agar pads. Live worms and fixed embryos were visualized using a Leica DMRA2

microscope equipped with epi-fluorescence and differential interference contrast optics. Imaging was carried out with a Hamamatsu digital camera and OpenLab software.

CHAPTER 3 RESULTS

3.1 Probing for additional asymmetric cell division defects in *dsh-2* mutants

3.2 The generation of many cells are affected in *dsh-2* mutants

Preliminary results suggest that in addition to the PHA lineage, division defects in other cell lineages may also be present in *dsh-2* mutants. Lack of *dsh-2* function often leads to losses of specific DD motor neurons as observed by a DD neuron-specific GFP marker (N. Hawkins, unpublished results). In total, there are six DD motor neurons, and their cell bodies reside along the ventral nerve cord. A lineage diagram for the DD neurons is shown in Figure 11. The ABplppap neuroblast divides asymmetrically to generate a posterior daughter that further divides to produce DD neurons 1, 3, and 5. The ABprppap neuroblast undergoes an identical division pattern but the posterior daughter generates DD2, 4, and 6 instead. A GFP reporter that specifically expresses in all the DD motor neurons was used to examine the number of DD neurons in *dsh-2* mutants. In *dsh-2* (M- Z-) mutants, losses of either DD1, 3, and 5 or DD2, 4, and 6 were often observed. These patterns of cells losses are consistent with a cell fate transformation where the posterior daughter cell has adopted an anterior daughter-like fate (Figure 11). Interestingly, the defective division also occurs at about 180 minutes into embryogenesis, the same time at which the division in the PHA lineage is defective. Furthermore, lineage analysis of *dsh-2* embryos revealed ectopic and delayed cell deaths, which are also suggestive of additional cell division defects (N. Hawkins, unpublished results).

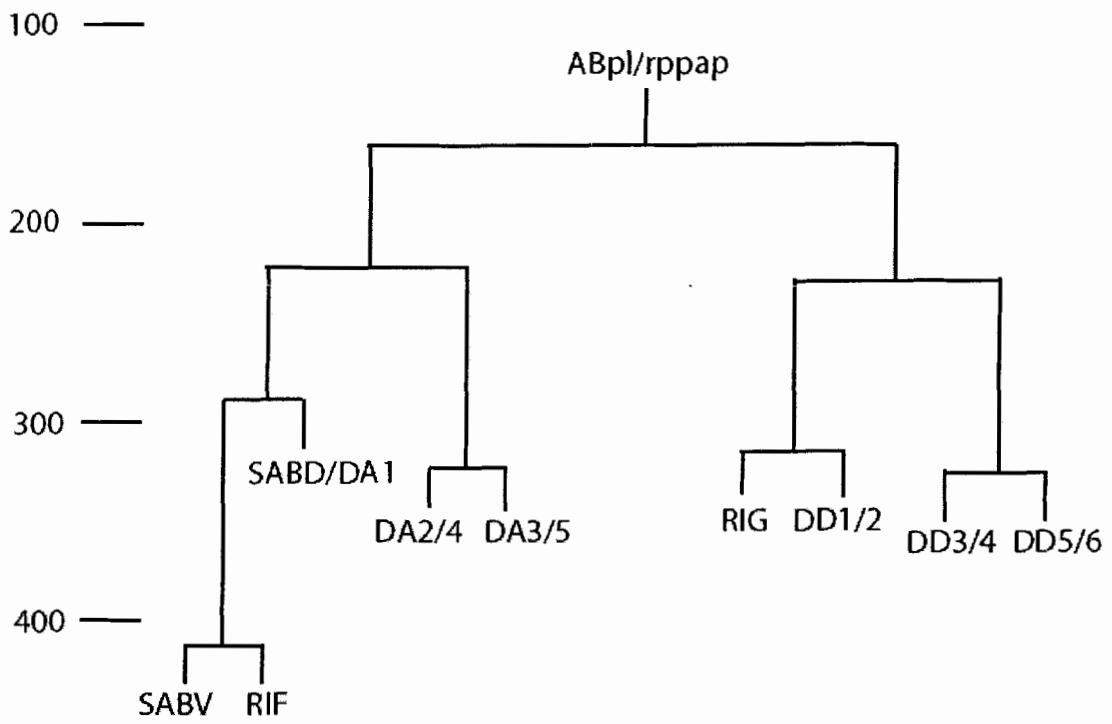

Figure 11 *dsh-2* may regulate asymmetric cell division in the DD motor neuron lineage. Numbers on the left denotes minutes after fertilization. The ABplppap and ABprppap neuroblasts divide asymmetrically at about 180 minutes of embryogenesis, and the posterior daughter cells go on to generate the DD motor neurons. The left posterior daughter generates DD1, 3, and 5 whereas the right posterior daughter generates DD2, 4, and 6. The DD motor neurons are evenly spaced along the ventral nerve cord, with DD1 being the most anterior and DD6 being the most posterior. In *dsh-2* mutants, either the DD1, 3, 5 or the DD2, 4, 6 neurons are lost. This is consistent with a cell fate transformation where the posterior daughter cell of ABpl/rppap has adopted an anterior daughter-like fate.

To identify additional lineages affected, we obtained *C. elegans* strains carrying different promoter::GFP fusions that express GFP in specific subsets of cells. Several criteria were followed in the selection of cell-specific reporters. Since *dsh-2* (M+ Z-) mutants are viable, maternal DSH-2 protein is sufficient for proper embryonic development and asymmetric cell division. Therefore, it is expected that cell losses and duplications would be more readily observed in mutants lacking both maternal and zygotic *dsh-2* function. However, *dsh-2* (M- Z-) mutants have gross morphological defects. If a marker expresses GFP in many cells, any cells losses and duplications could not be unambiguously attributed to a specific cell. Therefore, markers that specifically express GFP in one cell were preferred. Markers that are active in two cells were also chosen, especially if the cells are far apart from each other and can be easily distinguished. In addition, markers that are stably integrated into the genome were preferred. If unavailable, markers present as extrachromosomal arrays were selected.

In total, 12 strains containing different GFP fusions were obtained, allowing us to assay 18 different cells (16 neurons and two non-neuronal cells). Two of the 16 neurons are born post-embryonically as are both of the non-neuronal cells. For cells that are born during embryogenesis, the number of cells was determined in the first larval stage (L1); numbers for cells born post-embryonically were determined no later than the L3 stage. Each of the 12 strains was crossed into two *dsh-2* mutant alleles: *or302* and *ez25*. The *or302* allele is a 1 kb deletion/frame shift mutation that is predicted to produce a truncated protein containing the first 146 amino acids. Since the deletion spans part of the DIX and PDZ domains and remove most of the protein, *or302* is likely a null (Figure 12). The *ez25* allele is a nonsense mutation that just precedes the PDZ domain, the second of

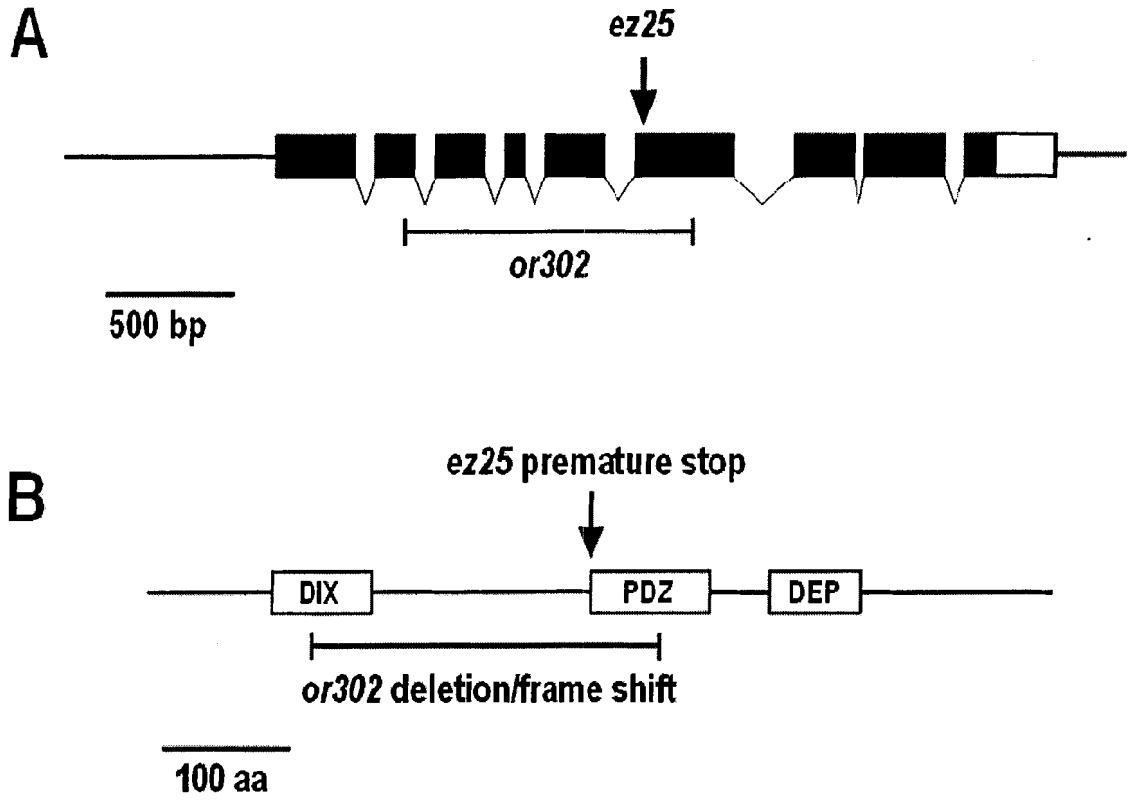

Figure 12 The *dsh-2* gene and the *or302* and *ez25* alleles.

A) Schematic showing the *dsh-2* genomic locus. The region deleted by the *or302* mutation is shown below the genomic structure; the nonsense mutation of *ez25* is depicted above. B) A schematic showing the DSH-2 protein and the three conserved domains. The *or302* deletion removes most of the DSH-2 protein and is a null. The *ez25* mutation is predicted to produce half of the protein but lacks the latter two domains. It is likely a strong loss-of-function or a null mutation.

three DSH-2 domains. This mutation is predicted to produce the first 360 amino acids of the DSH-2 protein. Therefore, *ez25* is likely a strong loss-of-function or null (Chang et al., 2005; Figure 12). The number of GFP-expressing cells was analyzed in *dsh-2* (M+ Z-) and (M- Z-) mutants. As a control, the markers were also analyzed in *dsh-2(or302)/mIn1* animals. These animals carry a wildtype copy of *dsh-2* on the balancer chromosome *mIn1* and thus are phenotypically wildtype. Losses and/or duplications were found for 16 out of the 18 cells (Table 3; Appendix). As expected, *dsh-2* (M- Z-) mutants exhibited more penetrant cell losses and duplications than *dsh-2* (M+ Z-) mutants.

Between the two alleles of *dsh-2*, cell losses and duplications occur at very similar frequencies (compare Table 3 with Appendix 1). When the difference in penetrance is greater than 10%, the *or302* allele was the more severe allele in three out of four cases (DTC, ASE, AWB). This was expected since *dsh-2(or302)* is likely a null whereas *dsh-2(ez25)* could be a hypomorph (Chang et al., 2005). The only exception was the ASH neuron, where losses were observed at a frequency of 19% in *dsh-2(ez25)* (M- Z-) mutants compared to only 5% in *dsh-2(or302)* (M- Z-) counterparts.

3.2.1 In-depth analysis of select lineages with divisional defects

Although losses and duplications of cells are indicative of cell fate transformation due to defects in asymmetric cell division, other explanations exist to account for a change in the number of specific cells. For instance, cells may inappropriately express or fail to express a GFP marker due to defects in cell fate determination. In order to determine if the cell losses/duplications were indeed caused by asymmetric cell division defects, analysis of lineally-related cells is required. One criterion was to focus on

Table 3 The production of many cells is affected in *dsh-2* mutants.

Cell	Genotype	% Loss	% Duplication	N
ALM	*dsh-2(or302)/mln1; zdIs5*	0	0	108
	dsh-2(or302) (M+ Z-); *zdIs5*	0	2	83
	dsh-2(or302) (M- Z-); *zdIs5*	1	6	106
AQR	*dsh-2(or302)/mln1; adEx1296*	n.d.	n.d.	n.d.
	dsh-2(or302) (M+ Z-); *adEx1296*	n.d.	n.d.	n.d.
	dsh-2(or302) (M- Z-); *adEx1296*	0	0	12
ASH	*dsh-2(or302)/mln1; hdIs26*	0	0	100
	dsh-2(or302) (M+ Z-); *hdIs26*	0	0	78
	dsh-2(or302) (M- Z-); *hdIs26*	6	0	90
ASI	*dsh-2(or302)/mln1; kyIs128*	0	0	44
	dsh-2(or302) (M+ Z-); *kyIs128*	n.d.	n.d.	n.d.
	dsh-2(or302) (M- Z-); *kyIs128*	18	3	33
AVM	*dsh-2(or302)/mln1; zdIs5*	0	0	42
	dsh-2(or302) (M+ Z-); *zdIs5*	0	1	90
	dsh-2(or302) (M- Z-); *zdIs5*	0	0	7
DA + DB	*dsh-2(or302)/mln1; juIs14*	0	0	124
	dsh-2(or302) (M+ Z-); *juIs14*	4	4	93
	dsh-2(or302) (M- Z-); *juIs14*	n.d.	n.d.	n.d.
CAN	*dsh-2(or302)/mln1; gmIs18*	0	0	100
	dsh-2(or302) (M+ Z-); *gmIs18*	0	0	86
	dsh-2(or302) (M- Z-); *gmIs18*	19	14	104
PLM	*dsh-2(or302)/mln1; zdIs5*	0	0	108
	dsh-2(or302) (M+ Z-); *zdIs5*	0	2	87
	dsh-2(or302) (M- Z-); *zdIs5*	6	8	110
PQR	*dsh-2(or302)/mln1; adEx1296*	0	0	9
	dsh-2(or302) (M+ Z-); *adEx1296*	n.d.	n.d.	n.d.
	dsh-2(or302) (M- Z-); *adEx1296*	0	0	12
PVM	*dsh-2(or302)/mln1; zdIs5*	0	0	42
	dsh-2(or302) (M+ Z-); *zdIs5*	0	1	93
	dsh-2(or302) (M- Z-); *zdIs5*	n.d.	n.d.	n.d.
URX	*dsh-2(or302)/mln1; ynIs22*	0	0	88
	dsh-2(or302) (M+ Z-); *ynIs22*	0	0	98
	dsh-2(or302) (M- Z-); *ynIs22*	n.d.	n.d.	n.d.
	dsh-2(or302)/mln1; adEx1296	0	0	10
	dsh-2(or302) (M+ Z-); *adEx1296*	0	0	8
	dsh-2(or302) (M- Z-); *adEx1296*	17	3	30

n.d. = not determined

lineages with high frequencies of aberrant cell numbers in *dsh-2* mutants. Also, cell fate markers must be available for lineally-related cells. A good candidate was the CAN neuron as it was duplicated at a frequency of 14% in *dsh-2(or302)* (M- Z-) and 16% in *dsh-2(ez25)* (M- Z-) mutants. Unfortunately, the lack of suitable markers for cells in the CAN lineage precluded further analysis of this lineage. Instead, the lineages that generate the DTC/AC cells, the OLL neuron, and the PVQ neuron were further analyzed.

3.2.1.1 DTC/AC lineage

In L1 hermaphrodites, Z1 and Z4 are the somatic precursor cells in the primordial gonad. They divide asymmetrically to generate a total of two DTCs and an AC. The DTCs lead the migration of the anterior and posterior gonadal arms, while the AC induces vulval fates of the underlying hypodermis. Wnt signalling proteins act through POP-1/TCF to regulate the asymmetric division of Z1/Z4 (Siegfried and Kimble, 2002; Kidd et al., 2005). The division becomes symmetric in Wnt signalling mutants, and AC duplications and DTCs losses are observed.

Although Wnt signalling dictates the asymmetric division of Z1/Z4, a role for *dsh-2* has not been characterized. To determine if *dsh-2* also regulates the same asymmetric cell division in the Z1/Z4 precursors, DTC- and AC-specific GFP reporters were analyzed in *dsh-2* hermaphrodites. In wildtype animals, two DTCs and one AC are present as visualized by the *qIs19[lag-2::gfp]* and *syIs50[cdh-3::gfp]* GFP markers, respectively. In *dsh-2(or302)* and *dsh-2(ez25)* mutants lacking zygotic function, the DTCs were lost 61% and 48% of the time, respectively (Table 4; Appendix 2; Figure 13). Conversely, ACs were gained at frequencies of 42% in *dsh-2(or302)* (M+ Z-) and 40% in

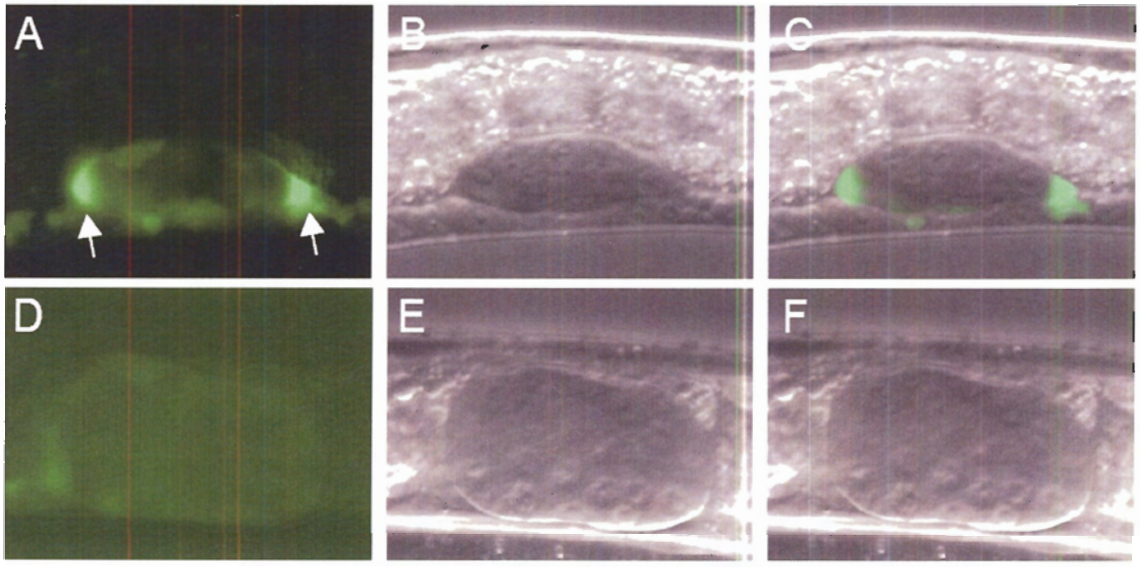

Figure 13 Losses of distal tip cells in *dsh-2* mutants.

The integrated array *qIs19[lag-2::gfp]* was used to visualize the DTCs in hermaphrodites. **A-C:** A wildtype animal at late L1/early L2 stage. A) Epi-fluorescence micrograph showing endogenous GFP in the two distal tip cells (DTCs; white arrows). B) Corresponding DIC image of the same animal. The anterior and posterior gonad arms are starting to elongate. C) A merge of the GFP and DIC images.
D-F: A *dsh-2(or302)* (M+ Z-) mutant at late L1/early L2 stage. D) Epi-fluorescence micrograph showing endogenous GFP. Both DTCs are lost as shown by the lack of bright GFP expression. E) DIC of the same animal. Gonad appears disorganized. F) Merge of GFP and DIC images.

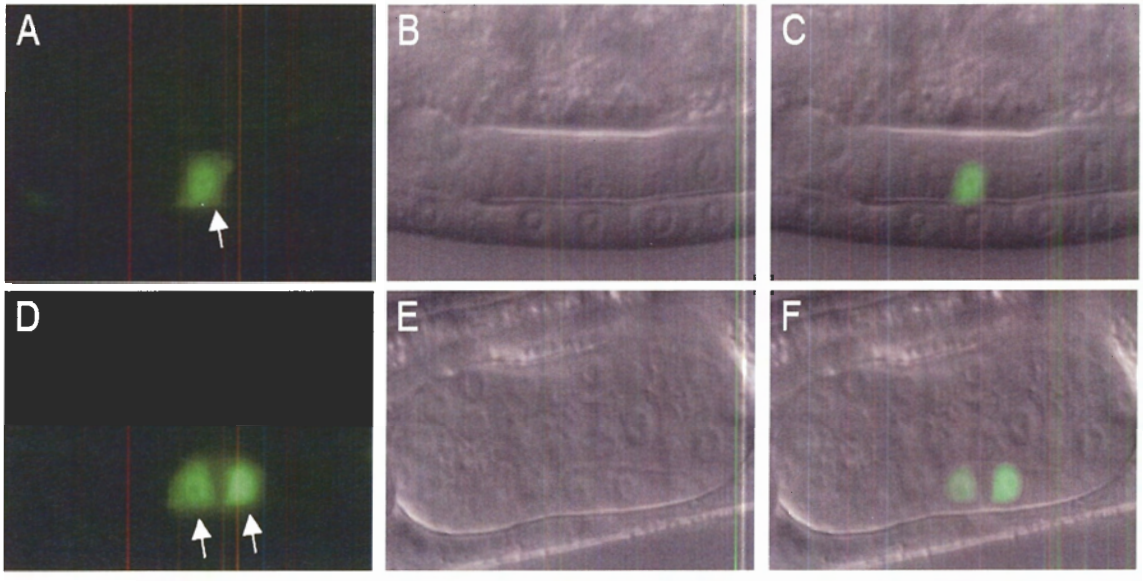

Figure 14 Anchor cell duplications in *dsh-2* mutants.

The integrated array *syIs50[cdh-3::gfp]* was used to visualize the ACs in hermaphrodites. **A-C**: A wildtype animal in the early L3 stage. A) Epi-fluorescence micrograph showing endogenous GFP in the single AC (arrow). B) Corresponding DIC image of the same animal. C) A merge of the GFP and DIC images.
D-F: A *dsh-2(or302)* (M+ Z-) hermaphrodite at L3 stage. D) Epi-fluorescence micrograph showing endogenous GFP. Two ACs are present as two cells express *cdh-3::gfp* (arrows). E) DIC of the same animal. F) Merge of D and E.

Table 4 Anchor cell duplications and distal tip cell losses are frequently observed in *dsh-2(or302)* (M+ Z-) mutants.

Cell	Genotype	% Loss	% Duplication	N
AC	***dsh-2(or302)/mln1; syls50***	0	< 1	104
	dsh-2(or302)* (M+ Z-); *syls50	0	42	90
DTC	***dsh-2(or302)/mln1; qls19***	3	0	110
	dsh-2(or302)* (M+ Z-); *qls19	61	0	82

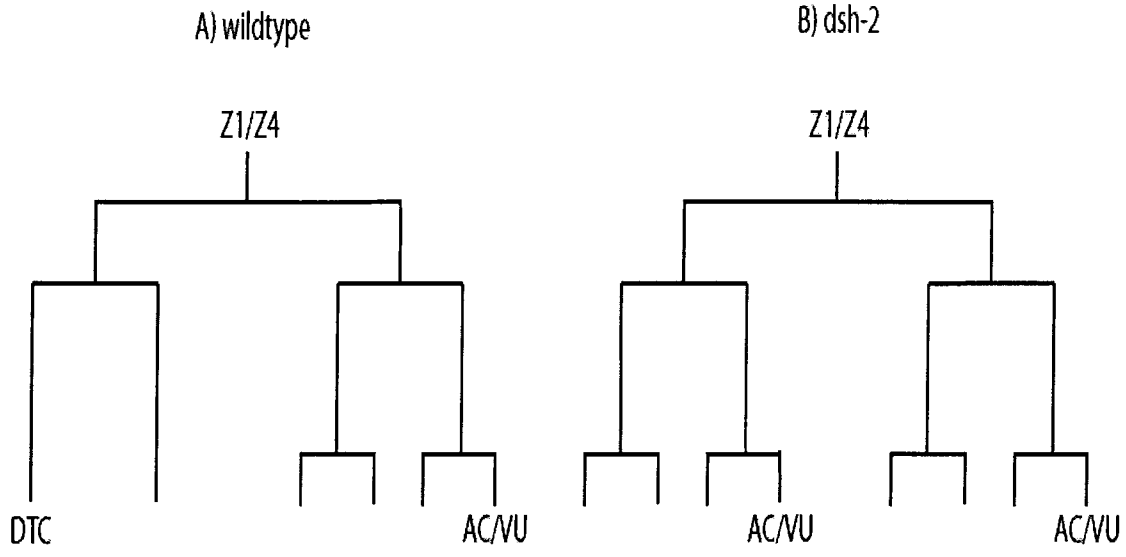

Figure 15 Proposed Z1/Z4 lineage defects in *dsh-2* mutants.

Both the Z1 and Z4 cells divide asymmetrically in wildtype hermaphrodites, generating a total of two DTCs and one each of AC and VU. In *dsh-2* mutants lacking zygotic function, both Z1 and Z4 divide symmetrically, and ACs are frequently gained at the expense of DTCs.

dsh-2(ez25) (M+ Z-) mutants (Table 4; Appendix 2; Figure 14). These observations suggest that in *dsh-2* mutants, the Z1/Z4 division also becomes symmetric (Figure 15).

3.2.1.2 OLL lineage

The OLL neuron is a putative mechanosensory neuron in the head (Wormatlas). The OLL neuron was frequently duplicated in *dsh-2* mutants (Table 5; Figure 16). In *dsh-2* (M+ Z-) mutants, OLL duplications were observed at a frequency of 27%. The penetrance increased slightly in *dsh-2* (M- Z-) mutants to 33%. This lineage is ideal for further analysis because, unlike other cells that are duplicated in *dsh-2* mutants, extra OLL neurons were readily observed even in *dsh-2* mutant animals lacking only zygotic function. The left OLL neuron is generated from the ABalpppp and the right OLL from the ABpraaap neuroblast. Since the two neuroblasts have identical downstream lineages, for simplicity only the right OLL lineage is shown in Figure 17. We focused on this portion of the OLL lineage because the division of the ABpraaap neuroblast occurs at 180 minutes, a time that is identical to the defective division in the PHA lineage. In wildtype, the ABpraaap neuroblast divides asymmetrically to produce distinct anterior and posterior daughter cells. Both cells divide further to produce exclusively neurons and cells that undergo apoptosis. The right OLL neuron is descended from the anterior daughter of the ABpraaap neuroblast. Specifically, we tested if extra OLL neurons were caused by a cell fate transformation that converted the posterior daughter to a second anterior daughter-like cell.

To determine if extra OLL neurons were generated by the proposed cell fate transformation, three transgenic strains carrying GFP markers for neurons derived from the posterior daughter (ADF, AWB, and ASE) were obtained and crossed into *dsh-2*

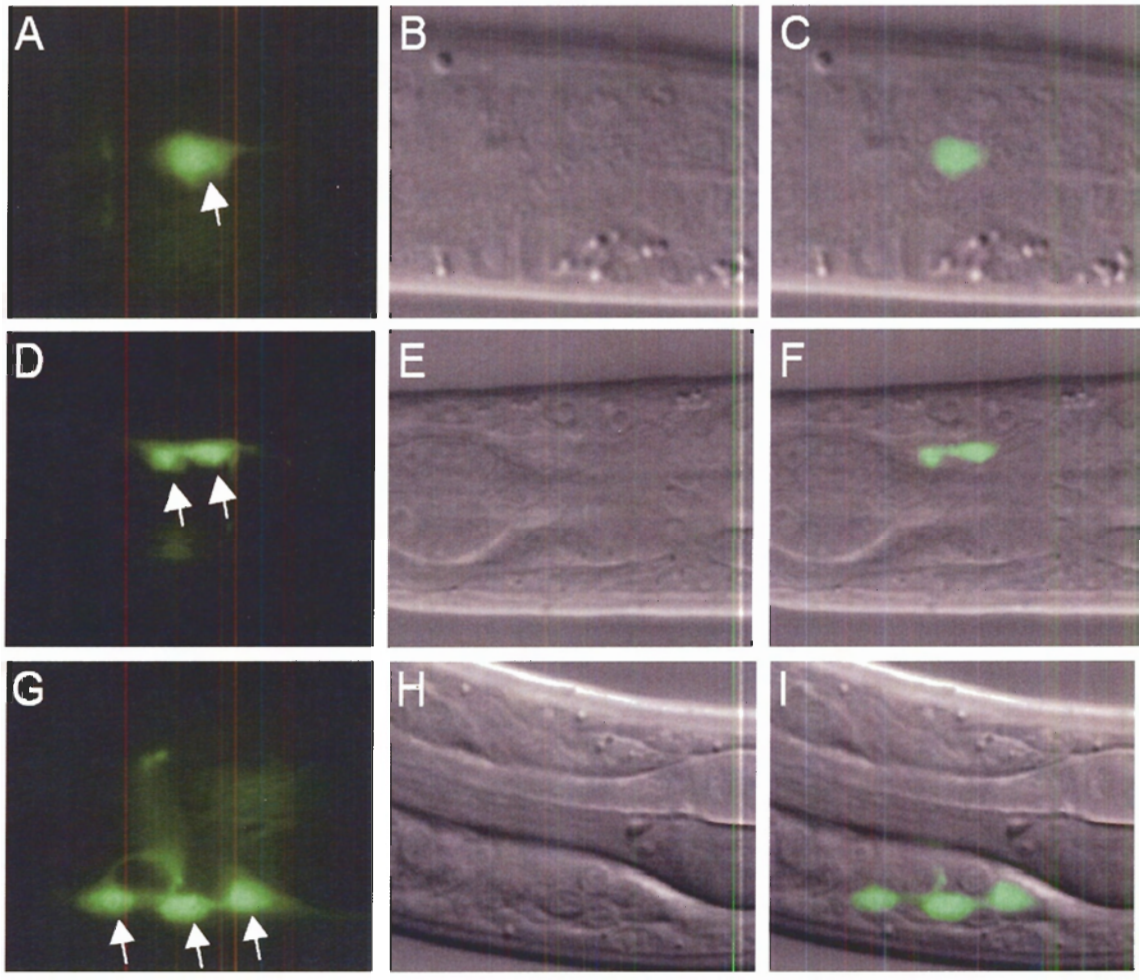

Figure 16 OLL duplications in *dsh-2* mutants.

The integrated array *otIs138[ser-2prom3::gfp]* was used to visualize the OLL neurons.
A-C: Wildtype larva. A) Epi-fluorescence micrograph showing endogenous GFP in an OLL neuron expressing *ser-2prom3::gfp* (arrow). B) Corresponding DIC image. C) Merge of GFP and DIC images.
D-F: A *dsh-2(ez25)* (M- Z-) larva. D) Epi-fluorescence micrograph showing endogenous GFP. Two cells express the *ser-2prom3::gfp* marker on the right side of the animal (two arrows). At a different focal plane, a single OLL on the left side also expresses GFP. E) DIC image of the same animal. F) Merge of GFP and DIC images.
G-I: Another *dsh-2(ez25)* (M- Z-) larva. G) On rare occasions, three cells express the *ser-2prom3::gfp* marker on one side of *dsh-2* mutants (three arrows). H) DIC image. I) Merge of GFP and DIC.

Table 5 Cell losses and duplications in the OLL lineage.

Cell	Genotype	% Loss	% Duplication	N
OLL	*dsh-2(or302)/mIn1; otIs138*	0	0	100
	dsh-2(or302) (M+Z-); *otIs138*	2	27	94
	dsh-2(or302) (M-Z-); *otIs138*	10	33 [a]	108
AWB	*dsh-2(or302)/mIn1; kyIs104*	0	0	92
	dsh-2(or302) (M+Z-); *kyIs104*	2	0	102
	dsh-2(or302) (M-Z-); *kyIs104*	19	0	119
ASE	*dsh-2(or302)/mIn1; ynIs22*	0	0	100
	dsh-2(or302) (M+Z-); *ynIs22*	7	0	98
	dsh-2(or302) (M-Z-); *ynIs22*	n.d. [b]	n.d. [b]	n.d. [b]
ADF	*dsh-2(or302)/mIn1; mgIs71*	0	0	100
	dsh-2(or302) (M+Z-); *mgIs71*	0	3	97
	dsh-2(or302) (M-Z-); *mgIs71*	n.d. [c]	n.d. [c]	n.d. [c]

n.d. = not determined

[a] 29% of the duplications observed resulted in two OLL neurons per side; 4% of the duplications led to three OLL neurons per side.

[b] *ynIs22* also expresses in another neuron called URX that is just anterior to ASE. These two cells could not be distinguished in *dsh-2* (M- Z-) mutants due to morphological defects. Thus, the number of ASEs was not scored.

[c] *mgIs71* also expresses in another neuron called NSM that is just anterior to ADF. These two cells could not be distinguished in *dsh-2* (M- Z-) mutants due to morphological defects. Thus, the number of ADFs was not scored.

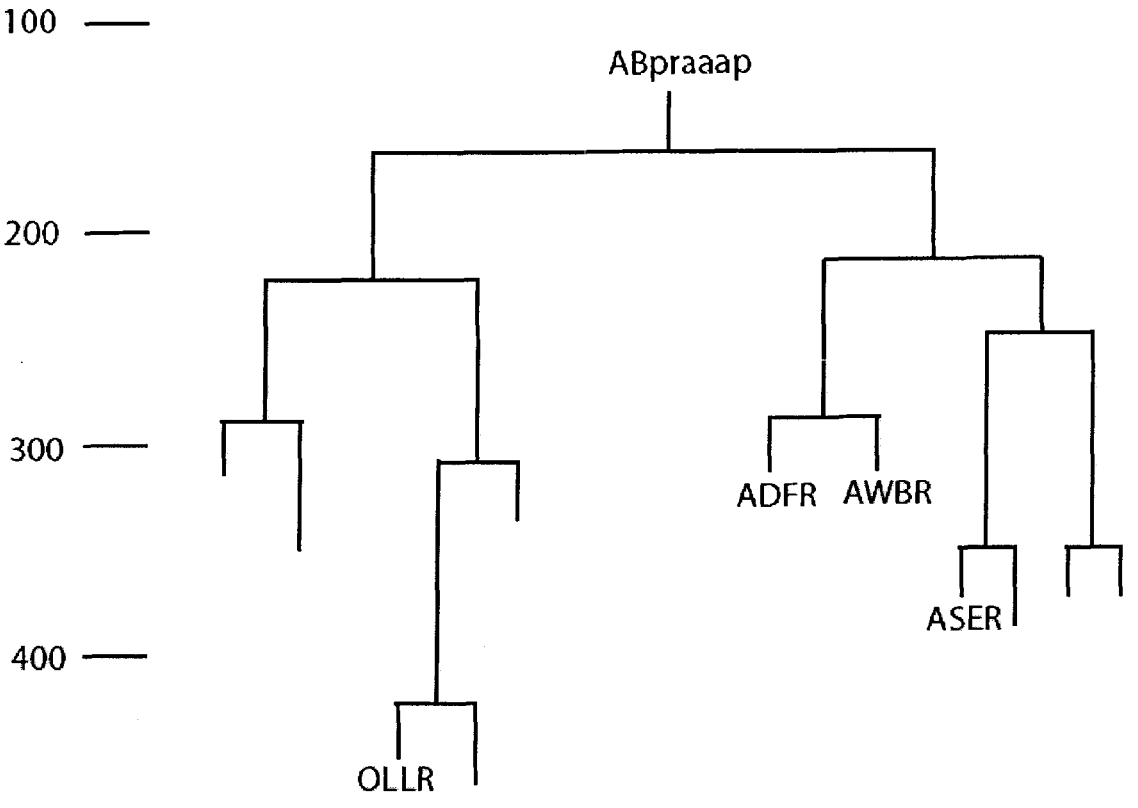

Figure 17 Lineage of the right OLL neuron.

The left OLL is generated from the ABalpppp neuroblast, and the right OLL is generated from the ABpraaap neuroblast. Since the downstream lineages of the two neuroblasts are identical, only the lineage diagram for the right OLL is shown. For simplicity, only cells that were analyzed with GFP markers are shown.

mutants. If the above hypothesis were correct, those cells may be lost at similar frequencies at which OLL duplications were observed. In *dsh-2(or302)* (M+ Z-) mutants, OLL is duplicated 27% of the time, and the frequency is 33% in maternal and zygotic mutants. However, in zygotic *dsh-2(or302)* mutants, AWB and ASE were only lost at 2% and 7%, respectively, and ADF was gained at 3% (Table 5). When both zygotic and maternal *dsh-2* function are lacking, AWB losses increased to a frequency of 19%. Unfortunately, we were unable to assay for the number of ASE and ADF neurons in *dsh-2* (M- Z-) mutants. Both neurons are found in the head, and the GFP markers are both expressed in additional neurons in the head. Thus, we could not unambiguously tell the cells apart in *dsh-2* (M- Z-) mutant animals due to severe morphological defects. Taken together, asymmetric cell division defect in the division of ABpraaap and ABalpppp at 180 minutes of embryogenesis is unlikely to be the cause of extra OLL neurons. However, our results indicate either cell fate determination or division defects later in the lineage may generate extra OLLs.

3.2.1.3 PVQ lineage

The PVQ neuron was found to be duplicated at 10% in *dsh-2(or302)* (M- Z-) mutants (Table 6; Figure 18). The lineage that generates the PVQ neuron is shown in Figure 19. We know that the lineally-related neuron phasmid neuron PHB is unaffected in *dsh-2* mutants (Hawkins et al., 2005). Thus, if the duplication of PVQ is due to an asymmetric cell division defect, the likely source of extra PVQs is the sister cell that normally undergoes apoptosis. If extra PVQs arose from the sister cell of the PVQ neuron, preventing the cell death from occurring in *dsh-2* mutants may significantly increase the incidence of PVQ duplications.

Table 6 PVQ duplications in *dsh-2(or302)* and *dsh-2(or302); ced-3(n717)* mutants.

Genotype	% Duplication	N
dsh-2(or302)/mIn1; oyIs14	2	116
dsh-2(or302)* (M+Z-); *oyIs14	3	88
dsh-2(or302)* (M-Z-); *oyIs14	10	98
oyIs14; ced-3(n717)	5	198
dsh-2(or302)/mIn1; ced-3(n717); oyIs14	11	132
dsh-2(or302)* (M+Z-); *ced-3(n717); oyIs14	33	79
dsh-2(or302)* (M-Z-); *ced-3(n717); oyIs14	50	102

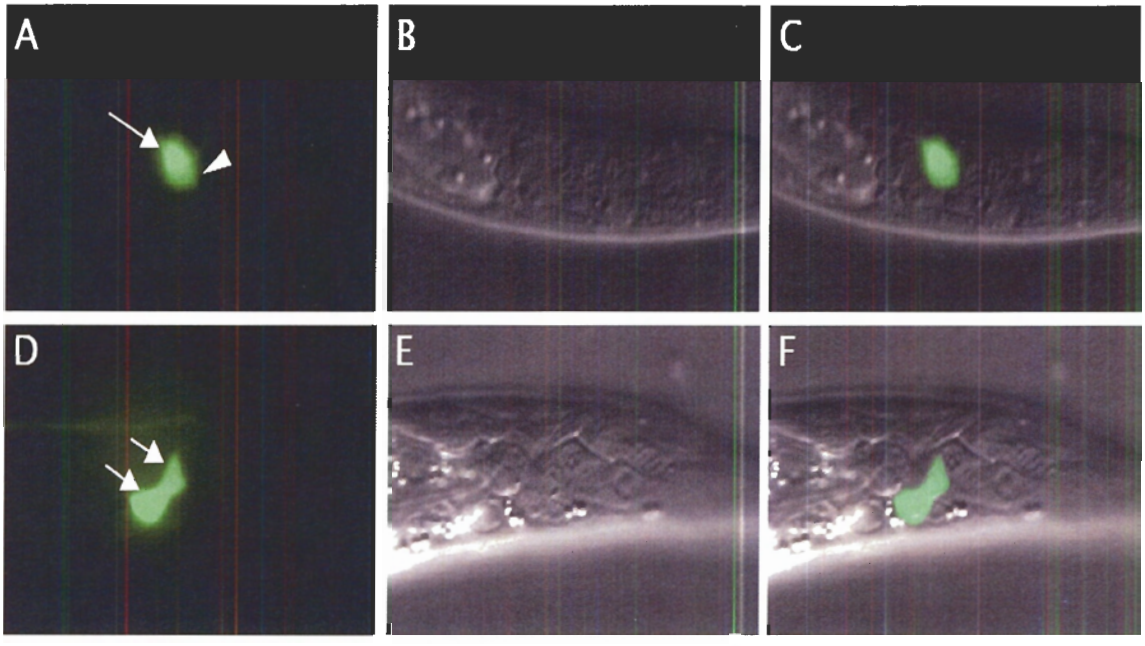

Figure 18 PVQ duplications in *dsh-2* mutants.

The integrated array *oyIs14[sra-6::gfp]* was used to visualize the PVQ neurons.
A-C: A wildtype larva. A) Epi-fluorescence micrograph showing endogenous GFP. One PVQ expresses *sra-6::gfp* (arrow); GFP from the other PVQ neuron is slightly out of focus (arrowhead). B) DIC image of the same animal in A. C) Merge of the GFP and DIC images.
D-F: A *dsh-2(or302)* (M+ Z-); *ced-3(n717)* mutant larva. D) Epi-fluorescence micrograph showing endogenous GFP. On the right side, two PVQ-like cells express *sra-6::gfp* (arrows). The PVQ neuron on the left side also expresses GFP. E) DIC of the same mutant animal. F) Merge of GFP and DIC images.

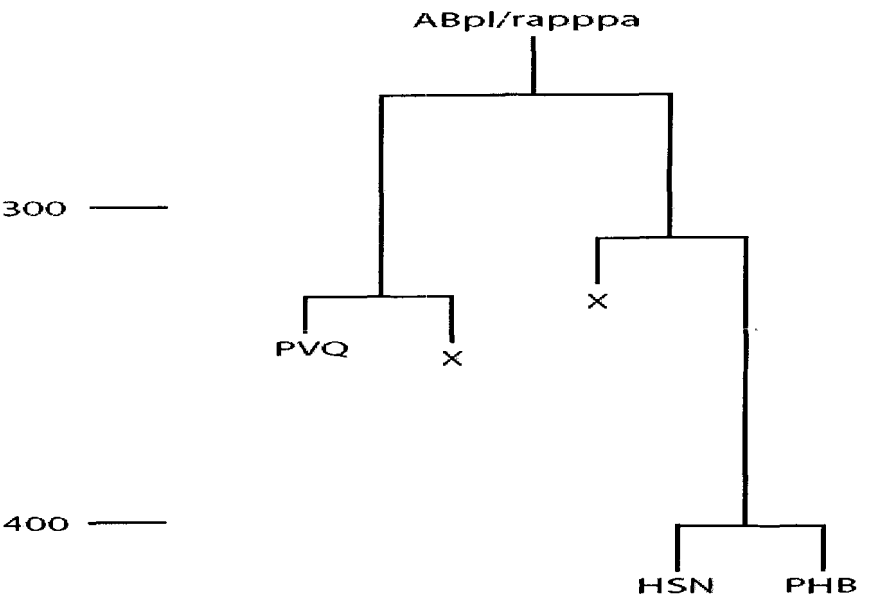

Figure 19 PVQ lineage diagram.

The ABpl/rapppa neuroblast divides asymmetrically at about 260 minutes. The anterior daughter divides to generate a PVQ neuron and a cell that undergoes apoptosis. The posterior daughter divides further to give rise to two neurons, HSN and PHB. The production of the HSN and PHB neurons are not affected in *dsh-2* mutants (Hawkins et al., 2005).

In wildtype, a total of 131 cells undergo apoptosis. Mutations in *ced-3,* a *C. elegans* caspase homolog, prevent all cell deaths from occurring. Therefore, we constructed *dsh-2; ced-3* double mutant strains that carried the PVQ-specific reporter *oyIs14[sra-6::gfp]*. In the *ced-3(n717)* background alone, PVQ duplications were observed at a low frequency of 5% (Table 6). *dsh-2(or302)/mIn1* animals have only one wildtype copy of *dsh-2*, and extra PVQs were observed at a slightly higher frequency of 11% when *ced-3* function was also lacking. In *dsh-2* (M+ Z-) mutants the penetrance of PVQ duplication was 3% and 33% with or without *ced-3* function, respectively. The absence of *ced-3* function also enhanced PVQ duplications from 10% to 50% in *dsh-2* (M- Z-) mutants, clearly indicating a synergistic effect between *dsh-2* and *ced-3* in the generation of PVQ neurons. Therefore, the PVQ duplications observed in *dsh-2* animals are likely due to a cell fate transformation of the PVQ sister cell.

3.3 Determining the temporal and spatial requirement of *dsh-2* function during ventral enclosure

dsh-2 mutants also have defects in ventral enclosure. We propose two models to explain this defect in morphogenesis. In the first model, ventral enclosure defects are a secondary consequence of earlier defects in asymmetric neuroblast divisions. Hypodermal cells migrate over a mixed population of neuroblasts, and the organization of the underlying neuroblasts has been shown to be essential for the migration of the hypodermal cells (George et al., 1998; Chin-Sang et al., 1999). In the second model, in addition to a role in regulating cell division, *dsh-2* function is independently required in the hypodermal cells, possibly for their polarization and migration. Therefore, to distinguish between these two models, I generated transgenic animals that specifically

expressed *dsh-2* either in hypodermal or neuronal cells. Rescue of lethality in *dsh-2* (M-Z-) mutant embryos was then examined.

In addition to assaying for rescue of *dsh-2* lethality, rescue of PHA duplications were also determined. To visualize the PHA neuron, the phasmid neuron-specific reporter *srb-6::gfp* was used as a co-injection marker in the generation transgenic animals. The *srb-6::gfp* plasmid expresses GFP in the PHA and PHB phasmid neurons. In animals carrying integrated arrays of *srb-6::gfp*, two cells express GFP on each side of the tail. In *dsh-2* mutants, three GFP-expressing cells are often observed due to duplication of the PHA neuron (Hawkins et al., 2005). However, when the *srb-6::gfp* plasmid is injected and contained in an extrachromosomal array, some degree of mitotic loss occurs during development, resulting in mosaicism. Therefore, the number of cells that express GFP may be an underestimation of the actual number of phasmid neurons.

To facilitate the assays for rescue of embryonic lethality and PHA duplications in *dsh-2* animals, all constructs were injected directly into *dsh-2(or302)/mIn1* hermaphrodites. In some cases, an extrachromosomal array was stably integrated into the genome to alleviate the problem of mosaicism. Before integration, the extrachromosomal array was first crossed into the N2 background. Once integrated lines were obtained, the *dsh-2(or302)* mutation was crossed back in for subsequent analysis.

3.3.1 DSH-2 expression in hypodermal cells failed to rescue *dsh-2* lethality

To express *dsh-2* specifically in hypodermal cells, we chose the *lin-26* promoter. The LIN-26 protein specifies hypodermal fate (Labouesse et al., 1994). Expression of the protein has been reported to begin in the 100-cell embryo, and a promoter::GFP fusion containing a 4 kb promoter fragment of *lin-26* is expressed in hypodermal cells before the

onset of ventral enclosure (Landmann et al., 2004). Thus, this 4 kb *lin-26* promoter fragment was used to construct the *lin-26p-dsh-2::gfp* plasmid.

To test for its ability to rescue *dsh-2* lethality, the construct was first injected into *dsh-2(or302)/mIn1* hermaphrodites at 5 ng/ul, and four independent lines were obtained. To investigate if the transgene can rescue embryonic lethality of M-Z- *dsh-2* mutants, the hatch rate of embryos laid by *dsh-2* (M+ Z-) transgenic animals was determined. However, no significant rescue of lethality was observed. Embryos lacking both maternal and zygotic *dsh-2* activity hatched 23% of the time, while the hatch rate of *dsh-2* (M+ Z-) animals expressing DSH-2 from the *lin-26* promoter was 31% (Table 7, *hkEx25*). Normally, *dsh-2* mutants cannot be maintained as a homozygote unless a rescuing array is present (Hawkins et al., 2005). *dsh-2* mutant animals carrying the *lin-26-dsh-2::gfp* extrachromosomal array at this low concentration also fail to maintain themselves as homozygotes. To determine if increasing the amount of transgene could lead to better rescue, the *lin-26p-dsh-2::gfp* construct was injected at a higher concentration of 20 ng/ul, and two lines were obtained. Again, rescue of *dsh-2* lethality was not observed as transgenic *dsh-2* mutants from either line were still unable to be maintained as homozygotes. A small percentage of *dsh-2(or302)/mIn1* animals carrying the *lin-26p-dsh-2::gfp* construct at 20 ng/ul showed major morphological defects (Figure 20). We predicted that injecting the plasmid at higher concentrations would lead to lethality and thus was not attempted.

The *lin-26p-dsh-2::gfp* transgenes are maintained as extrachromosomal arrays in the transgenic animals. A large population of hypodermal cells may require *dsh-2* function to undergo proper embryogenesis and ventral enclosure. However, mosaic

Table 7 Rescue of *dsh-2* lethality by extrachromosomal arrays expressing DSH-2 with either the *unc-119, lin-26,* or *F25B3.3* promoter.

Parental Genotype	% Hatch	N
dsh-2(or302)/mIn1	**98**	**615**
dsh-2(or302)/mIn1; hkEx20 [a] [unc-119p-dsh-2::gfp]	**n.d.**	**n.d.**
dsh-2(or302)/mIn1; hkEx21 [a] [unc-119p-dsh-2::gfp]	**n.d.**	**n.d.**
dsh-2(or302)/mIn1; hkEx22 [a] [unc-119p-dsh-2::gfp]	**93**	**264**
dsh-2(or302)/mIn1; hkEx31 [b] [unc-119p-dsh-2::gfp]	**96**	**274**
dsh-2(or302)/mIn1; hkEx25 [c] [lin-26p-dsh-2::gfp]	**96**	**196**
***dsh-2(or302)* (M+ Z-)**	**23**	**866**
dsh-2(or302)* (M+ Z-); *hkEx20 [a] [unc-119p-dsh-2::gfp]	**53**	**1412**
dsh-2(or302)* (M+ Z-); *hkEx21 [a] [unc-119p-dsh-2::gfp]	**38**	**790**
dsh-2(or302)* (M+ Z-); *hkEx22 [a] [unc-119p-dsh-2::gfp]	**51**	**1122**
dsh-2(or302)* (M+ Z-); *hkEx31 [b] [unc-119p-dsh-2::gfp]	**41**	**745**
dsh-2(or302)* (M+ Z-); *hkEx25 [c] [lin-26p-dsh-2::gfp]	**31**	**348**
dsh-2(or302)* (M+ Z-); *hkEx80 [d] [F25B3.3p-dsh-2::gfp]	**30**	**89**

n.d. = not determined

[a] construct injected at 20 ng/ul

[b] construct injected at 50 ng/ul

[c] construct injected at 5 ng/ul

[d] construct injected at 50 ng/ul

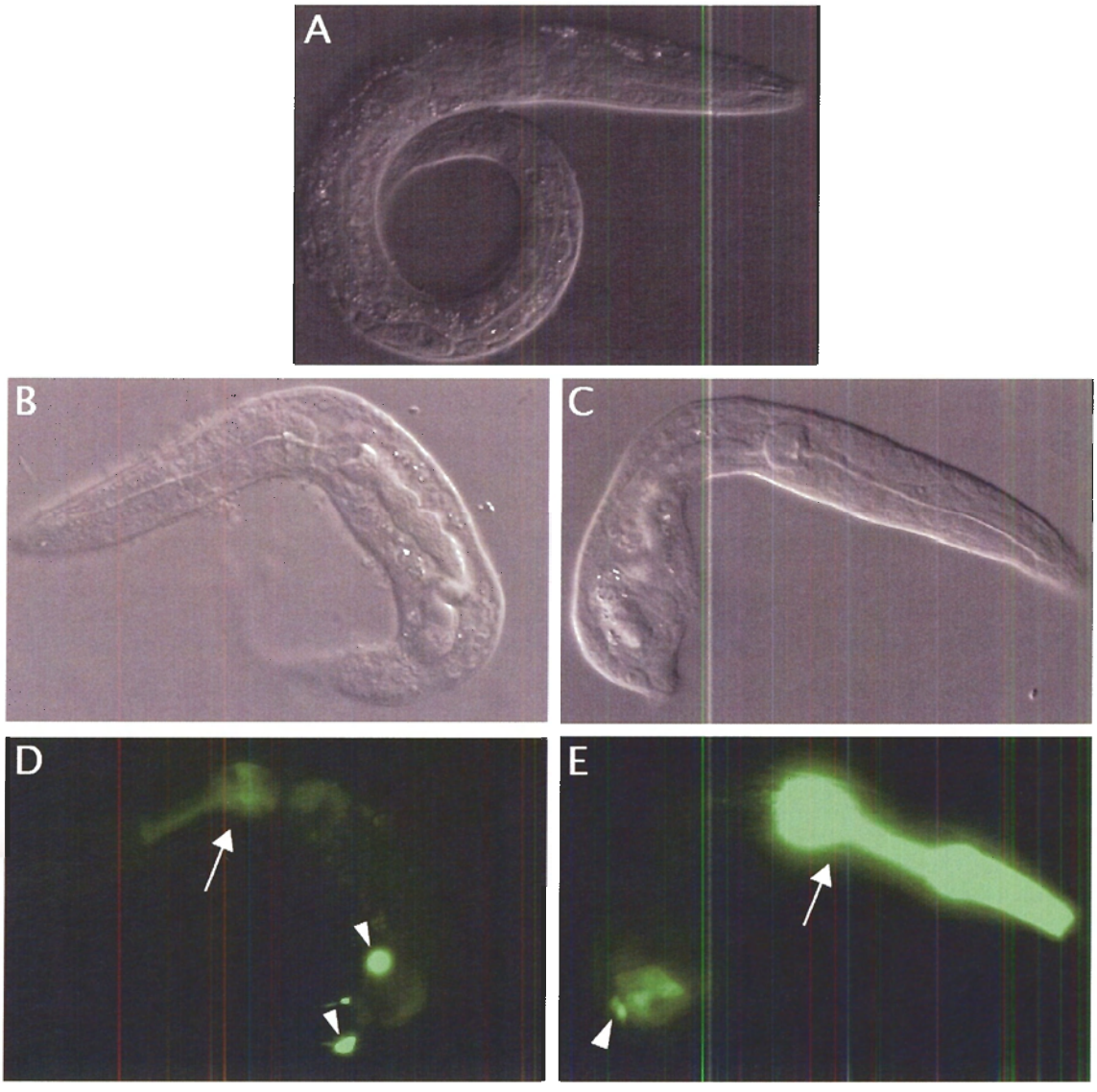

Figure 20 High copies of *unc-119p-dsh-2::gfp* and *lin-26p-dsh-2::gfp* cause morphological defects in *dsh-2(or302)/mIn1* animals.

A: DIC image showing morphology of a wildtype larva.
B and D: A *dsh-2/mIn1; hkEx29* animal carrying *unc-119p-dsh-2::gfp* at 100 ng/ul. B) Although morphology of the head appears normal, the body and the tail are severely deformed. Similar morphological defects were also observed when the construct was injected at lower concentrations 20 ng/ul and 50 ng/ul. D) Expression of *srb-6::gfp* (arrowheads) and pharyngeal GFP (arrow) shows that the animal carries the transgene as well as the *mIn1* balancer.
C and E: A *dsh-2/mIn1; hkEx27*animal carrying *lin-26p-dsh-2::gfp* at 20 ng/ul. C) Morphology of the tail is severely affected. E) Expression of *srb-6::gfp* (arrowhead) and pharyngeal GFP (arrow) shows that the animal carries both the transgene and the *mIn1* balancer.

inheritance of the extrachromosomal array may result in only a subset of those cells inheriting it. Therefore, the apparent inability of the *lin-26p::dsh-2::gfp* construct to rescue *dsh-2* lethality could be due to mosaicism. To bypass this problem, a transgenic line with the construct injected at 5 ng/ul (*hkEx25*) and a second carrying the construct at 20 ng/ul (*hkEx27*) were stably integrated into the genome via X-ray irradiation. Four integrated lines were obtained with the construct injected at 5 ng/ul and eight integrated lines obtained at the 20 ng/ul concentration. One representative line from each of the concentrations was further examined for rescue of *dsh-2* lethality. However, no significant rescue was observed even after integration (Table 8, *hkIs2* and *hkIs14*). These results indicate that DSH-2 expressed by the *lin-26p* is insufficient to rescue maternal effect embryonic lethality of *dsh-2* mutants.

3.3.2 PHA duplications were also not rescued by hypodermal DSH-2 expression

The *lin-26p::dsh-2::gfp* construct was also tested for its ability to rescue PHA neuronal duplications in *dsh-2* mutants. To determine the number of phasmid neurons in transgenic animals, we counted the number of cells expressing the phasmid neuron reporter *srb-6::gfp*. As expected for a hypodermal promoter, the two integrated lines *hkIs2* and *hkIs11* showed no significant rescue of PHA duplications (Table 9).

3.3.3 DSH-2 protein expressed under the *lin-26* promoter is expressed and properly localized prior to ventral enclosure

Next, we analyzed the expression and localization pattern of DSH-2::GFP expressed under control of the *lin-26* promoter. The *lin-26p-dsh-2::gfp* construct may not rescue *dsh-2* lethality because the resultant transgene is not expressed early enough to rescue ventral enclosure defects. In contrast, the exogenous protein may not be functional

Table 8 Rescue of *dsh-2* lethality by integrated *unc-119p-dsh-2::gfp* or *lin-26p-dsh-2::gfp* arrays.

Parental Genotype	% Hatch	N
dsh-2(or302)/mIn1; gmIs12[srb-6::gfp] [a]	98	299
dsh-2(or302)/mIn1; hkIs8[unc-119p-dsh-2::gfp] [b]	85	470
dsh-2(or302)/mIn1; hkIs2[lin-26p-dsh-2::gfp] [c]	97	273
dsh-2(or302)/mIn1; hkIs14[lin-26p-dsh-2::gfp] [d]	94	151
dsh-2(or302)* (M+ Z-); *gmIs12[srb-6::gfp] [a]	23	220
dsh-2(or302)* (M+ Z-); *hkIs8[unc-119p-dsh-2::gfp] [b]	65	499
dsh-2(or302)* (M+ Z-); *hkIs2[lin-26p-dsh-2::gfp] [c]	21	450
dsh-2(or302)* (M+ Z-); *hkIs14[lin-26p-dsh-2::gfp] [d]	17	290

[a] *gmIs12* = integrated *srb-6::gfp*
[b] *hkIs8* = integrated *hkEx22* (construct injected at 20 ng/ul)
[c] *hkIs2* = integrated *hkEx25* (construct injected at 5 ng/ul)
[d] *hkIs14* = integrated *hkEx27* (construct injected at 20 ng/ul)

Table 9 Rescue of PHA duplications by *lin-26p-dsh-2::gfp* and *unc-119p-dsh-2::gfp*.

	# phasmid neurons / side				
Genotype	**0 (%)**	**1 (%)**	**2 (%)**	**3 (%)**	**N**
dsh-2(or302)* (M- Z-); *gmIs12[srb-6::gfp] [a]	2	5	69	24	148
dsh-2(or302)* (M- Z-); *hkIs2[lin-26p-dsh-2::gfp] [b]	0	6	76	17	144
dsh-2(or302)* (M- Z-); *hkIs11[lin-26p-dsh-2::gfp] [c]	0	13	71	15	150
dsh-2(or302)* (M- Z-); *hkEx22[unc-119p-dsh-2::gfp] [d]	3	20	72	6	123
dsh-2(or302)* (M- Z-); *hkIs8[unc-119p-dsh-2::gfp] [e]	0	< 1	98	2	121

[a] integrated *srb-6::gfp*
[b] construct injected at 5 ng/ul
[c] construct injected at 20 ng/ul
[d] construct injected at 20 ng/ul
[e] construct injected at 20 ng/µl

due to its mislocalization. To determine the temporal and spatial expression pattern of the construct, embryos carrying the integrated transgene *hkIs1* were collected and stained with anti-GFP antibodies. The embryos were co-stained with the monoclonal antibody MH27. This antibody is specific for AJM-1, an adherens junction protein (Francis and Waterston, 1991). Expression of AJM-1 begins when hypodermal cells are first born, and its expression is maintained throughout development. Therefore, staining embryos with MH27 demarcates the hypodermal cells prior to and during ventral enclosure. When the stained embryos were examined, cells that expressed DSH-2::GFP also expressed AJM-1. Thus, we concluded that DSH-2::GFP was expressed in hypodermal cells before, during, and after ventral enclosure (Figure 21). In addition, the protein was found at the membrane, which correlates with endogenous DSH-2 localization (Hawkins et al., 2005).

3.3.4 Expression of *dsh-2* under the *unc-119* promoter partially rescued *dsh-2* lethality

To express *dsh-2* specifically in neuroblasts, an *unc-119p-dsh-2::gfp* construct previously made in the lab by Amy Leung was used to generate transgenic animals. It is an ideal promoter because UNC-119 expression is detected at the 60-cell stage of embryogenesis and remains active in neuronal lineages (Maduro and Pilgrim, 1995). To determine if neuronal-specific *dsh-2* expression can rescue *dsh-2* embryonic lethality, the construct was first injected into *dsh-2(or302)/mIn1* hermaphrodites at 5 ng/ul. Three independent lines were obtained. As described above, only 20% of *dsh-2* (M- Z-) embryos hatch, and *dsh-2* mutants cannot be maintained as homozygotes. However, *dsh-2* mutants carrying one of the three transgenes could be maintained as a homozygote due to the transgenes at least partially rescuing lethality. Because the degree of rescue was

Figure 21 *lin-26p-dsh-2::gfp* is expressed in hypodermal cells.

Embryos carrying the array *hkIs1* (*lin-26-dsh-2::gfp*) were co-stained with α-GFP antibodies (to visualize DSH-2::GFP, panels A and B) and the monoclonal MH27 antibody (to mark the hypodermal cells, panels C and D). Anterior is to the left.
A, C, E, G: Dorsal view of an embryo before ventral enclosure. A) DSH-2::GFP is primarily membrane-associated. C) Hypodermal cells have started dorsal intercalation and are becoming wedge-shaped. E) Merge shows that DSH-2::GFP is expressed in hypodermal cells. G) Enlarged view of the boxed region in panel E.
B, D, F, H: Ventral view of an embryo at the end of ventral enclosure. B)DSH-2::GFP is primarily localized to the membrane. D) Majority of the hypodermal cells have met at the ventral midline. F) A merge of shows that DSH-2::GFP is expressed in hypodermal cells. H) Enlarged view of boxed region in F.

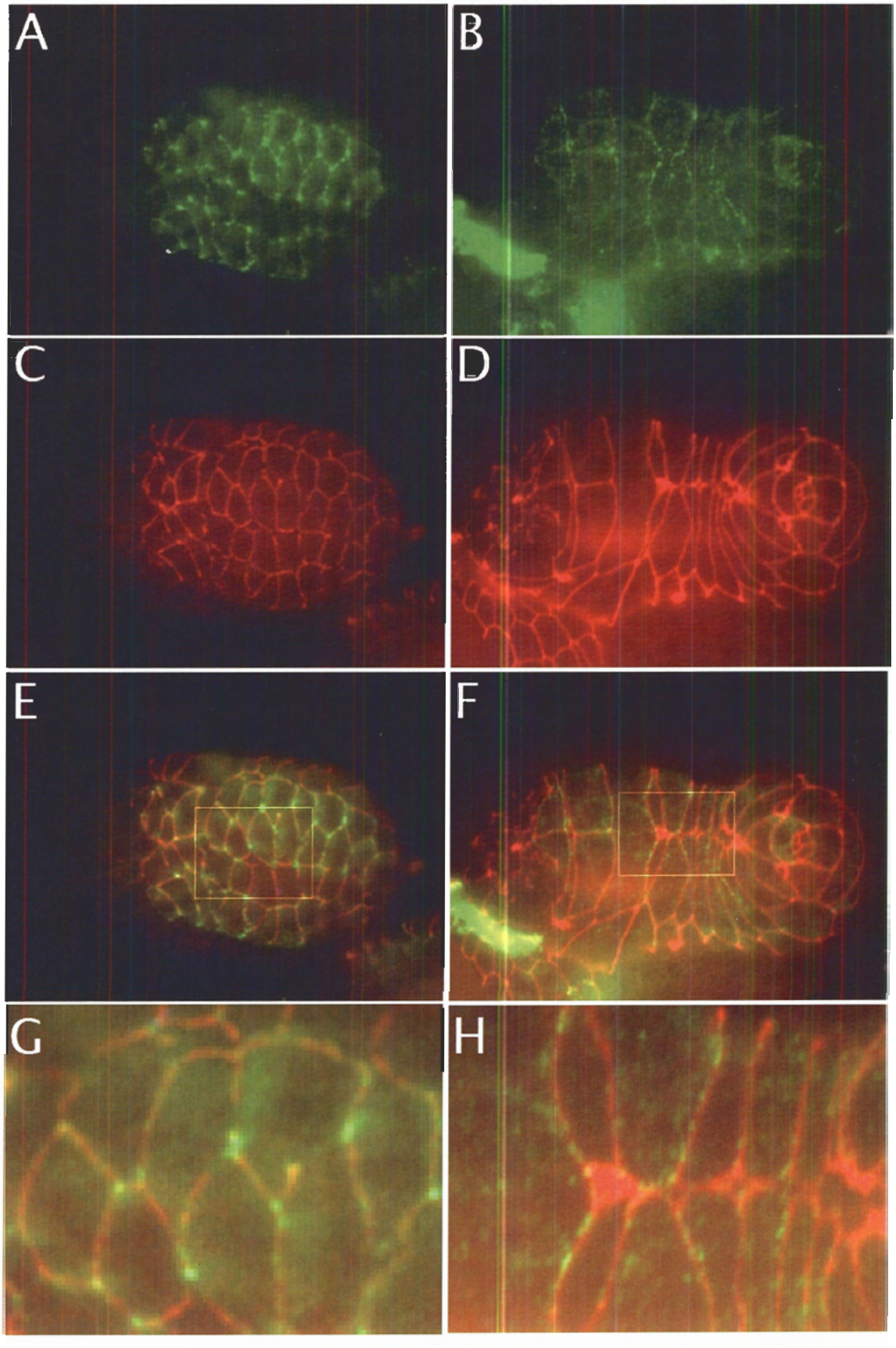
A
B
C
D
E
F
G
H

weak when the *unc-119p-dsh-2::gfp* construct was injected at 5 ng/ul, the construct was re-injected at a higher concentration of 20 ng/ul. Three independent lines were obtained, and all three lines were also capable of maintaining *dsh-2(or302)* mutants as a homozygote. Thus, we could conclude that the transgenes must be partially rescuing *dsh-2* lethality.

We then quantified the hatch rate of *dsh-2* (M- Z-) mutant embryos for the three lines. Respectively, the hatch rates were 53%, 38%, and 51% (Table 7, *hkEx20, hkEx21,* and *hkEx22*), a significant rescue compared to 23% for non-transgenic *dsh-2* (M- Z-) mutants. Because the rescue was incomplete, the construct was injected at higher concentrations of 50 and 100 ng/ul. Two lines were obtained at 50 ng/ul, but rescue of embryonic lethality did not improve as the hatch rate of embryos produced by transgenic *dsh-2* (M+ Z-) mutants was 41% (Table 7, *hkEx31*). One line at 100 ng/ul was also obtained, but the construct caused high lethality in transgenic animals, thus rescue of *dsh-2* lethality was not determined. Similar to the *lin-26p-dsh-2* construct at 20 ng/ul, the *unc-119::dsh-2* construct injected at concentrations higher than 5 ng/ul resulted in morphological defects in *dsh-2(or302)/mIn1* animals (Figure 20).

While it is evident that expressing DSH-2 under control of the *unc-119* promoter significantly improved the hatch rates of *dsh-2* (M- Z-) embryos from 20% to 52%, this rescue is likely an underestimate due to mosaic inheritance of the extrachromosomal array (described above). To more accurately quantify the rescuing ability of the *unc-119p-dsh-2* construct, a transgenic line carrying the construct at 20 ng/ul (*hkEx22*) was stably integrated into the genome by X-ray irradiation. Five independent lines were obtained, and one line was further examined for rescue of *dsh-2* lethality. Upon

integration, 65% of *dsh-2* (M- Z-) embryos hatched compared to only 24% in the control group (Table 8, *hkIs8*). Similar to the extrachromosomal *unc-119p-dsh-2::gfp* arrays, *dsh-2* mutants carrying the integrated array were also able to be maintained as homozygotes. Taken together, these results suggest that expression of *dsh-2* in neuronal lineages is able to partially rescue *dsh-2* maternal effect embryonic lethality.

3.3.5 DSH-2 expressed under the *unc-119* promoter rescued PHA duplications

After observing rescue of *dsh-2* lethality, we next determined if PHA duplications were also rescued by the *unc-119p-dsh-2::gfp* construct. To determine if *dsh-2* expressed under the *unc-119* promoter can rescue PHA duplications, the number of cells expressing the co-injection marker *srb-6::gfp* was examined in *dsh-2* mutants that carried the construct at 20 ng/ul. PHA duplications occur at a frequency of about 22% in *dsh-2* (M-Z-) mutants. Significant rescue was observed as PHA duplications were only seen at 6% in *dsh-2* (M- Z-) mutants (Table 9, *hkEx25*). After integration of the extrachromosomal array, the number of phasmid neurons was again examined. PHA duplications were further reduced to 2% (Table 9, *hkIs8*). Therefore, expression of *dsh-2* with the *unc-119* promoter resulted in almost complete rescue of PHA duplications in *dsh-2* mutants.

3.3.6 DSH-2 expressed under the *unc-119* promoter is not restricted to neuronal lineages

To examine the expression pattern of the DSH-2::GFP protein, embryos carrying the *hkIs5* integrated array were collected and stained with anti-GFP antibody. The embryos were also stained with the monoclonal antibody MH27 to identify the hypodermal cells. As expected, DSH-2::GFP was found to associate closely with the membrane. Surprisingly, some cells that stained with GFP also stained with MH27. This

indicated that the DSH-2::GFP was not only expressed in neuroblasts but also in hypodermal cells during ventral enclosure (Figure 22). Expression of DSH-2::GFP was also observed post-embryonically in the head, possibly in the hypodermis (Figure 23). Therefore, the *unc-119* promoter is not completely specific to neuronal lineages. More importantly, even though the *unc-119p-dsh-2::gfp* construct rescued *dsh-2* maternal effect lethality, we cannot rule out the possibility that this rescue is due to expression of *dsh-2* in both neuroblasts and hypodermal cells.

3.3.7 Expressing *dsh-2* with *F25B3.3p*, a second neural-specific promoter, did not rescue *dsh-2* lethality

By using either *lin-26* or *unc-119* promoter, I hoped to determine if specifically expressing *dsh-2* in the hypodermis or neuroblasts could rescue ventral enclosure defects in *dsh-2* mutants. Using the *lin-26* promoter, it was evident that *dsh-2* expression in the hypodermis alone is not sufficient to rescue *dsh-2* lethality. Although rescue was observed when using the *unc-119p*, we discovered that the promoter was found to be active in both neuronal and hypodermal cells. Therefore, we could not unambiguously determine if *dsh-2* function exclusively in neuroblasts is sufficient for proper ventral enclosure.

To further examine this question, a second neural-specific promoter from the *F25B3.3* gene was utilized. This gene is a homolog of a *ras* nucleotide exchange factor that is expressed in the vertebrate nervous system (Ebinu et al., 1998), and the promoter has been previously used as a neurons-specific marker (Gilleard and McGhee, 2001). To generate a *F25B3.3p-dsh-2::gfp* translational fusion, stitching PCR was performed. The PCR product was initially injected at 20 ng/ul, and three lines were obtained. No rescue

Figure 22 *unc-119p-dsh-2::gfp* is expressed in both neuronal and hypodermal lineages.

Embryos carrying the array *hkIs5* (*unc-119p-dsh-2::gfp*) were co-stained with α-GFP antibodies to visualize DSH-2::GFP (in panels A and B) and the monoclonal MH27 antibody to mark the hypodermal cells (panels C and D). Anterior is to the left.
A, C, E, G: Dorsal view of an embryo before ventral enclosure. A) DSH-2::GFP is primarily membrane-associated. C) Hypodermal cells have just been born and start to stain for MH27. E) A merge shows that DSH-2::GFP is expressed in some cells that are also MH27-positive. G) Enlarged view of the boxed region from panel E. Some cells expressing DSH-2::GFP were not stained by MH27 (arrow), indicating that they are neuroblasts. Conversely, some cells are also MH27-positive (arrowhead), indicating that they are hypodermal cells.
B, D, F, H: Ventral view of an embryo at the end of ventral enclosure. B) DSH-2::GFP is primarily localized to the membrane. D) The hypodermal cells have met at the ventral midline to close the ventral hole. F) A merge of shows that DSH-2::GFP, in addition to being expressed in neuroblasts, is also expressed in hypodermal cells. H) Enlargement of the boxed region from panel F. Arrow shows a neuroblast beneath the hypodermal cells that expressed DSH-2::GFP; arrowhead shows expression of DSH-2::GFP in a hypodermal cell.

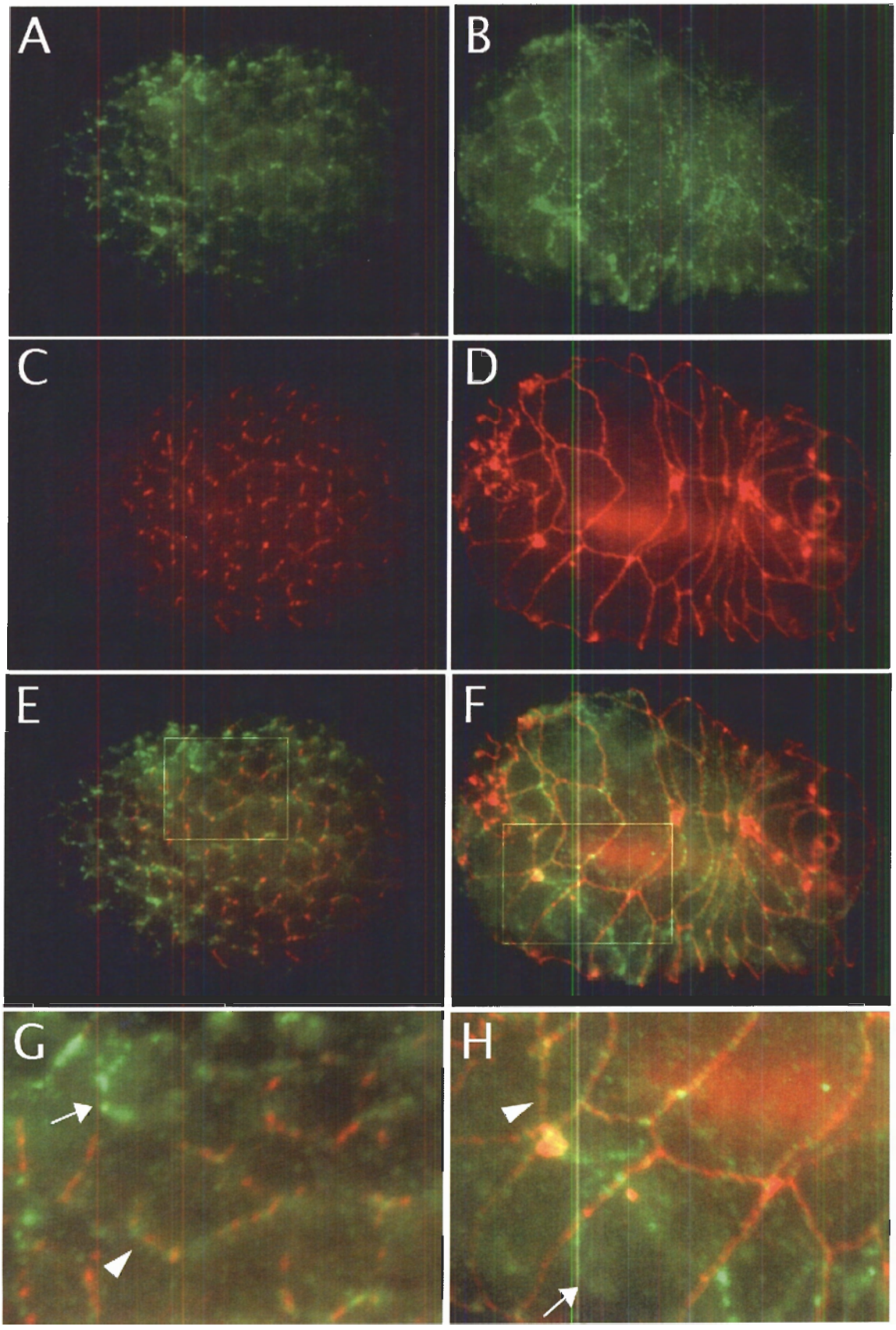
A
B
C
D
E
F
G
H

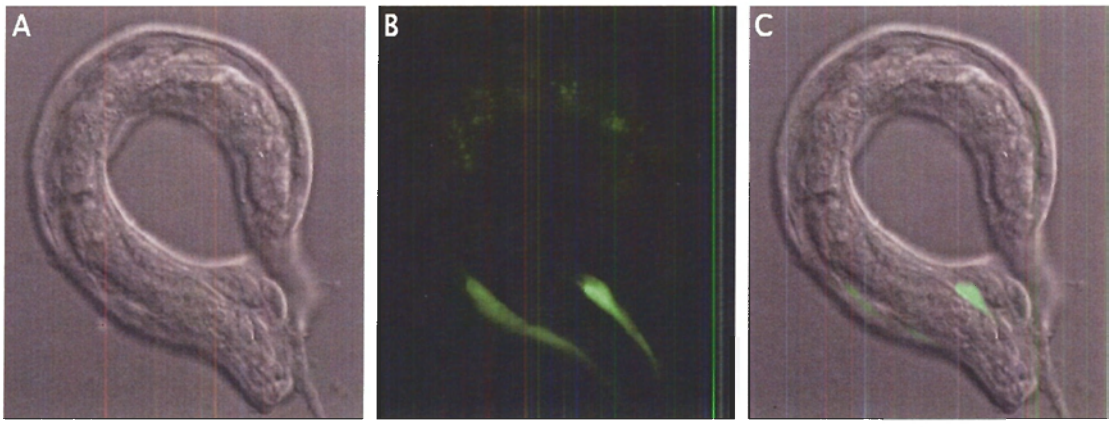

Figure 23 Expression of *unc-119p-dsh-2::gfp* in non-neuronal cells of larva.

A *dsh-2* (M- Z-) mutant larva expressing *hkEx22* (*unc-119p-dsh-2::gfp* injected at 20 ng/ul). Panel A shows the DIC image of the animal. In panel B, GFP is expressed in the head, potentially in the hypodermis. Panel C is the merge of panels A and B.

of *dsh-2* lethality was observed as *dsh-2* homozygotes containing the extrachromosomal arrays could not be maintained. Instead of quantifying the hatch rate of these transgenics, the construct was immediately re-injected at 50 ng/ul. Seven lines were obtained, but none achieved significant rescue of embryonic lethality: transgenic *dsh-2* homozygotes were unable to maintain themselves. The hatch rate of *dsh-2* mutants was determined for one line and was found to be 30%, further supporting the lack of significant rescue (Table 7, *hkEx80*).

3.3.8 The *F25B3.3* promoter was unable to express *dsh-2* before or during ventral enclosure

The expression pattern of DSH-2::GFP under the *F25B3.3* promoter was then examined. The transgene may not be expressed early enough in neuroblasts before ventral enclosure, resulting in failure to rescue *dsh-2* embryonic lethality. To determine if the *F25B3.3p-dsh-2::gfp* construct is expressed early enough, embryos from gravid hermaphrodites carrying the *hkEx80* array were collected and stained with anti-GFP antibodies. Again, the embryos were stained with MH27 to mark the hypodermal cells during ventral enclosure. As shown in Figure 24, DSH-2::GFP is expressed in neurons of larvae and embryos that have completed ventral enclosure. However, the first detectable expression of GFP was in embryos at the end of ventral enclosure as indicated by MH27 staining. Therefore, the *F25B3.3* promoter is unable to express *dsh-2* in neuronal cells early enough to possibly rescue *dsh-2* ventral enclosure defects.

3.4 Domain analysis of *dsh-2*

There is a differential requirement for the three conserved domains of Dsh in different signalling pathways. The DIX domain is required for the canonical Wnt

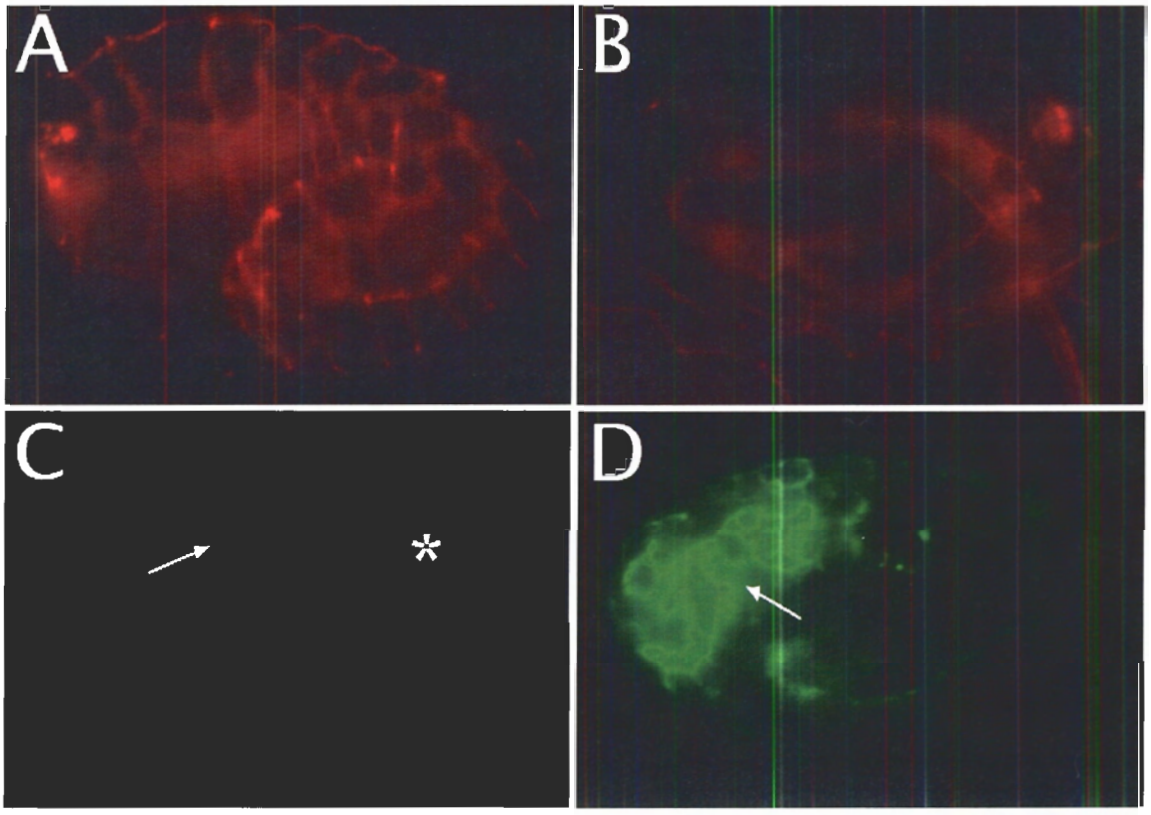

Figure 3 *F25B3.3p-dsh-2::gfp* is not expressed early enough in neuroblasts.

Embryos from *dsh-2(or302)/mIn1; hkEx80* (*F25B3.3p-dsh-2::gfp* injected at 50 ng/ul) animals were collected and co-stained with α-GFP antibodies to visualize DSH-2::GFP (panels C and D) and MH27 antibodies to outline the hypodermal cells (panels A and B). Anterior is to the left and ventral side down.

A and C: A *dsh-2(or302)/mIn1; hkEx80* embryo. A) MH27 staining pattern. The embryo has completed ventral enclosure and has started to elongate. **C) Some neuronal cells in** the head express faint DSH-2::GFP (arrow). Signal more posterior to these cells is from out-of-focus gut GFP expressed from the *mIn1* balancer chromosome (star).

B and D: A *dsh-2(or302)/dsh-2(or302); hkEx80* embryo. B) MH27 staining pattern. The embryo has elongated to the 2 ½ fold stage. D) DSH-2::GFP is strongly expressed in many neurons in the head (arrow).

signalling pathway while the DEP domain is essential for the PCP pathway. Mutants lacking *dsh-2* function have defects in asymmetric cell division and ventral enclosure. However, it is unclear which signalling pathway(s) *dsh-2* activates to regulate these two processes. To address this question, two *dsh-2::gfp* deletion constructs were obtained (T. Walston and J. Hardin, University of Wisconsin, Madison; Figure 25). Both constructs were placed under the control of the endogenous *dsh-2* promoter. The first construct is missing amino acid 101 to 185 in the DSH-2 protein and thus lacks the entire DIX domain (ΔDIX). The second construct removes amino acid 535 to 609 of DSH-2, thereby lacking all but 23 amino acids in the DEP domain (Δ*EP). These two constructs were used to generate transgenic animals and assayed for rescue of embryonic lethality and PHA duplications in *dsh-2* mutants.

3.4.1 Δ*EP *dsh-2* failed to rescue embryonic lethality in *dsh-2* mutants

The Δ*EP *dsh-2* construct was injected at increasing concentrations and tested for rescue of *dsh-2* lethality. Initially, the Δ*EP *dsh-2* construct was injected at 0.5 ng/ul, and three transgenic lines were obtained. At this concentration, no rescue of *dsh-2* embryonic lethality was observed since the *dsh-2* mutant was not maintainable as a homozygote. These transgenic animals carry the constructs as extrachromosomal arrays. As described above, the apparent inability to rescue *dsh-2* lethality may be attributed to mosaicism of the array. Therefore, one transgenic line carrying the array *hkEx39* was integrated into the genome via X-ray irradiation, and five independent lines were obtained. The line *hkIs25* was examined for its ability to rescue *dsh-2* embryonic lethality. Rescue of embryonic lethality was still not observed as transgenic *dsh-2* animals could not maintained as

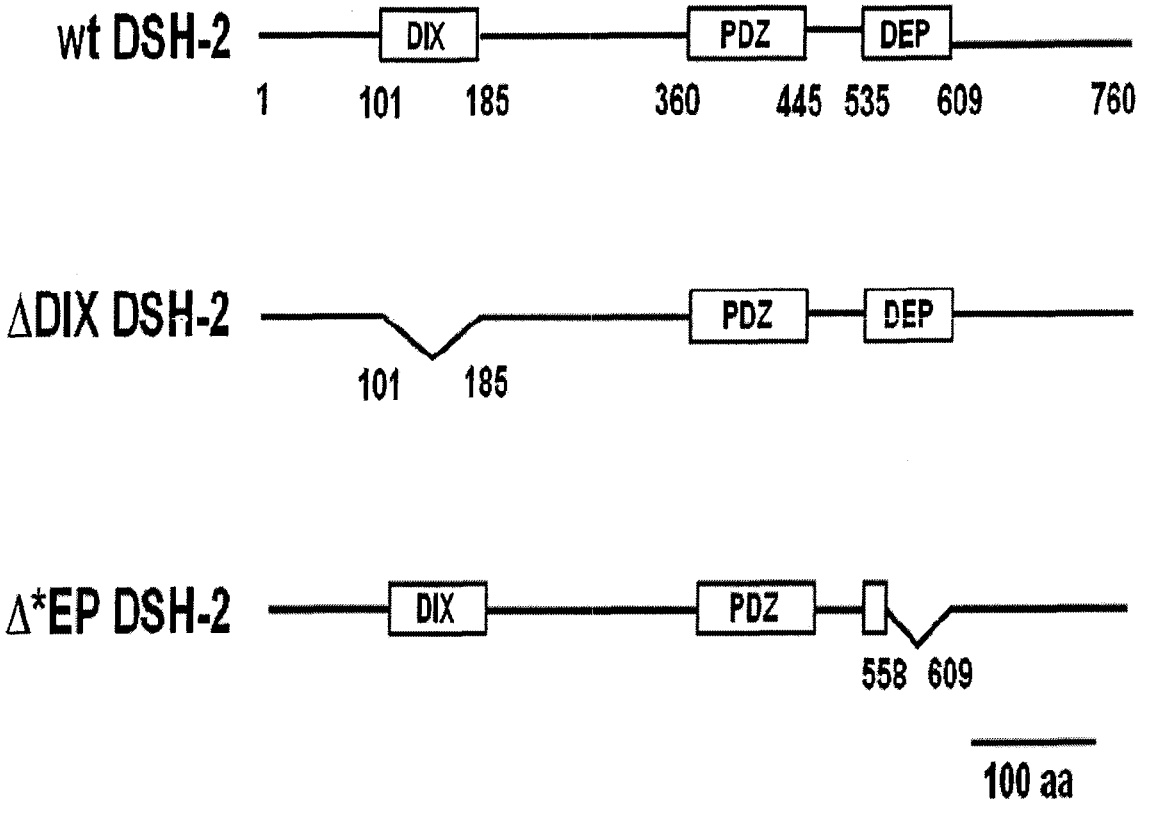

Figure 25 Schematic of DSH-2 truncations.

Wildtype DSH-2 is shown at the top. The DIX, PDZ, and DEP domains are shown, with numbers underneath indicating the amino acid positions of the respective domains. Both truncations are fused in-frame with GFP at the C-terminus and expressed under control of the endogenous *dsh-2* promoter. Amino acid 101-185 is deleted in ΔDIX DSH-2::GFP, removing the entire DIX domain. Amino acid 558-609 is deleted in Δ*EP DSH-2::GFP, removing the majority of the DEP domain.

homozygotes. Therefore, at a low concentration, the Δ*EP *dsh-2* construct was unable to rescue *dsh-2* maternal effect embryonic lethality.

To determine if injecting the Δ*EP *dsh-2* construct at a higher concentration could rescue *dsh-2* lethality, the plasmid was injected at 2.5 ng/ul. Nine transgenic lines were obtained, but none showed rescue of *dsh-2* lethality as determined by their inability to maintain a *dsh-2* homozygote mutant strain. Hatch rates of *dsh-2* (M- Z-) embryos were quantified for three lines to be 28%, 18%, and 23% of the time, respectively (Table 10, *hkEx54, hkEx57,* and *hkEx61*), further supporting the lack of *dsh-2* lethality rescue. When the construct was injected at 10 ng/ul, no lines were obtained. One explanation could be that high concentrations of the construct caused lethality. Taken together, the DEP domain of *dsh-2* appears to be essential for ventral enclosure.

3.4.2 Δ*EP *dsh-2* also failed to rescue PHA neuronal duplications

Next, the Δ*EP *dsh-2* construct was assayed for its ability to rescue PHA neuronal duplications in *dsh-2* mutants. First, transgenic lines obtained at the injection concentration of 0.5 ng/ul were analyzed. Since the *srb-6::gfp* phasmid neuron-specific reporter was used as a co-injection marker, the number of phasmid neurons could be immediately determined. As shown in Table 11 (*hkEx39*), Δ*EP *dsh-2* did not appear to rescue duplications of the PHA neuron. Transgenic *dsh-2* (M- Z-) mutants have an extra phasmid neuron 16% of the time as compared to 24% in control *dsh-2* (M- Z-) animals. Since the phasmid neurons marker was present as part of the extrachromosomal array, the 16% PHA neuronal duplication is likely an underestimation due to mosaicism. Therefore, the Δ*EP *dsh-2* construct showed no apparent rescue of PHA duplications. To alleviate

Table 10 Rescue of *dsh-2* lethality by Δ*EP DSH-2::GFP and ΔDIX DSH-2::GFP.

Parental Genotype	% hatch	N
***dsh-2(or302)* (M+ Z-)**	**23**	**866**
dsh-2(or302)* (M+ Z-); *hkEx54* [a] *[Δ*EP dsh-2::gfp]	**28**	**115**
dsh-2(or302)* (M+ Z-); *hkEx57* [a] *[Δ*EP dsh-2::gfp]	**18**	**186**
dsh-2(or302)* (M+ Z-); *hkEx61* [a] *[Δ*EP dsh-2::gfp]	**23**	**221**
dsh-2(or302)* (M+ Z-); *hkEx52* [b] *[ΔDIX dsh-2::gfp]	**41**	**83**

[a] construct injected at 2.5 ng/ul
[b] construct injected at 2.5 ng/ul

Table 11 Rescue of phasmid neuron duplications in transgenic animals carrying Δ*EP DSH-2::GFP or ΔDIX *dsh-2::gfp*::GFP arrays.

	# phasmid neurons / side				
Genotype	**0 (%)**	**1 (%)**	**2 (%)**	**3 (%)**	**N**
dsh-2(or302)/mln1; gmIs12[srb-6::gfp]	0	0	100	0	134
dsh-2(or302)/mln1; hkEx39[Δ*EP dsh-2::gfp] [a]	0	3	96	< 1	117
dsh-2(or302)/mln1; hkEx36[ΔDIX dsh-2::gfp] [b]	0	10	90	0	80
dsh-2(or302)/mln1; hkIs20[ΔDIX dsh-2::gfp] [c]	0	0	100	0	120
dsh-2(or302)* (M+ Z-); *gmIs12[srb-6::gfp]	0	4	91	4	89
dsh-2(or302)* (M+ Z-); *hkEx39[Δ*EP dsh-2::gfp] [a]	0	9	89	2	102
dsh-2(or302)* (M+ Z-); *hkEx36[ΔDIX dsh-2::gfp] [b]	6	48	44	2	94
dsh-2(or302)* (M+ Z-); *hkIs20[ΔDIX dsh-2::gfp] [c]	0	8	88	4	96
dsh-2(or302)* (M- Z-); *gmIs12[srb-6::gfp]	2	5	69	24	148
dsh-2(or302)* (M- Z-); *hkEx39[Δ*EP dsh-2::gfp] [a]	3	20	60	16	128
dsh-2(or302)* (M- Z-); *hkEx36[ΔDIX dsh-2::gfp] [b]	8	38	49	6	80
dsh-2(or302)* (M- Z-); *hkIs20[ΔDIX dsh-2::gfp] [c]	< 1	15	60	23 [d]	113

[a] injected at 0.5 ng/ul
[b] injected at 0.5 ng/ul
[c] integrated *hkEx32*
[d] <1% had 4 cells per side

the problem of mosaicism and more accurately determine if Δ*EP *dsh-2* injected at 0.5 ng/ul could rescue PHA duplications, we wanted to determine the number of phasmid neurons in *dsh-2* mutants carrying the integrated array *hkIs25*. Unfortunately, expression of *srb-6::gfp*, the phasmid neuron GFP marker, was too faint for reliable visualization of phasmid neurons. *srb-6::gfp* expression was brighter in the other four integrated lines but they were not crossed into *dsh-2* mutants to score for rescue of PHA duplications due to time constraints. Therefore, rescue of PHA duplications was not determined for integrated arrays of Δ*EP *dsh-2* injected at 0.5 ng/ul.

We then tested if higher injection concentrations of Δ*EP *dsh-2* could rescue PHA duplications. We examined the nine lines obtained by injecting the Δ*EP *dsh-2* construct at 2.5 ng/ul for rescue of PHA duplications. Unfortunately, all nine lines carrying extrachromosomal arrays showed very high mosaicism. One way to quantify PHA duplications would be to integrate an extrachromosomal array carrying the Δ*EP *dsh-2* construct at 2.5 ng/ul. However, another approach was taken. We attempted to inject Δ*EP *dsh-2* at the higher concentration of 10 ng/ul. Unfortunately, injecting the construct at such high concentration resulted in lethality. Nonetheless, results from transgenics carrying the construct at a low concentration suggest that the DEP domain of DSH-2 may be important for regulating asymmetric cell division in the PHA lineage.

3.4.3 Expression of the Δ*EP DSH-2 protein was not detected

To examine the expression of the Δ*EP DSH-2 protein during embryogenesis, embryos were collected from the five integrated lines expressing Δ*EP *dsh-2* at 0.5 ng/ul. Since the deletion construct was tagged with GFP at the C-terminus, the resultant DSH-

2::GFP protein could be detected by staining embryos with an anti-GFP antibody. Surprisingly, no staining was observed in embryos or larvae. This lack of staining could simply be due to the low concentration at which the construct was injected. Therefore, to examine the expression of the Δ*EP *dsh-2* construct when injected at the higher concentration of 2.5 ng/ul, embryos were collected from *dsh-2(or302)/mIn1* animals carrying the extrachromosomal array *hkEx58*. Similarly, expression of the Δ*EP DSH-2 protein was not detected after staining with anti-GFP antibodies. The *dsh-2* deletion construct was confirmed to be fused in-frame with the C-terminal GFP (T. Walston and J. Hardin, University of Wisconsin, Madison). Also, the lack of signal was not due to over-fixation of the embryos. Some of the embryos carry the *mIn1* balancer, which carries the integrated array *mIs14* that expresses GFP in gut precursor cells during embryogenesis. This GFP protein was effectively detected by α-GFP antibodies. Therefore, the injection concentrations of 0.5 and 2.5 ng/ul may be too low to detect expression of the Δ*EP *dsh-2* construct.

3.4.4 ΔDIX *dsh-2* partially rescued *dsh-2* embryonic lethality

After determining that the DEP domain is essential for *dsh-2* function, we next tested a requirement for the DIX domain. First, we determined the ability of the ΔDIX *dsh-2* construct to rescue *dsh-2* embryonic lethality. Six transgenic lines were obtained when the ΔDIX *dsh-2* construct was injected at 0.5 ng/ul, but none of the lines appeared to rescue *dsh-2* lethality as transgenic *dsh-2* mutants failed to be maintained as homozygotes. As previously mentioned, a lack of rescue may be a consequence of mosaic inheritance of the extrachromosomal arrays. Therefore, two extrachromosomal

arrays, *hkEx32* and *hkEx36*, were integrated. Six lines were obtained in total, and two lines, *hkIs20* and *hkIs22* were tested for rescue of *dsh-2* lethality. However, significant rescue of *dsh-2* lethality was not observed as neither integrated array was able to maintain a *dsh-2* homozygous mutant.

Next, the construct was injected at higher concentrations and analyzed for rescue of *dsh-2* embryonic lethality. Two lines were obtained when the construct was injected at 2.5 ng/ul. One line did not show rescue. However, for the second line, significant rescue was observed as 41% of *dsh-2* (M- Z-) embryos hatched (Table 10, *hkEx52*), and this array was able to maintain a *dsh-2* mutant line as a homozygote. To further show that the ΔDIX *dsh-2* construct can rescue *dsh-2* lethality, the injection concentration of the construct was increased to 10 ng/ul. Three lines were obtained, and rescue was also observed to be significant as transgenic *dsh-2* mutants from all three lines could propagate as homozygotes. Therefore, the DIX domain of DSH-2 appears to be dispensable for function. Taken together with the earlier results that showed a requirement for the DEP domain, DSH-2 may transduce a PCP-like signal to regulate ventral enclosure.

3.4.5 ΔDIX *dsh-2* may affect the production of a phasmid neuron

The ΔDIX *dsh-2* construct was next tested for its ability to rescue PHA neuronal duplications. First, animals that carry the ΔDIX *dsh-2* construct at 0.5 ng/ul were examined. In control *dsh-2(or302)/mIn1* animals carrying the integrated array *gmIs12[srb-6::gfp]*, two cells in the tail would express GFP 100% of the time. In transgenic *dsh-2(or302)/mIn1* larvae, two phasmid neurons were detected 90% of the

time and a single neuron observed at a frequency of 10% (Table 11, *hkEx36*). The lost of *srb-6::gfp* expression in a phasmid neuron was likely caused by mosaicism since the GFP reporter was part of the extrachromosomal array. When the number of phasmid neurons was examined in *dsh-2* (M+ Z-) animals, the frequency of observing one GFP-expressing cell in the tail increased significantly to 48% (Table 11; *hkEx36*). Such high losses were unlikely to be caused by mosaicism, and may suggest the loss of a phasmid neuron in *dsh-2* (M+ Z-) mutants carrying ΔDIX *dsh-2*.

To better determine if the ΔDIX *dsh-2* construct causes the loss of a phasmid neuron in zygotic *dsh-2* mutants, two transgenic lines with ΔDIX *dsh-2* injected at 0.5 ng/ul were integrated. A total of six lines were obtained, and the number of phasmid neurons was determined in *dsh-2* mutants carrying the integrated array *hkIs20*. Unexpectedly, phasmid neurons were no longer lost at significant frequencies. Losses of a phasmid neuron were only observed at 8% in *dsh-2* (M+ Z-) mutants carrying *hkIs20* compared to 4% in the control group (Table 11). Intriguingly, for *dsh-2* (M- Z-) mutants, in addition to observing a 23% duplication of a phasmid neuron, losses were also detected at 15%. These losses appear to be significant because control *dsh-2* (M- Z-) animals were found to lose a phasmid neuron only 5% of the time. Therefore, the ΔDIX *dsh-2* construct showed no rescue of PHA neuronal duplications when injected at 0.5 ng/ul. However, as described earlier, rescue of *dsh-2* embryonic lethality was also not observed at this injection concentration.

To determine if increased amounts of ΔDIX *dsh-2* could rescue PHA duplications, the two lines obtained from injections at 2.5 ng/ul were examined. Unfortunately, the arrays were highly mosaic and the expression of *srb-6::gfp* was frequently absent in a

phasmid neuron in heterozygote *dsh-2* and homozygous *dsh-2* animals (Appendix 5, *hkEx52*). Thus, we were unable to test for rescue of PHA duplications at this injection concentration. One method to alleviate array mosaicism is to integrate the array. However, since it is a very time-consuming process, a different approach was taken. When the ΔDIX *dsh-2* construct was injected at the higher concentration of 10 ng/ul, a *dpy-30p::dsRed* plasmid (courtesy of S. Cordes and G. Garriga, University of California, Berkeley) was used in place of *srb-6::gfp* as the co-injection marker. *dpy-30p::dsRed* expresses *dsRed* in most cells and expression can be used to identify transgenic animals. Three transgenic lines were obtained (*hkEx84*, *hkEx85*, *hkEx86*). The integrated array *gmIs12[srb-6::gfp]* was then crossed into *dsh-2(or302)/mIn1; hkEx86* hermaphrodites to generate *dsh-2(or302)/mIn1; gmIs12; hkEx86* animals. When these worms were assayed for rescue of PHA duplications in *dsh-2* (M- Z-) mutants, complete rescue was observed (N=83) (Table 12, *hkEx86*). This indicates that the DIX domain is not required for regulating asymmetric cell division in the PHA lineage.

3.4.6 ΔDIX DSH-2 is properly localized to the membrane

To determine the expression pattern of the ΔDIX DSH-2::GFP protein, embryos were first collected from the 6 integrated lines carrying the construct at 0.5 ng/ul. Similar to the Δ*EP *dsh-2* construct, no GFP was detected upon staining with anti-GFP antibodies. Again, this could be due to the low concentration at which the ΔDIX *dsh-2* plasmid was injected. Therefore, embryos were collected from homozygous *dsh-2* mutants carrying the extrachrosmomal array *hkEx84*, which was generated by injection of the ΔDIX *dsh-2* plasmid at 10 ng/ul. In these embryos, ΔDIX DSH-2 protein was detected. Similar to the endogenous DSH-2 protein, ΔDIX DSH-2 was localized

Table 2 Rescue of PHA duplications by ΔDIX *dsh-2::gfp* injected at 10 ng/ul.

	# phasmid neurons / side				
Genotype	**0 (%)**	**1 (%)**	**2 (%)**	**3 (%)**	**N**
dsh-2(or302)/mIn1; gmIs12	0	0	100	0	134
dsh-2(or302)/mIn1; gmIs12; hkEx86[ΔDIX dsh-2::gfp] [a]	0	0	100	0	78
dsh-2(or302)* (M- Z-); *gmIs12	2	5	69	24	148
dsh-2(or302)* (M- Z-); *gmIs12; hkEx86[ΔDIX dsh-2::gfp] [a]	0	0	100	0	83

[a] construct injected at 10 ng/ul

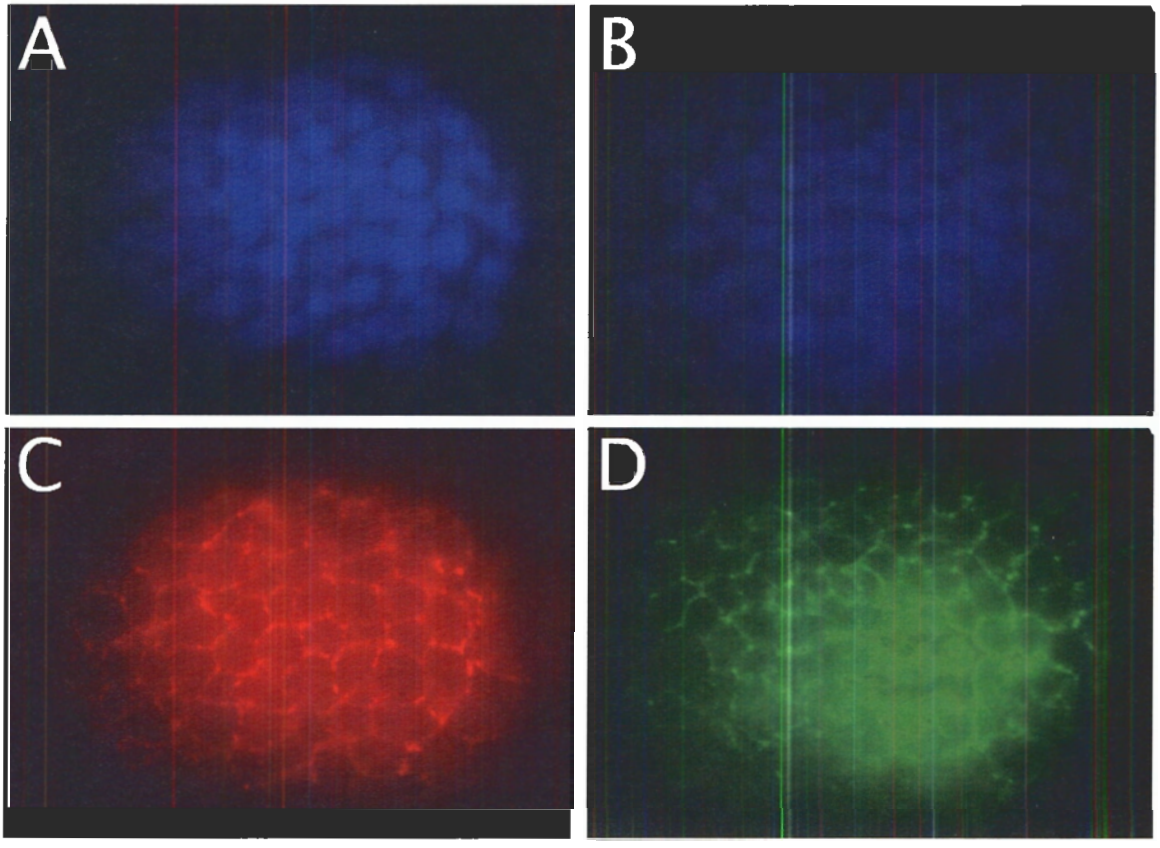

Figure 4 ΔDIX DSH-2::GFP is localized to the membrane.

A and C: Wildtype N2 embryo. A) DAPI staining. C) α-DSH-2 staining shows that the endogenous DSH-2 protein is localized to the membrane.
B and D: Embryo expressing *hkEx84[ΔDIX dsh-2::gfp]* (construct injected at 10 ng/ul). B) DAPI staining. D) α-GFP staining. ΔDIX DSH-2::GFP is also primarily localized to the membrane.

primarily at the membrane (Figure 26). Therefore, the DIX domain is not required for membrane localization of DSH-2.

3.5 Other genes that may function with *dsh-2* in regulating asymmetric cell division in the PHA lineage

In addition to *dsh-2*, the only other gene known to also regulate asymmetric cell division in the PHA lineage is *mom-5*, a Frizzled homologue. The PHA neuron is duplicated at a frequency of only 22% in *dsh-2* (M- Z-) mutants. Such incomplete penetrance suggests that many additional genes function with *dsh-2* to regulate asymmetric cell division in the PHA lineage.

3.5.1 VAB proteins

dsh-2 (M- Z-) hatched larvae often have severe morphological defects due to faulty ventral enclosure. Strong loss-of-function mutants in the *vab* (variable abnormal morphology) gene family also have morphological defects that are comparable to *dsh-2* mutants. VAB-2/EFN-1 is one of four Ephrin ligands, and VAB-1 is the only Ephrin receptor in *C. elegans*. During ventral enclosure, VAB-1 and VAB-2 are expressed in non-overlapping subsets of neuroblasts, and the proteins function to organize the neuroblasts for proper migration of the overlying hypodermal cells (Chin-Sang et al., 1999). However, a potential role in asymmetric cell divisions had not been examined. Therefore, we tested for PHA lineage defects in *vab-1* and *vab-2* mutants.

3.5.1.1 Ephrin signalling may play a minor role in the generation of a phasmid neuron

To test if an Ephrin ligand regulates asymmetric division in the PHA lineage, *gmIs12[srb-6::gfp]* was crossed into *vab-2(e96)* mutants to visualize the phasmid

neurons. The *vab-2(e96)* allele carries a nonsense mutation, and is one of the strongest *vab-2* loss-of-function mutations available (Chin-Sang et al., 1999). However, as shown in Table 13, no phasmid neuron defects were observed in *vab-2(e96)* mutants.

To further assess if Ephrin signalling regulates asymmetric division in the PHA lineage, *gmIs12* was crossed into *vab-1(dx31)* mutants. The lack of phasmid neuronal duplications in *vab-2/efn-1* mutants could be explained by functional redundancy between the Ephrin ligands. VAB-1 is the only Ephrin receptor in the *C. elegans* genome. Removing function of the VAB-1 receptor has been shown to be equivalent to knocking down functions in three of the four Ephrins (Wang et al., 1999). Therefore, although removing the function of a single Ephrin did not result in a change in the number of phasmid neurons, knocking out the function of the Ephrin receptor might. By analyzing *gmIs12* in *vab-1(dx31)* mutants, phasmid neuronal duplications were only observed at the very low frequency of 1% (N=77; Table 13). However, since *gmIs12[srb-6::gfp]* is expressed in both PHA and PHB neurons, we could not unambiguously determine which one of the neurons was duplicated. Due to the minute instances of neuronal duplications, Ephrin signalling mutants were not pursued any further.

3.5.2 G proteins

C. elegans G proteins regulate the asymmetric cell division in the one celled zygote. In *C. elegans*, the genes *goa-1* and *gpa-16* encode the Gα subunits (Jansen et al., 1999). In the one-celled zygote, GPA-16 and GOA-1 act redundantly to position the mitotic spindle toward the posterior side of the zygote (Gotta and Ahringer, 2001). *gpb-1* encodes the only Gβ subunit in *C. elegans*. In *gpb-1(pk44)* mutants, orientation of the

Table 13 Phasmid neuron duplications in G protein and *vab* mutants.

	# phasmid neurons / side				
Genotype	**0 (%)**	**1 (%)**	**2 (%)**	**3 (%)**	**N**
gmIs12	0	0	100	0	118
vab-2(e96); gmIs12	0	0	100	0	145
vab-1(dx31); gmIs12	0	0	99	1	70
gpb-1(pk44); gmIs12	0	0	100	0	86
gpa-16(it143); gmIs12 [a]	0	1	98	1	97
gpa-16(it143); gmIs12 [b]	0	0	100	0	86

[a] at non-permissive temperature of 25°C

[b] at semi-permissive temperature of 20°C

mitotic spindle is defective in many divisions during early embryogenesis (Zwaal et al., 1996). For divisions in the PHA lineage, however, a role for G proteins had not been examined. To determine if G proteins regulate divisions in the PHA lineage, the integrated array *gmIs12[srb-6::gfp]* was crossed into G protein mutants and assayed aberrant phasmid neuron numbers.

3.5.2.1 The G proteins do not affect the asymmetric cell division in the phasmid neuron lineages

To examine if the β subunit of G proteins regulate asymmetric cell division in the PHA lineage, *gpb-1(pk44)* animals were obtained. The integrated array *gmIs12[srb-6:;gfp]* was then crossed into *gpb-1(pk44)* mutants to assay for the number of phasmid neurons. However, no duplications were observed (Table 13).

We then sought to determine if the Gα subunits regulate asymmetric cell division in the PHA lineage. First, we obtained *gpa-16(it143)* mutants. The *it143* mutation is a temperature sensitive allele. At the permissive temperature of 15°C, homozygous *gpa-16(it143)* mutants are viable. However, homozygous mutants exhibit embryonic lethality of 70% and 30% when propagated at 25°C and 20°C, respectively (Bergmann et al., 2003). To determine if PHA duplications are present in *gpa-16(it143)* mutants, the *gmIs12[srb-6::gfp]* marker was crossed in to score for phasmid neuron duplications. No duplications were observed when the mutants were produced at the semi-permissive temperature of 20°C. When the mutants were grown at the non-permissive temperature of 25°C, phasmid neuronal losses and duplications were both observed at a frequency of 1% (Table 13). Due to low penetrance, further tests on G protein mutants were not performed.

CHAPTER 4 DISCUSSION

4.1 Additional genes that function with DSH-2 in asymmetric cell division

Previously, *dsh-2* has been shown to regulate cell division during embryogenesis in the lineage that generates the PHA sensory neuron (Hawkins et al., 2005). PHA duplications only occur at a frequency of 22% in mutants lacking both maternal and zygotic *dsh-2* function. This indicates that many other genes also regulate asymmetric cell division in the PHA lineage. We attempted to identify some of those genes by assaying for PHA duplications in a specific subset of signalling mutants. These mutants have either been shown to have defects in asymmetric cell division or morphogenesis during embryogenesis. Unfortunately, the mutants tested showed very rare or no duplications of a phasmid neuron.

Recent work in the lab by L. Nykilchuk has identified the Wnt ligand *cwn-1* to function with *dsh-2* in regulating asymmetric division in the PHA lineage. When RNAi was performed to knock down *cwn-1* function in wildtype animals, no PHA duplications were observed. PHA duplications are observed 3% of the time in *dsh-2* (M+ Z-) mutants. However, when *cwn-1* function was also compromised in *dsh-2* (M+ Z-) mutants, PHA duplications increased to 10-15%. Therefore, the effect of reducing *cwn-1* function was only uncovered when the knock down was done in the "sensitized genetic background" of *dsh-2* (M+ Z-) mutants. Thus, the same approach can be taken to further investigate mutants that gave rare phasmid neuron duplications. Both *vab-1* and *gpa-16(it143)*

mutants show rare duplications of 1%. Performing RNAi of these two genes in *dsh-2* mutants lacking just zygotic function may further reveal their roles in regulating asymmetric neuroblast division.

4.2 Asymmetric division or fate specification of many cells may be disrupted in *dsh-2*

Preliminary analysis suggested that *dsh-2* is likely required for cell divisions in lineages other than the one that generates PHA. Therefore, using cell-specific GFP markers, we assayed for defects in the production of 18 cells. Many cell losses and duplications were observed. These cell losses/duplications could be the result of cell division defects. However, defects in cell fate specification could also account for gains and losses of cells. For instance, three homeobox-containing transcription factors CEH-10, TTX-3, and CEH-10 are required for differentiation of a specific class of interneurons. In the respective mutants, specific interneurons are lost (Altun-Gultekin et al., 2001). Another homeobox-containing protein LIN-11 specifies fate in a subset of olfactory and mechanosensory neurons. In *lin-11* mutants, neuronal losses and duplications are observed (Sarafi-Reinach et al., 2001).

Wnt signalling has been shown to regulate expression of homeobox genes. In post-embryonic development, descendants of the left and right Q neuroblasts migrate in opposite directions. Wnt signalling proteins participate in a canonical Wnt pathway to dictate the direction in which the cells migrate. It was shown that Wnt signalling regulates this process by modulating the expression of the homeobox gene *mab-5* in Q neuroblast descendents (Maloof et al., 1999; Whanbgo and Kenyon, 1999). *mig-5* is the only Dsh homolog that has been shown to affect migration of the Q neuroblasts (cited as

PhD thesis by Guo, 1995 in Maloof et al., 1999). Although no reports have been published, *mig-5* has been proposed to function with the other Wnt signalling proteins in regulating *mab-5* expression. Therefore, Wnt signalling can activate transcription factors to specify cell fate. More importantly, this cell fate specification occurs independently of asymmetric cell divisions.

Thus, in *dsh-2* mutants, although many cell losses and duplications are observed, they may either be caused by defects in cell fate specification or asymmetric cell division. To determine if it is defects in the latter that leads to aberrant cell numbers, cell-specific GFP markers for lineally related cells were also analyzed.

4.2.1 DSH-2 may function with Wnt signalling proteins to regulate the asymmetric cell division of the Z1/Z4 precursor cells

The Z1/Z4 precursor cells divide asymmetrically in the proximal-distal axis. The distal daughters become DTCs while one of the proximal daughters become an AC. Losses of DTCs and duplications of ACs in *dsh-2* mutants indicate that the Z1/Z4 divisions were often symmetric (Figure 15). Core components of the canonical Wnt signalling pathway, including LIN-17/Frizzled, SYS-1/WRM-1/β-catenin, and POP-1/Tcf, have been shown to regulate the same division. Recently, the *dsh-2(ez25)* allele was isolated in a genetic screen for mutants with gonadogenesis defects (Chang et al., 2005). In that study, POP-1 asymmetry in the Z1/Z4 daughters was found to be reversed in *dsh-2* mutants. Therefore, similar to other Wnt signalling proteins, DSH-2 regulates the Z1/Z4 divisions by controlling POP-1 levels in the descendents of the Z1/Z4 cells. As for asymmetric cell divisions in the PHA lineage, no role has been implicated for either

LIN-17 or POP-1. Therefore, DSH-2 appears to participate in distinct signalling cascades in governing the divisions of the Z1/Z4 gonadal precursor and the ABpl/rpppa neuroblast.

4.2.2 PVQ and OLL lineages may have asymmetric cell division defects

4.2.2.1 PVQ lineage

Our results indicate that, in *dsh-2* mutants, a cell fate transformation in the PVQ lineage occurs at 315 minutes to convert the sister cell that normally undergoes apoptosis to become a second PVQ neuron (Figure 27). However, it remains unclear whether this transformation is caused by a defect in asymmetric cell division or cell fate specification. Since the cell fate transformation occurs at a terminal division, we cannot distinguish between these two possibilities using lineally-related GFP markers. Nonetheless, since the defective division in the PVQ lineage occurs 135 minutes after the division that is defective in the PHA lineage, *dsh-2* appears to function at various time points during embryogenesis in the generation of different neurons.

4.2.2.2 OLL lineage

OLL duplications were observed at a frequency of 27% and 33% in *dsh-2* (M+ Z-) and (M- Z-) mutants, respectively. Due to penetrant OLL duplications in mutants lacking only zygotic *dsh-2* function and the availability of GFP markers for other cells in the lineage, we tested if OLL duplications were a result of asymmetric cell division defects. We decided to examine the division in the lineage that occurs at 180 minutes during embryogenesis (Figure 28A, division #1). The ABplpppp and ABpraaap neuroblasts generate the left and right OLL, respectively. We specifically tested the hypothesis that extra OLLs were due to the posterior daughter cells transforming into

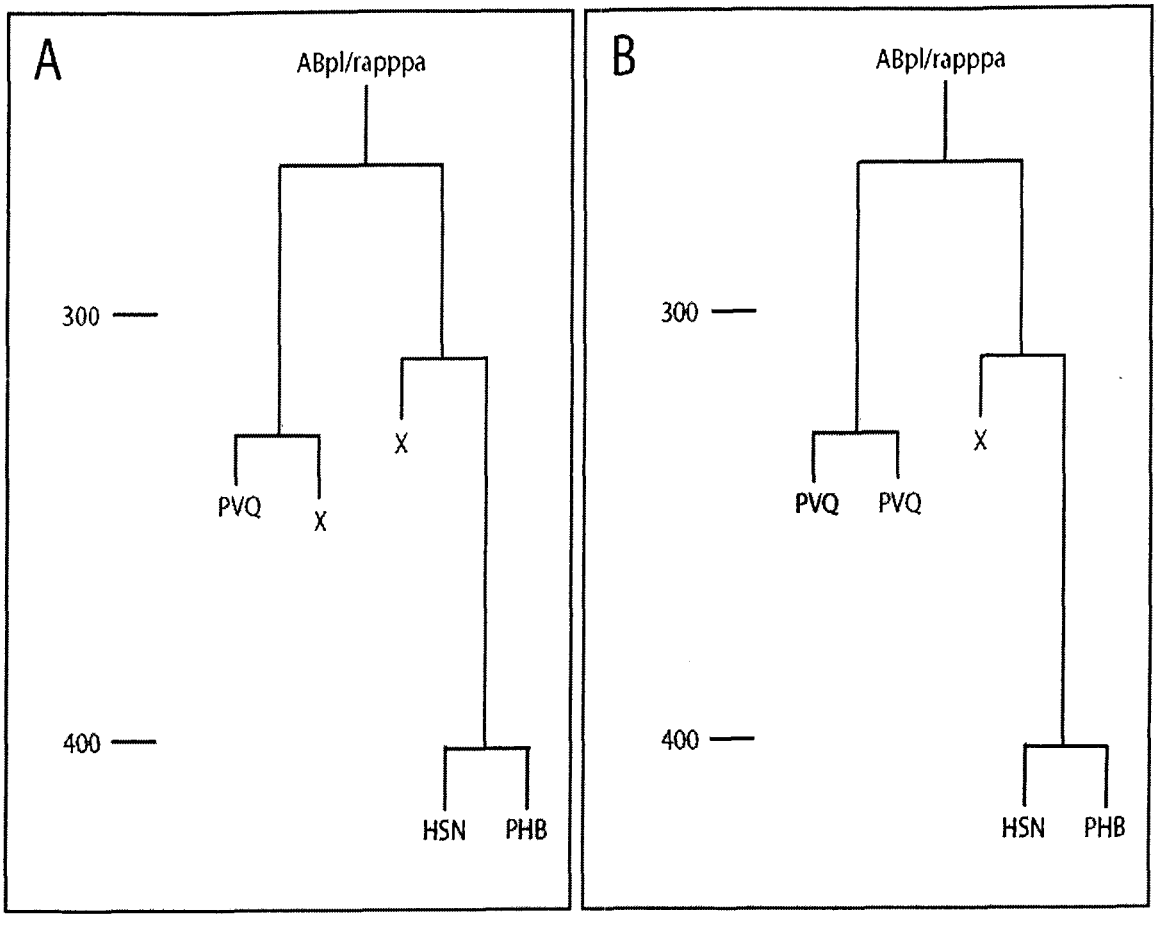

Figure 27 *dsh-2* may regulate a division in the PVQ lineage

The PVQ sister cell, which undergoes apoptosis, is often transformed into a second PVQ neuron in *dsh-2*. A) PVQ lineage diagram of wildtype. B) Proposed lineage transformation in *dsh-2* mutant.

Figure 28 Possible division defects in OLL lineage of *dsh-2* mutants.

A: Wildtype lineage. Results from this study showed that OLL duplications are not caused by a cell fate transformation at division #1. Therefore, OLL duplications may be caused by division defects further down in the lineage.

B: If OLL duplications are caused by a defect in division #2, the anterior daughter may adopt the fate of the posterior daughter cell. In this case, the ADL neuron would be lost at the expense of extra OLL neurons.

C: If it is division #3 that is affected in *dsh-2* mutants, the posterior daughter that normally undergoes apoptosis at about 310 minutes may be transformed into a second anterior daughter-like cell.

D: If it is division #4 that is affected, the posterior daughter cell that undergoes apoptosis at about 420 minutes may be transformed into another OLL-like cell.

E: Three OLLs would be generated if division #3 produces two anterior daughter-like cells and one of the two divisions at timepoint #4 is also affected.

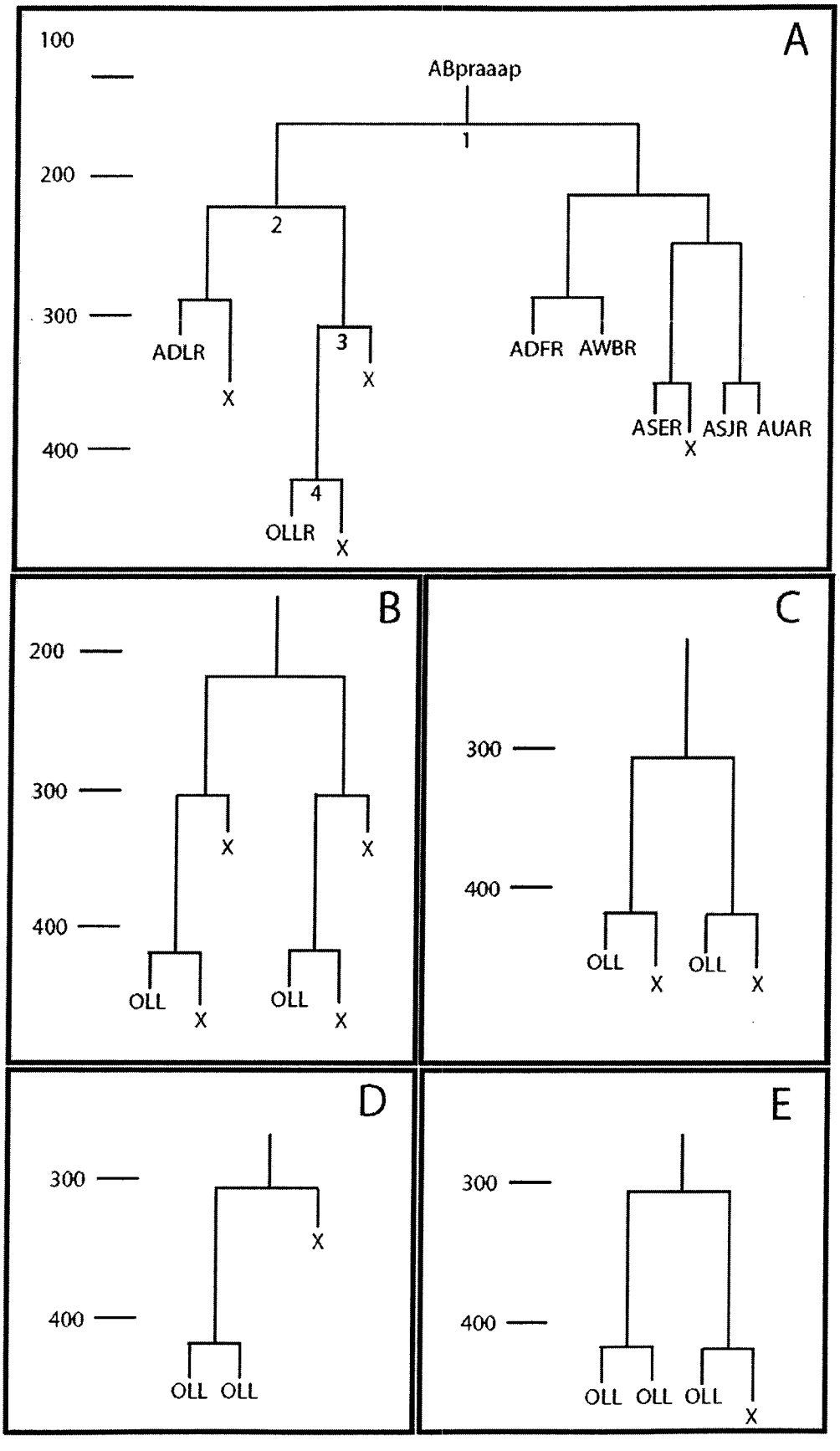
A
100
200
300
400
ABpraaap
1
2
3
4
ADLR
X
X
ADFR
AWBR
ASER
X
ASJR
AUAR
OLLR
X
B
200
300
400
X
X
OLL
X
OLL
X
C
300
400
OLL
X
OLL
X
D
300
400
X
OLL
OLL
E
300
400
OLL
OLL
OLL
X

anterior-like daughter cells. Thus, we would predict a loss of neurons derived from the posterior daughter cells at a similar frequency that OLL is duplicated. Therefore, we scored for losses of the ADF, AWB, and ASE neurons in *dsh-2* (M+ Z-) and (M- Z-) mutants. However, our results were not consistent with defects of the ABplpppp or ABpraaap neuroblast at 180 minutes of embryogenesis. Therefore, OLL duplications could be due to defects in divisions further down the lineage or defects in cell fate specification.

Further experiments could be performed to determine if extra OLLs are caused by asymmetric cell division defects after the 180 minutes mark. The three possibilities are highlighted in Figure 28B-E. If division #2 is affected in *dsh-2* mutants and both daughter cells adopt the posterior cell fate, the ADL neuron would be lost at the expense of extra OLLs (Figure 28B). GFP markers for ADL are available; however, they are not cell-specific as the reporters also express GFP in two or three other neurons in close proximity of the ADL neuron. Nonetheless, if a cell-specific ADL marker becomes available, it can be crossed into *dsh-2* mutants and assayed for any ADL losses or duplications.

Moreover, defects in division #3 or #4 in could also lead to OLL duplications. If division #3 became symmetric, the cell death occurring at about 320 minutes of embryogenesis may be transformed to subsequently produce an extra OLL neuron (Figure 28C). The entire *C. elegans* cell lineage has been determined, and all cell deaths can be identified in live embryos under Nomarski optics. OLL duplications occur at 27% in *dsh-2* (M+ Z-) mutants. Since these mutants have maternal *dsh-2* function, embryogenesis is not perturbed, and the presence or absence of this death could

potentially be determined. If this cell death is indeed found to be missing in a subset of zygotic *dsh-2* embryos, those embryos can be allowed to hatch and scored for corresponding OLL duplications. Another method to determine if extra OLLs are derived from division #3 is to score for OLL duplications in *dsh-2; ced-3* double mutants. In *dsh-2* mutants, if division #3 is affected, the apoptotic cell that is transformed would likely undergo apoptosis, thereby masking OLL duplications. A significant increase of OLL duplications could be observed in *dsh-2* mutants if apoptosis was prevented from occurring during embryogenesis.

Analysis of *dsh-2; ced-3* double mutants could also show a significant increase of OLL duplications if division #4 is affected (Figure 28D). In this case, the sister cell of OLL that normally undergoes apoptosis could be transformed into a second OLL neuron. In addition, in *dsh-2* (M- Z-) mutants, 29% of the time two OLL neurons were observed on one side of an animal, and 4% of the time three OLLs were found on a side (Table 5). Three OLL neurons could be explained if DSH-2 regulates more than one asymmetric division in the lineage: for instance, at division #3 and #4 (Figure 28E). In spite of this, even if both cell fate transformations occurred in the same *dsh-2* mutant, the transformed cells would undergo apoptosis most of the time and mask the production of three OLLs. However, in *dsh-2; ced-3* mutants, if both of the cell deaths stemming from divisions #3 and 4 become transformed, they would survive to generate OLL neurons. Thus, in these mutants, the frequency of observing three OLLs on a side would significantly increase relative to *dsh-2* mutants alone.

4.2.2.3 ADF/AWB lineage

Our analysis of cells lineally related to the OLL neuron suggests that asymmetric cell division defects may be present in the ADF/AWB lineage. ADF and AWB are sister cells (Figure 17). In mutants lacking only zygotic *dsh-2* function, AWB is lost at a frequency of 2%, while ADF is duplicated 3% of the time (Table 5). In mutants lacking both maternal and zygotic *dsh-2* function, AWB losses increased to 19%. Unfortunately, the number of ADF neurons was unable to be determined in *dsh-2* (M- Z-) mutants. The ADF marker *mgIs71[tph-1::gfp]* is also expressed in another head neuron called NSM, which lies just anterior to ADF. Therefore, in *dsh-2* (M- Z-) mutants, the ADF and NSM neurons could not be distinguished due to defects in morphology. Nonetheless, the marker could still be scored to see if there are any changes in the number of GFP-expressing cells. Currently, no marker is specific to the NSM neuron. If one becomes available and subsequent analysis reveals no changes in the number of NSM neuron in *dsh-2* mutants, then by process of elimination, any cell losses/duplications showed by the *tph-1::gfp* marker could be attributed to the ADF neuron.

4.2.3 Lineages for future studies

4.2.3.1 CAN lineage

Defects in the CAN lineage warrant further investigation. The CAN neuron is lost 19% of the time and duplicated at a frequency of 14% in *dsh-2* (M- Z-) mutants. The CAN neuron has a unique cellular morphology, and it is the only neuron that is born in the head and migrates posteriorly to reside just anterior of the vulva. When duplications were observed, the two GFP-expressing cells resemble the CAN neuron morphology (Figure 29). Also, both cells would be observed right next to each other and in the middle

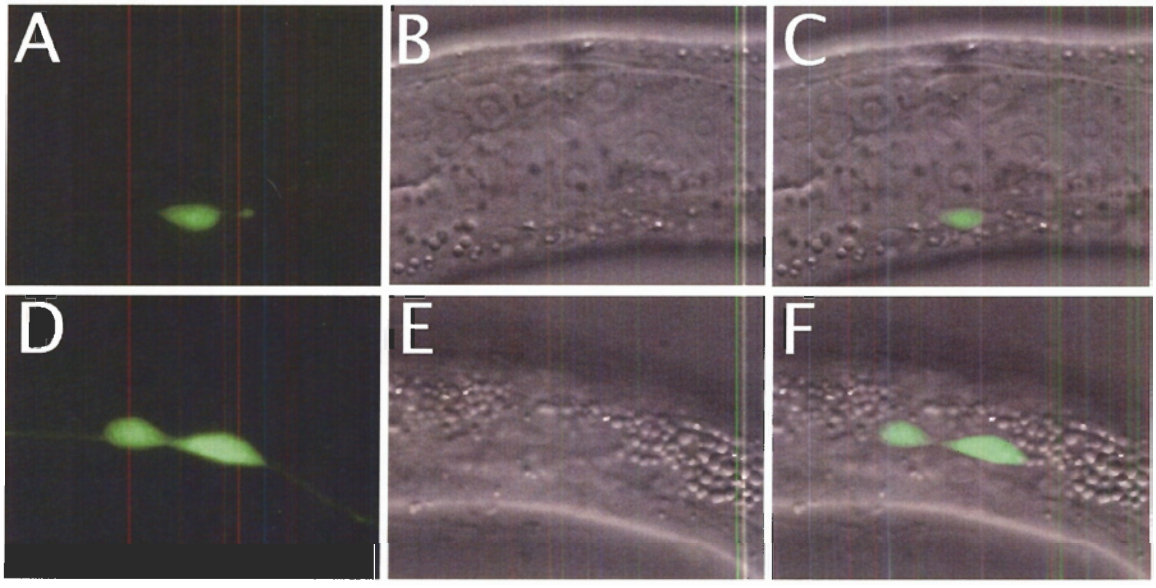

Figure 29 CAN duplications in *dsh-2* mutants.

The CAN neurons are visualized using the integrated array *gmIs18[ceh-23::gfp]*.
A, B, C: wildtype. A) GFP image shows the single CAN neuron in the animal. B) DIC image of the same animal. C) Merge of DIC and GFP images.
D, E, F: *dsh-2(ez25)* (M- Z-) mutant. A) Two CAN neurons express *ceh-23::gfp*. Processes of the CAN neurons could also be observed. B) DIC image of the same mutant animal. C) Merge of DIC and GFP images.

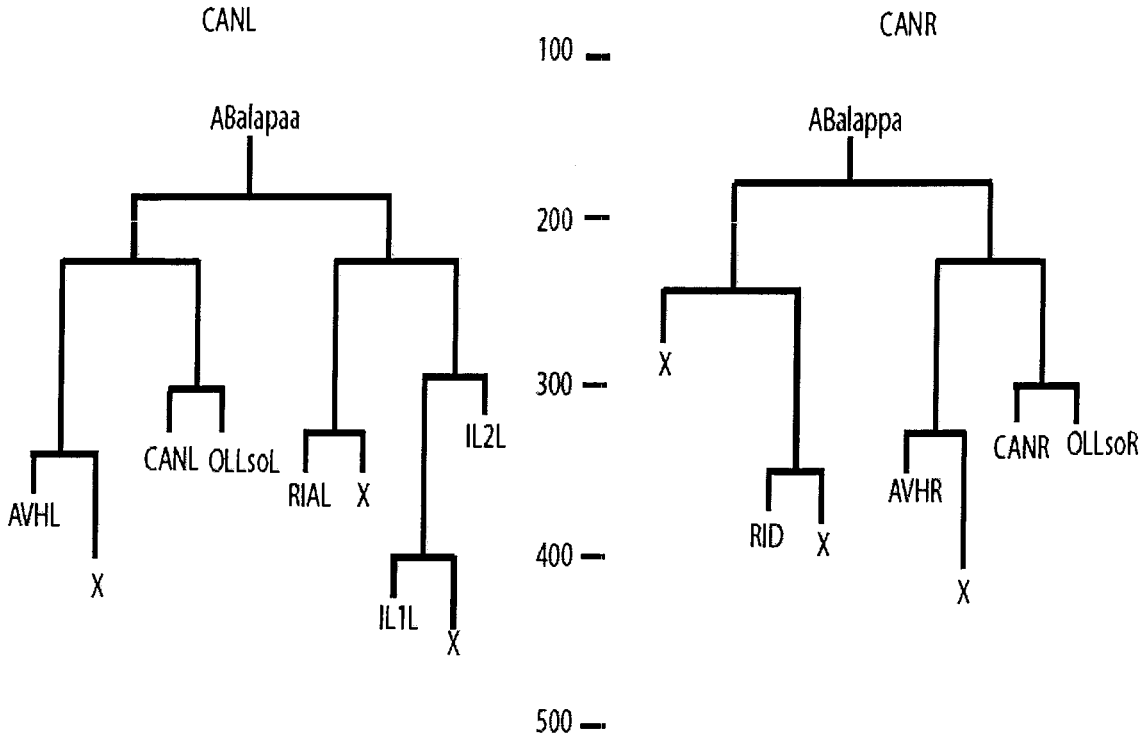

Figure 30 Lineage diagrams for the CAN neurons.

of the animal where CAN neurons are expected to be. Therefore, it is highly unlikely that, in *dsh-2* mutants, an extra GFP-expressing cell is a lineally-unrelated neuron that has fully differentiated into a second CAN neuron. Nonetheless, evidence from lineally-related cells is required to support CAN neuronal duplications as defects in asymmetric cell division. Figure 30 is the lineage diagrams for CANL, CANR, and lineally-related cells. Potentially, the RIAL neuron, lineally-related to CANL, could be examined using the *glr-6::gfp* marker (Brockie et al., 2001). However, this array is extrachromosomal and thus may complicate analysis. Also, the OLLso cells, which are sister cells of the CAN neuron, could also be examined using *ITXp::gfp* (WormAtlas: http://www.wormatlas.org/handbook/hypodermis/IL.OLimagegallery.htm). However, analysis of this marker may be limited to *dsh-2* (M+ Z-) mutants since it is also expressed in two other pairs of socket cells in the head. Moreover, the integrated marker *lqIs4* could be crossed into *dsh-2* mutants to assay for losses or duplications of the RID neuron, which is lineally-related to CANR (Tsalik et al., 2003). This marker is also expressed in another head neuron called AIY as well as the CAN neuron. However, these two neurons appear to be far enough away from the RID neuron for it to be unambiguously identified in *dsh-2* (M+ Z-) and (M- Z-) mutants.

4.2.3.2 ASI lineage

Even though the ASI lineage was not further examined for asymmetric cell division defects, analysis of this lineage may provide a link between asymmetric cell division and ventral enclosure. In *dsh-2* (M- Z-) mutants, the ASI neuron was lost 18% and duplicated 3% of the time (N=33). The sample number was low because the ASI marker had very faint GFP expression and thus was difficult to detect. In the ASI lineage,

the ABpl/raap cell divides asymmetrically at 140 minutes of embryogenesis (Figure 31). The anterior daughter gives rise to non-neuronal and neuronal cells, including ASI, whereas the posterior daughter divides to subsequently generate four hypodermal cells. Two of those four cells are called the leading cells (Figure 31, arrows), and they are important for initiating and guiding the migration of the hypodermis during ventral enclosure (Williams-Masson et al., 1997). Laser ablation of all or a subset of these leading cells affects various stages of epidermal morphogenesis such as cell migration, ventral enclosure, and elongation. ASI neuronal losses may be caused by defects in the asymmetric division of the ABpl/raap cell, thereby transforming the anterior daughter into a second posterior daughter (Figure 31). As a result, leading cells might be duplicated in *dsh-2* (M- Z-) mutants.

The consequence of extra leading cells during morphogenesis and ventral enclosure has not been investigated. The leading cells make extensive filopodial contacts with each other and the underlying substrate (Williams-Masson et al., 1997). Therefore, extra leading cells may result in ectopic filopodial connections either among themselves or with the underlying substrate, thereby disrupting ventral enclosure. Although no GFP markers exist for the leading cells, they could be identified by Nomarski optics (Williams-Masson et al., 1997). However, morphological defects of *dsh-2* (M- Z-) mutant embryos could complicate such identification. Another approach to determine if leading cells are duplicated is to analyze GFP markers for lineally-related cells. Cell-specific GFP reporter are available for both the AWA and ASG neurons. An integrated version of *odr-7::gfp* has been shown to be only expressed in AWA, and the integrated array

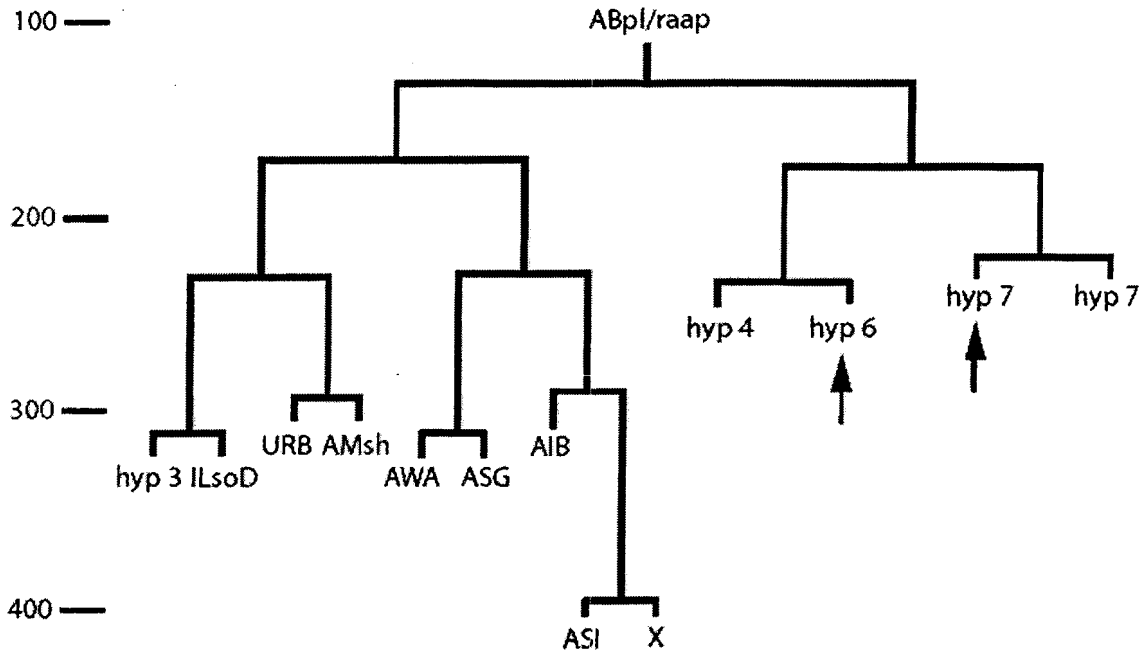

Figure 31 Lineage diagram for the ASI neuron and leading cells.

The ASI neuron is often lost in *dsh-2(or302)* mutants. The hyp6 and hyp7 cells are the leading cells for ventral enclosure (arrows) and are lineally related to the ASI neuron.

oyIs26[ops-1::gfp] has been reported to be specific to the ASG and ADL neurons (Sarafi-Reinach et al., 2001). Similar to the ASI neuron, AWA and ASG are descended from the anterior daughter of the ABpl/raap neuroblast. Therefore, the markers could be used to assay for AWA and ASG neuronal losses in *dsh-2* mutants.

4.3 *dsh-2* may be required in both the neuroblasts and hypodermis for ventral enclosure

By expressing DSH-2 under different tissue-specific promoters, we aimed to determine where *dsh-2* function is required for ventral enclosure. Expressing DSH-2 with the hypodermal promoter *lin-26* led to no significant rescue of *dsh-2* maternal effect embryonic lethality. Expression of the DSH-2 protein under the *lin-26* promoter was detected soon after the hypodermal cells are born (Figure 21). Therefore, it appears that expressing the DSH-2 protein in the intercalating and migrating hypodermal cells is not sufficient to rescue *dsh-2* embryonic lethality. *dsh-2* (M- Z-) embryos have defects at various stages of epidermal morphogenesis, such as intercalation of the dorsal hypodermis, migration of the leading cells, and fusion of the ventral cells (T. Walston and J. Hardin, personal communication). Our results clearly showed that the *lin-26p-dsh-2::gfp* construct was unable to rescue embryonic lethality of *dsh-2* mutants. However, it would be interesting to determine if the construct is able to rescue one or more of the ventral enclosure defects normally observed in *dsh-2* (M- Z-) mutants.

Expressing *dsh-2* under the control of the *unc-119* promoter was able to partially rescue *dsh-2* embryonic lethality. In addition, there was almost complete rescue of PHA duplications. Several implications can be drawn from these two findings. First, ventral enclosure begins at about 310 minutes, and the defective division in the PHA lineage

occurs at 180 minutes. Therefore, the observation that the *unc-119* promoter can rescue PHA duplications means that the promoter can express DSH-2 long before the onset of ventral enclosure. Second, since the rescue of PHA duplications and ventral enclosure were coupled, defects in ventral enclosure may be, at least partially, a secondary consequence of earlier defects in asymmetric neuroblast divisions. In this study, the production of many neurons was found to be affected, which may be indicative of asymmetric cell division defects. If the various neuronal losses/duplications could also be rescued by expressing DSH-2 with the *unc-119* promoter, it would further support the model that ventral enclosure is dependent on earlier division defects of neuroblasts.

However, experiments revealed that expression of DSH-2 under the *unc-119* promoter was not restricted to neuronal lineages; expression was also detected in hypodermal cells. Had the *unc-119p-dsh-2::gfp* construct specifically expressed DSH-2 in neuroblasts as we had intended, a strong claim could be made that *dsh-2* is required in the neuroblasts for ventral enclosure. However, there is likely a requirement in neuroblasts since hypodermal-specific *dsh-2* expression alone was insufficient to rescue *dsh-2* lethality. At this point we cannot rule out a requirement in both tissues.

To further investigate the requirement for *dsh-2* in neuroblasts, a second neuronal-specific promoter from the *F25B3.3* gene was used. However, no rescue of embryonic lethality was observed when the promoter was used to express DSH-2 in *dsh-2* (M- Z-) mutants. Subsequent analysis showed that even though the promoter was neuroblast-specific, it was not active prior to the onset of ventral enclosure. The *F25B3.3* promoter has been previously used to generate a neuronal-specific reporter, and promoter activity was also observed only after ventral enclosure (Altun-Gultekin et al., 2001; Gilleard and

McGhee, 2001). Therefore, the lack of *dsh-2* embryonic lethality rescue by *F25B3.3p-dsh-2::gfp* was likely due to the late onset of expression.

Further experiments could be performed to resolve the tissue-specific requirements of *dsh-2* in ventral enclosure. First, other promoters could be used to express *dsh-2* in the hypodermis. *dsh-2* function may be required in the hypodermal precursor cells before ventral enclosure. One candidate promoter for expressing *dsh-2* in early hypodermal precursor cells is *elt-1*, a gene that specifies hypodermal cell fate and is expressed even earlier than *lin-26* in embryogenesis (Page et al., 1997; Gilleard and McGhee, 2001). If using this promoter to express *dsh-2* is still unable to rescue *dsh-2* lethality, then it further supports the claim that *dsh-2* function is not required in the hypodermis for ventral enclosure. On the other hand, *dsh-2* could be expressed with yet another neuronal promoter, *unc-33*. Similar to the *unc-119* promoter, the *unc-33* promoter is reportedly active only in neuroblasts (Altun-Gultekin et al., 2001). However, the tissue specificity of the promoter must be carefully examined. Results gained from these experiments may provide further insight into the cell type(s) that requires *dsh-2* function during morphogenesis.

4.4 *dsh-2* may participate in a PCP-like signalling pathway

Dsh proteins are characterized by the presence of three evolutionarily conserved domains. Studies from various organisms have shown that two of the conserved domains, DIX and DEP, are preferentially required for different signalling pathways. In flies, Dsh deletion constructs lacking the DIX domain but have the rest of the protein are able to rescue PCP but not canonical Wnt signalling defects in flies (Axelrod et al., 1998). On the other hand, constructs lacking the DEP domain but possess the rest of the protein can

rescue Wnt but not PCP signalling mutants (Axelrod et al., 1998), and expressing ΔDEP Xdsh in wildtype *Xenopus* animals causes dominant negative Wnt signalling defects (Rothbacher et al., 2000). Although we have evidence that *C. elegans dsh-2* regulates asymmetric cell division and ventral enclosure, it is uncertain if DSH-2 functions in a canonical Wnt pathway or a PCP-like pathway to regulate the two processes.

We aimed to distinguish between these two signalling pathways by expressing *dsh-2* deletion constructs that lack specific domains. Our results showed that the deletion construct lacking the DIX domain is able to rescue both ventral enclosure defects and PHA duplications in *dsh-2* (M- Z-) mutants, and expression of the ΔDIX DSH-2 protein can be detected. In contrast, neither phenotype was rescued when a *dsh-2* deletion construct lacking part of the DEP domain was expressed. Moreover, expression of the Δ*EP DSH-2 protein was not observed. This could be due to the low concentrations at which the Δ*EP *dsh-2* construct was injected. On the other hand, the lack of expression from the construct could be due to the Δ*EP DSH-2 protein being degraded for unknown reasons. If this were the case, it could account for the inability of the Δ*EP *dsh-2* construct to rescue embryonic lethality or PHA neuronal duplications of *dsh-2* mutants.

Nonetheless, our results suggest that DIX, the domain important for Wnt signaling, is dispensable for DSH-2 function. This is consistent with a previous finding that loss-of-function *pop-1/Tcf* mutants showed no defects in the generation of PHA neurons (M. Roh, M.Sc thesis), suggesting that the canonical Wnt signalling pathway does not regulate asymmetric divisions in the PHA lineage. Conversely, we showed that DEP, the domain important for PCP signalling, is required for DSH-2 function. This

implicates a role for a PCP-like signalling cascade, not only in regulating asymmetric neuroblast division, but also in ventral enclosure. Expressing just the DIX or DEP domain alone in *dsh-2* mutants and assaying for rescue of ventral enclosure defects and PHA duplications should more accurately define the domain that is important for *dsh-2* function.

Additional findings also suggest DSH-2 to participate in a PCP-like signalling pathway. The endogenous DSH-2 protein is localized to the plasma membrane (Hawkins et al., 2005; Walston et al., 2004). In this study, ΔDIX DSH-2::GFP (with an intact DEP domain) also showed cortical localization. In flies, Dsh is also localized to the cell cortex when transducing PCP signals. The DEP domain is necessary and sufficient for targeting Dsh protein to the membrane, and membrane localization is a prerequisite for Dsh to function in PCP signalling (Axelrod et al., 1998). Likewise, *Xenopus* Xdsh is recruited to the membrane in cells undergoing CE (Wallingford et al., 2000), and the DEP domain is also required for localization at the cell cortex (Park et al., 2005). Therefore, both the membrane localization of *C. elegans* DSH-2 and the domain required for this localization is consistent with Dsh proteins from other organisms that function in PCP signalling. Future experiments expressing the DEP domain alone should reveal if it is sufficient to mimic the function and localization of the endogenous DSH-2 protein.

In addition, phenotypes of *dsh-2* loss-of-function and overexpression also suggest DSH-2 to function in a PCP-like signalling pathway. For genes functioning in canonical Wnt signalling, loss or reduction in function produces opposite phenotypes as overexpression. For instance, EGL-20, a *C. elegans* Wnt ligand, activates a canonical Wnt pathway to regulate the direction of migration in Q neuroblasts descendents. In

wildtype, QL descendents migrate posteriorly while the QR descendents migrate anteriorly. Loss of *egl-20* function results in all cells migrating to the anterior. Conversely, EGL-20 overexpression causes all cells to migrate to the posterior (Whangbo and Kenyon, 1999). However, phenotypes of reducing PCP signalling are similar to over-activation. In zebrafish, *silberblick/wnt11* mutants have defects in convergent extension, and overexpressing the DEP domain from Xdsh causes similar defects (Heisenberg et al., 2000). In *C. elegans*, the lack of *dsh-2* function led to PHA neuronal duplications. The same phenotype was observed with overexpression of a genomic *dsh-2* construct in wildtype animals. In this study, although the ΔDIX *dsh-2* construct injected at 10 ng/ul was able to rescue PHA duplications in *dsh-2* mutants, this injection concentration was unable to duplicate PHA neurons in wildtype animals. An explanation could be that the construct needs to be injected at higher concentrations in order for ectopic neuronal duplications to be observed. Also, it is be possible that although the DIX domain is dispensable for rescuing PHA duplications in mutants, its function is required to cause PHA duplications in wildtype.

In the *C. elegans* genome, core PCP signalling components have been identified. PAR-3/Bazooka, PAR-6, RhoA GTPases, and JNK have all been characterized, and they have been shown to regulate diverse developmental processes. PAR-3 and PAR-6 control the asymmetric division of the one-celled zygote (Hung and Kemphues, 1999; Watts et al., 1996). MIG-2 and CED-10 are RhoA GTPase homologues, and they have roles in regulating the migration and axonal guidance of specific neurons during development (Zipkin et al., 1997; Lundquist et al., 2001). JNK-1 has been shown to regulate lifespan and stress resistance (Oh et al., 2005). Additional core PCP components such as

strabismus, *prickle*, and *flamingo* have also been identified through BLAST searches (M. Roh, M.Sc thesis), but their roles have not been well-characterized.

An RNAi screen has been previously performed in our lab to determine if the above-mentioned PCP signalling genes regulate asymmetric neuroblast division (M. Roh, M.Sc thesis). Unfortunately, reducing function of the PCP genes did not result in significant losses or duplications of the PHA neuron. In addition, knocking down the function of PCP genes did not cause ventral enclosure defects. Therefore, even though our results showed that the DEP domain is required for DSH-2 to regulate asymmetric neuroblast division and ventral enclosure, one must be cautious in placing DSH-2 in a PCP-like pathway. A genetic screen in flies isolated Dsh mutations in the DEP domain that specifically affects Wnt signalling (Penton et al., 2002). Therefore, further evidence is required before DSH-2 can be concluded to transduce a PCP-like signal.

To identify novel genes that function with *dsh-2* in ventral enclosure and asymmetric cell division, students in our lab have performed a genetic screen to isolate suppressors of *dsh-2(or302)* lethality (J. Gleaves, K. Hingwing, and N. Hawkins, unpublished results). From the screen, both recessive and dominant suppressors were identified. The majority of the suppressors also happen to suppress PHA duplications, suggesting that ventral enclosure defects in *dsh-2* mutants are likely a secondary consequence of earlier defects in asymmetric neuroblast division. Experiments are underway to clone and molecularly characterize the suppressor genes. Of particular interest to our lab are the dominant suppressors. Since these suppressors suppress a null allele of *dsh-2*, the dominant suppressors could be activating mutations that function downstream of DSH-2. For instance, an activating mutation of GSK-3β would indicate

that DSH-2 participates in the Wnt pathway to control development. In contrast, an activating mutation in JNK or Rho GTPase would suggest DSH-2 to function in a PCP-like pathway. It is also possible that the activating mutation is in a novel gene, placing DSH-2 in a yet unidentified signalling pathway. Molecular characterization of the suppressors should clarify the signalling specificity of DSH-2 during development.

4.4.1 May ΔDIX and Δ*EP *dsh-2* affect other cells?

We showed in this study that ΔDIX *dsh-2* injected at 10 ng/ul completely rescued PHA duplications in *dsh-2* mutants. This study also showed that in addition to PHA, many additional cells are either lost or duplicated in *dsh-2* mutants. It would be informative to determine if those cell losses/duplications can also be rescued by the ΔDIX *dsh-2* construct. Of particularly interest would be to assay for the ability of the two deletion constructs to rescue division defects of the Z1/Z4 somatic gonad precursor cells. DSH-2 functions with other Wnt signalling proteins to regulate POP-1 levels in governing this asymmetric division (Chang et al., 2005). Since the DIX domain of Dsh protein in other organisms have been shown to transduce canonical Wnt signals, it is possible that the DIX domain of DSH-2 is required to regulate the Z1/Z4 division. Therefore, the DTC- and AC-specific GFP reporters could be crossed into animals carrying the ΔDIX *dsh-2* construct at 10 ng/ul and those carrying the Δ*EP *dsh-2* construct at 2.5 ng/ul. These animals can then be assayed for rescue of DTC losses/AC duplications in *dsh-2* (M+ Z-) mutants. Results obtained from these experiments should indicate if DSH-2 employs the same mechanism in regulating different asymmetric cell divisions during development.

APPENDICES

Appendix 1 Cell losses and duplications in *dsh-2(ez25)* mutants.

Cell	Genotype	% Loss	% Duplication	N
ALM	*dsh-2(ez25)/mln1; zdls5*	0	0	118
	dsh-2(ez25) (M+ Z-); *zdls5*	0	4	96
	dsh-2(ez25) (M- Z-); *zdls5*	1	7	140
ASH	*dsh-2(ez25)/mln1; hdls26*	0	0	100
	dsh-2(ez25) (M+ Z-); *hdls26*	1	0	100
	dsh-2(ez25) (M- Z-); *hdls26*	19	0	93
AVM	*dsh-2(ez25)/mln1; zdls5*	0	0	50
	dsh-2(ez25) (M+ Z-); *zdls5*	0	3	108
	dsh-2(ez25) (M- Z-); *zdls5*	2	5	66
CAN	*dsh-2(ez25)/mln1; gmls18*	0	0	170
	dsh-2(ez25) (M+ Z-); *gmls18*	0	0	102
	dsh-2(ez25) (M- Z-); *gmls18*	18	16	116
PLM	*dsh-2(ez25)/mln1; zdls5*	0	0	118
	dsh-2(ez25) (M+ Z-); *zdls5*	0	0	96
	dsh-2(ez25) (M- Z-); *zdls5*	2	6	141
PVM	*dsh-2(ez25)/mln1; zdls5*	0	0	62
	dsh-2(ez25) (M+ Z-); *zdls5*	0	< 1	107
	dsh-2(ez25) (M- Z-); *zdls5*	6	2	65
URX	*dsh-2(ez25)/mln1; ynls22*	0	0	100
	dsh-2(ez25) (M+ Z-); *ynls22*	0	6	88
	dsh-2(ez25) (M- Z-); *ynls22*	0	15	26

Appendix 2 Distal tip cell losses and anchor cell duplications in *dsh-2(ez25)* mutants.

Cell	Genotype	% Loss	% Duplication	N
AC	*dsh-2(ez25)/mln1; syls50*	0	1	96
	dsh-2(ez25) (M+ Z-); *syls50*	0	40	65
DTC	*dsh-2(ez25)/mln1; qls19*	3	0	105
	dsh-2(ez25) (M+ Z-); *qls19*	48	0	94

Appendix 3 Cell losses and duplications in the OLL lineage in *dsh-2(ez25)* mutants.

Cell	Genotype	% Loss	% Duplication	N
OLL	*dsh-2(ez25)/mln1; otIs138*	0	0	100
	dsh-2(ez25) (M+ Z-); *otIs138*	0	12 [a]	104
	dsh-2(ez25) (M- Z-); *otIs138*	2	43 [b]	90
AWB	*dsh-2(ez25)/mln1; kyIs104*	0	0	86
	dsh-2(ez25) (M+ Z-); *kyIs104*	3	1	86
	dsh-2(ez25) (M- Z-); *kyIs104*	10	1	84
ASE	*dsh-2(ez25)/mln1; ynIs22*	0	0	100
	dsh-2(ez25) (M+ Z-); *ynIs22*	0	0	91
	dsh-2(ez25) (M- Z-); *ynIs22*	8	0	13

[a] 9% of sides had 2 OLLs per side, while 3% had 3 OLLs per side
[b] 40% of sides had 2 OLLs per side, while 3% had 3 OLLs per side

Appendix 4 PVQ duplications in *dsh-2(ez25)* mutants.

Genotype	% Duplication	N
dsh-2(or302)/mln1; hdIs26 [a]	0	96
dsh-2(or302) (M+ Z-); *hdIs26*	1	79
dsh-2(or302) (M- Z-); *hdIs26*	24	91
dsh-2(ez25)/mln1; hdIs26	0	99
dsh-2(ez25) (M+ Z-); *hdIs26*	0	88
dsh-2(ez25) (M- Z-); *hdIs26*	11	89
dsh-2(ez25)/mln1; oyIs14 [b]	1	107
dsh-2(ez25) (M+ Z-); *oyIs14*	4	90
dsh-2(ez25) (M- Z-); *oyIs14*	8	112
ced-3(n717); dsh-2(ez25)/mln1; oyIs14	29 [c]	92
ced-3(n717); dsh-2(ez25) (M+ Z-); *oyIs14*	37	103
ced-3(n717); dsh-2(ez25) (M- Z-); *oyIs14*	54	106

[a] *hdIs26[sra-6::dsRed]*
[b] *oyIs14[sra-6::gfp]*
[c] 28% had 2 PVQs per side, 1% had 3 PVQs per side

Appendix 5 High mosaicism of *srb-6::gfp* expression in transgenics carrying extrachromosomal arrays of Δ*EP DSH-2::GFP or ΔDIX DSH-2::GFP.

	# phasmid neurons / side				
Genotype	**0 (%)**	**1 (%)**	**2 (%)**	**3 (%)**	**N**
dsh-2(or302)/mIn1; gmIs12[srb-6::gfp] [a]	0	0	100	0	134
dsh-2(or302)/mIn1; hkEx57[Δ*EP dsh-2::gfp] [b]	4	14	72	0	74
dsh-2(or302)/mIn1; hkEx62[Δ*EP dsh-2::gfp] [c]	1	19	80	0	90
dsh-2(or302)/mIn1; hkEx52[ΔDIX dsh-2::gfp] [d]	6	31	63	0	49
dsh-2(or302)* (M+ Z-); *gmIs12[srb-6::gfp] [a]	0	4	91	4	89
dsh-2(or302)* (M+ Z-); *hkEx57[Δ*EP dsh-2::gfp] [b]	10	43	42	5	21
dsh-2(or302)* (M+ Z-); *hkEx62[Δ*EP dsh-2::gfp] [c]	7	64	25	4	28
dsh-2(or302)* (M+ Z-); *hkEx52[ΔDIX dsh-2::gfp] [d]	8	67	25	0	12
hkEx57[Δ*EP dsh-2::gfp] [b]	1	34	65	0	93
hkEx52[ΔDIX dsh-2::gfp] [d]	4	31	65	0	98

[a] integrated *srb-6::gfp* as control
[b] hkEx57 = construct injected at 2.5 ng/ul
[c] hkEx62 = construct injected at 2.5 ng/ul
[d] hkEx52 = construct injected at 2.5 ng/ul

Appendix 6 Scheme for crossing *flp-8:gfp* into *dsh-2(or302)* mutants.

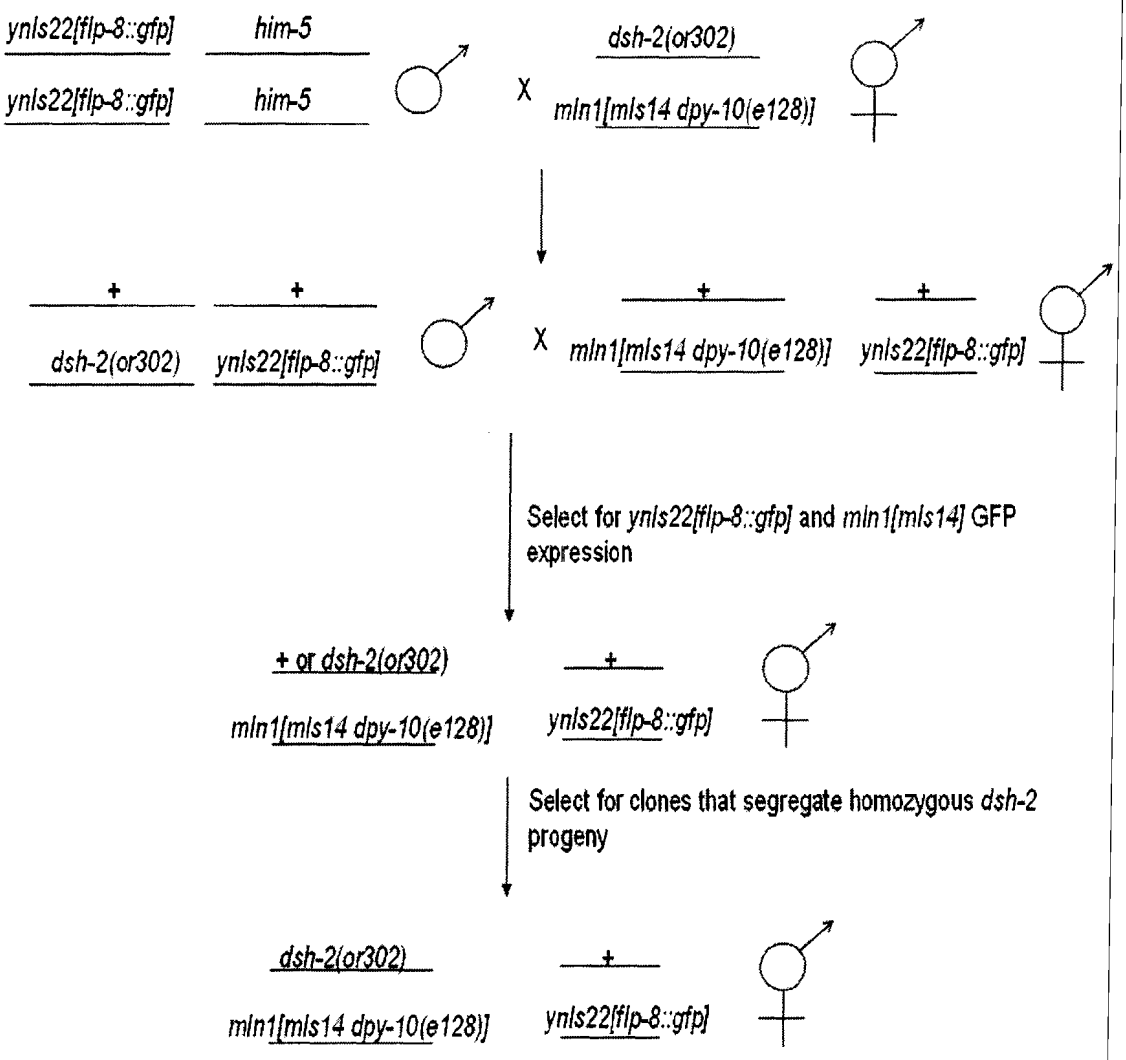

Appendix 7 Scheme for crossing *In[prom::gfp]* into *dsh-2(or302)* mutants.

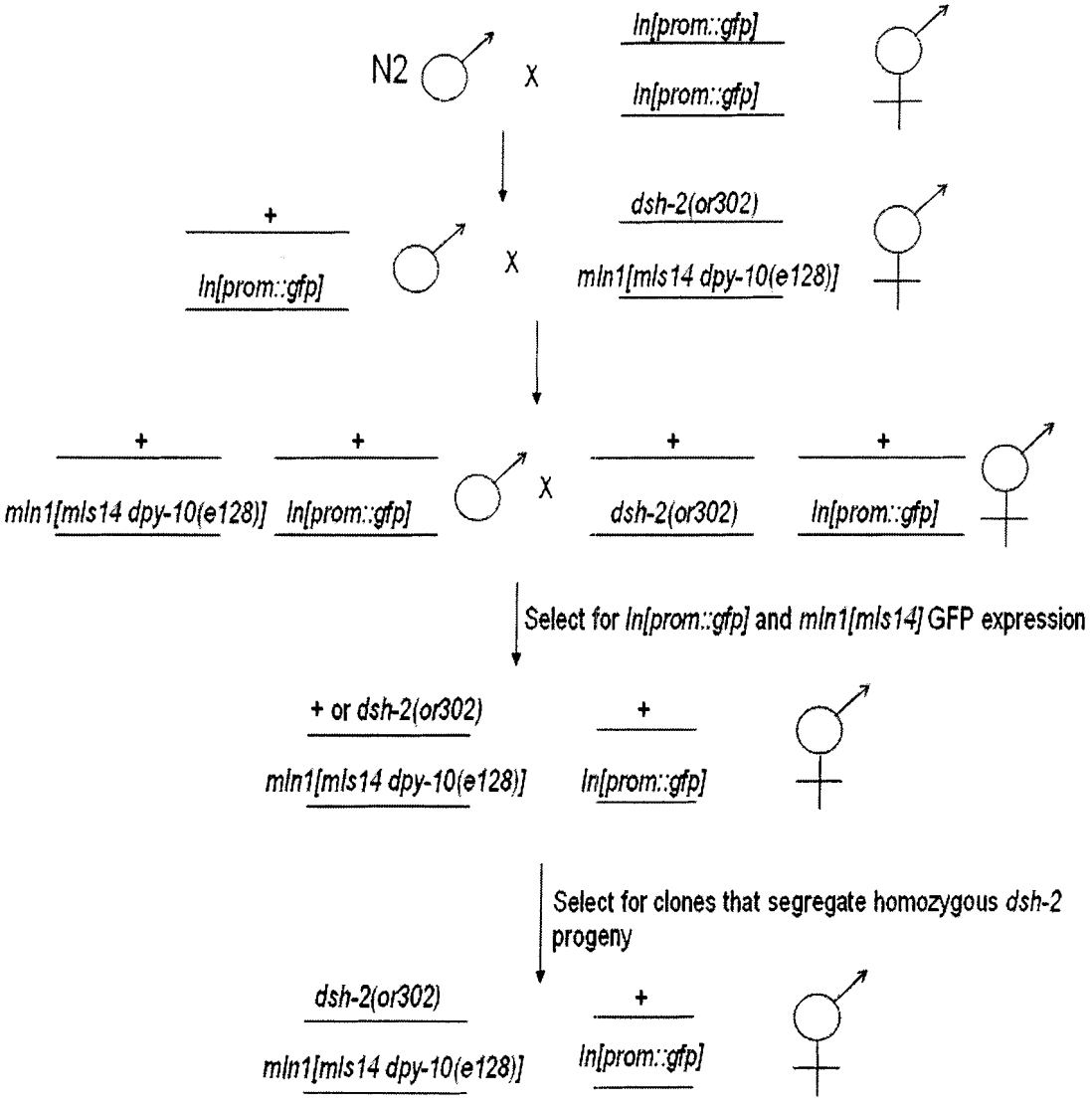

Appendix 8 Scheme for obtaining *dsh-2/mIn1; gmIs12; hkEx86.*

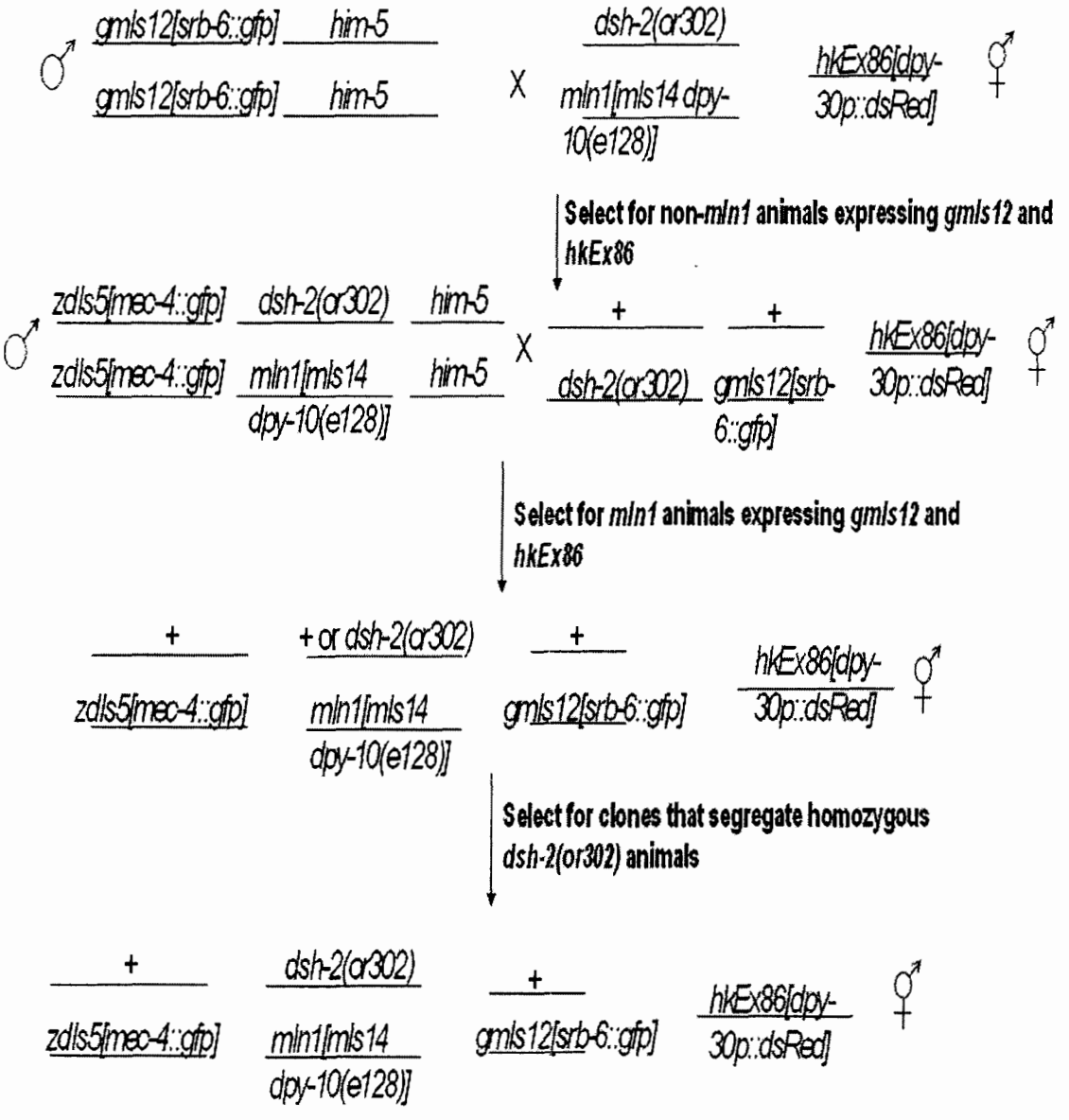

Appendix 9 Scheme for backcrossing integrated strains.

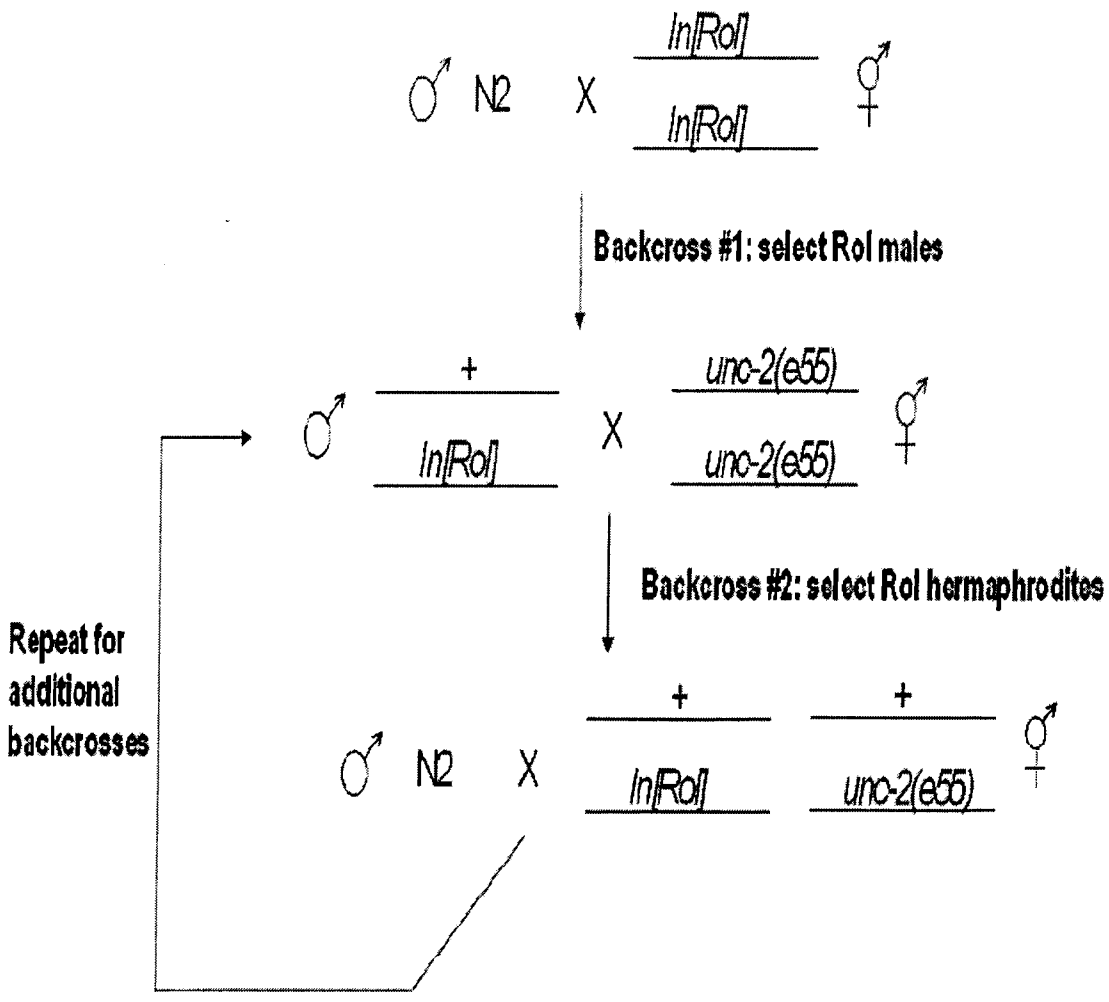

Appendix 10 Scheme for crossing integrated arrays into *dsh-2/mIn1*.

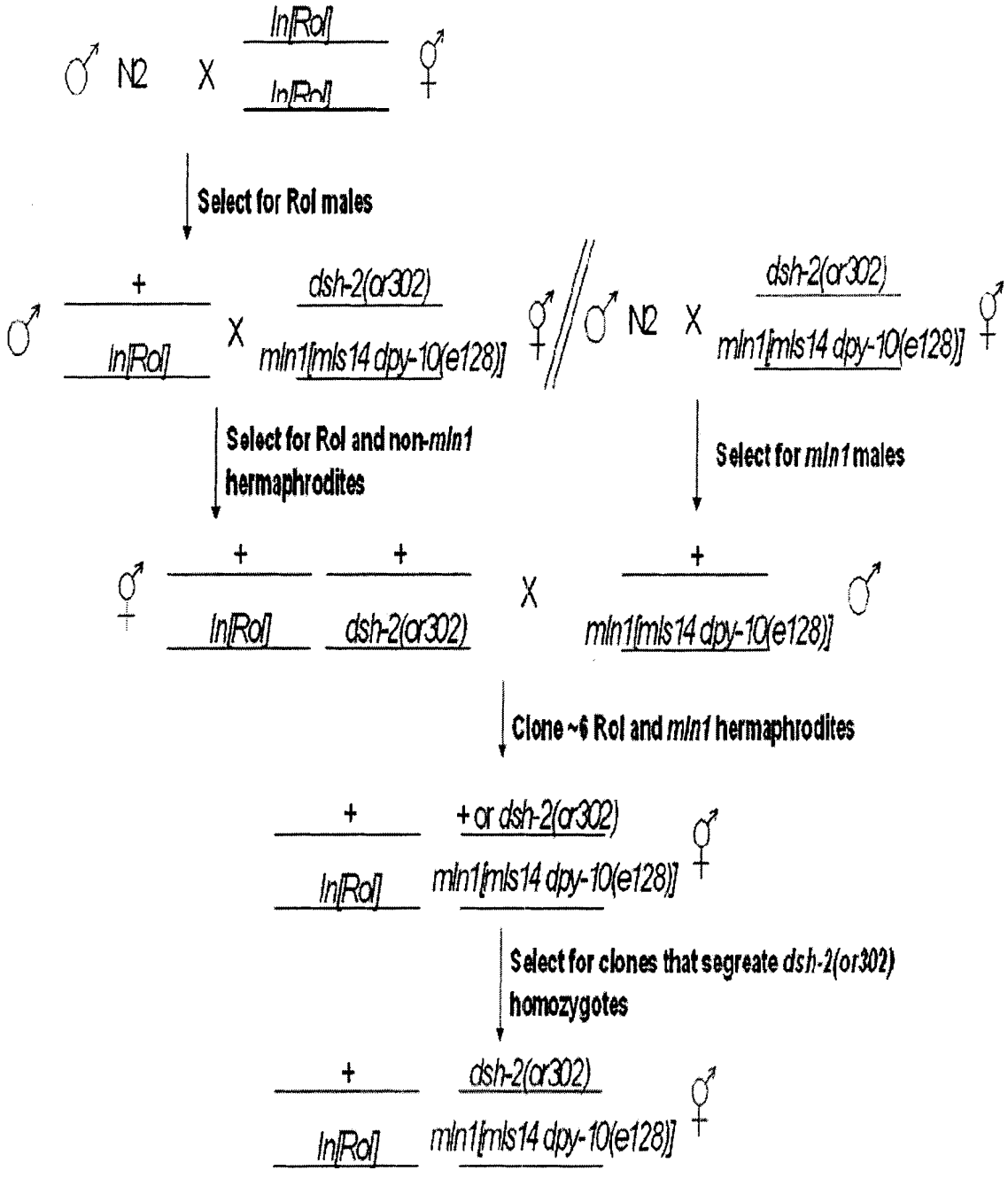

Appendix 11 Scheme for crossing extrachromosomal arrays into N2 before integration.

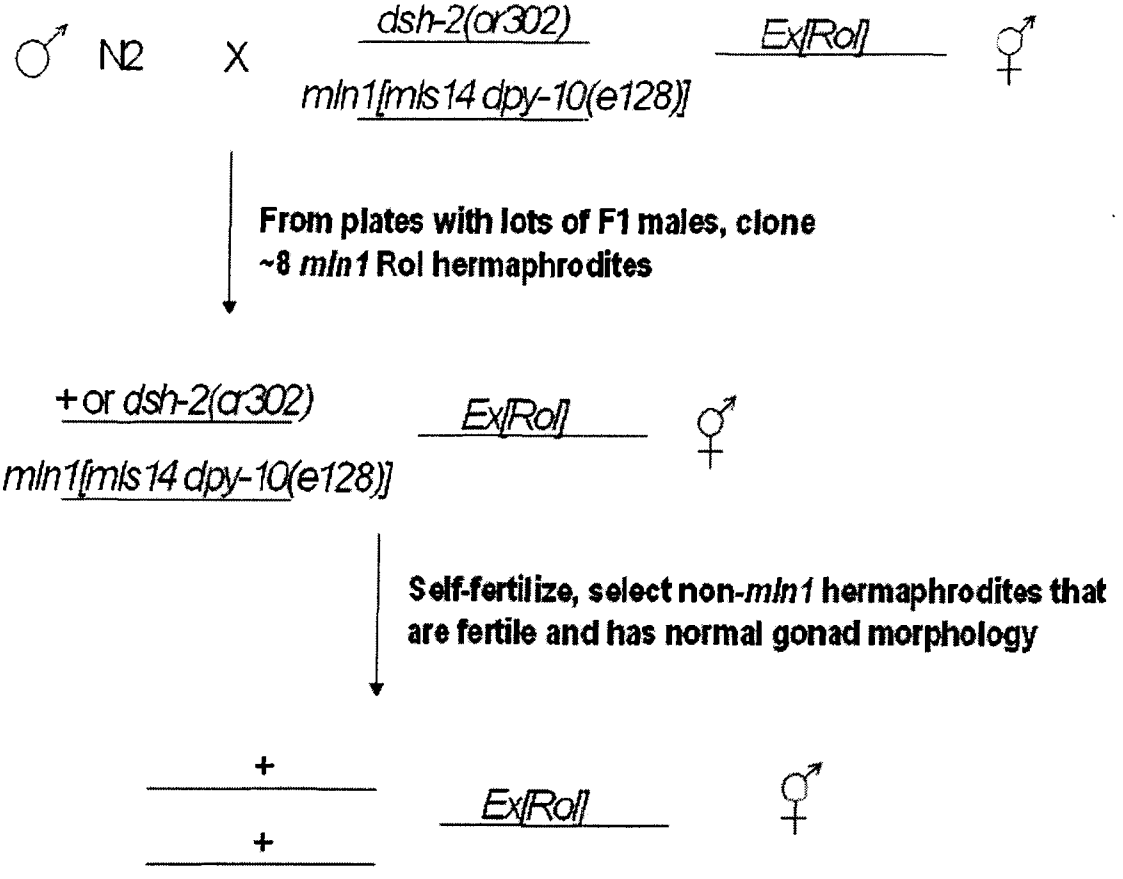

Appendix 12 Scheme for crossing *gmIs12* into *vab-1* or *vab-2* mutants.

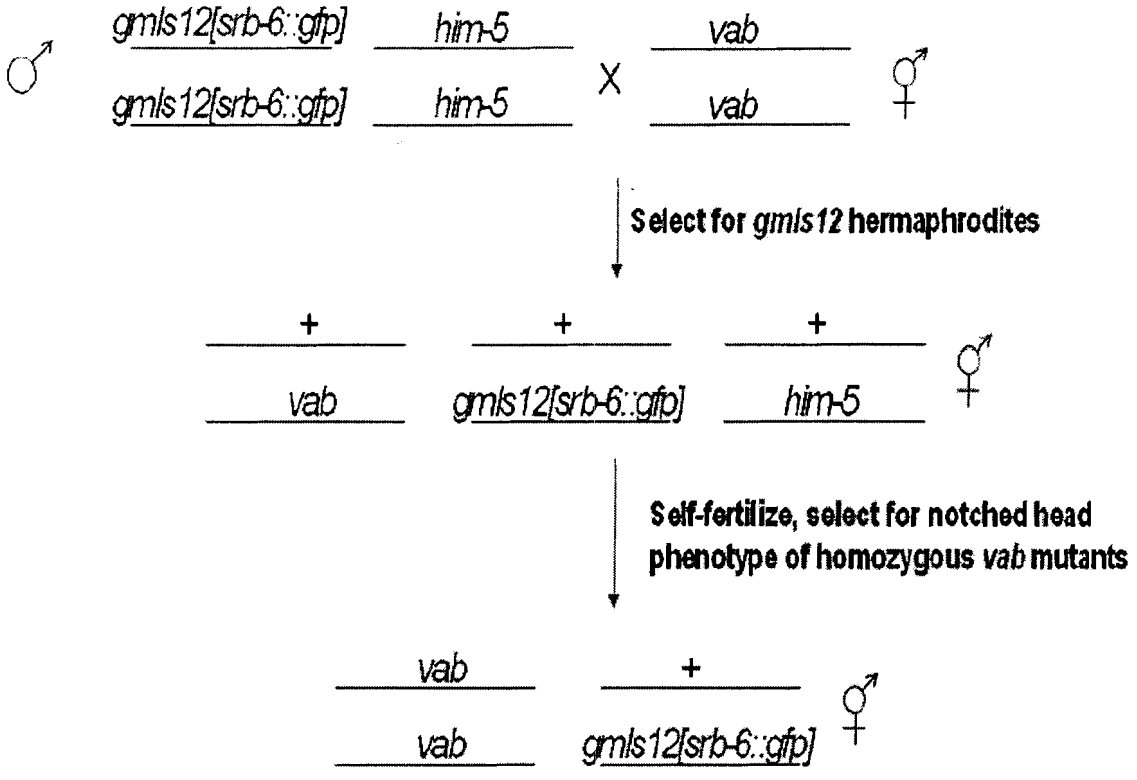

Appendix 13 Scheme for crossing *gmIs12* into *gpb-1* mutants.

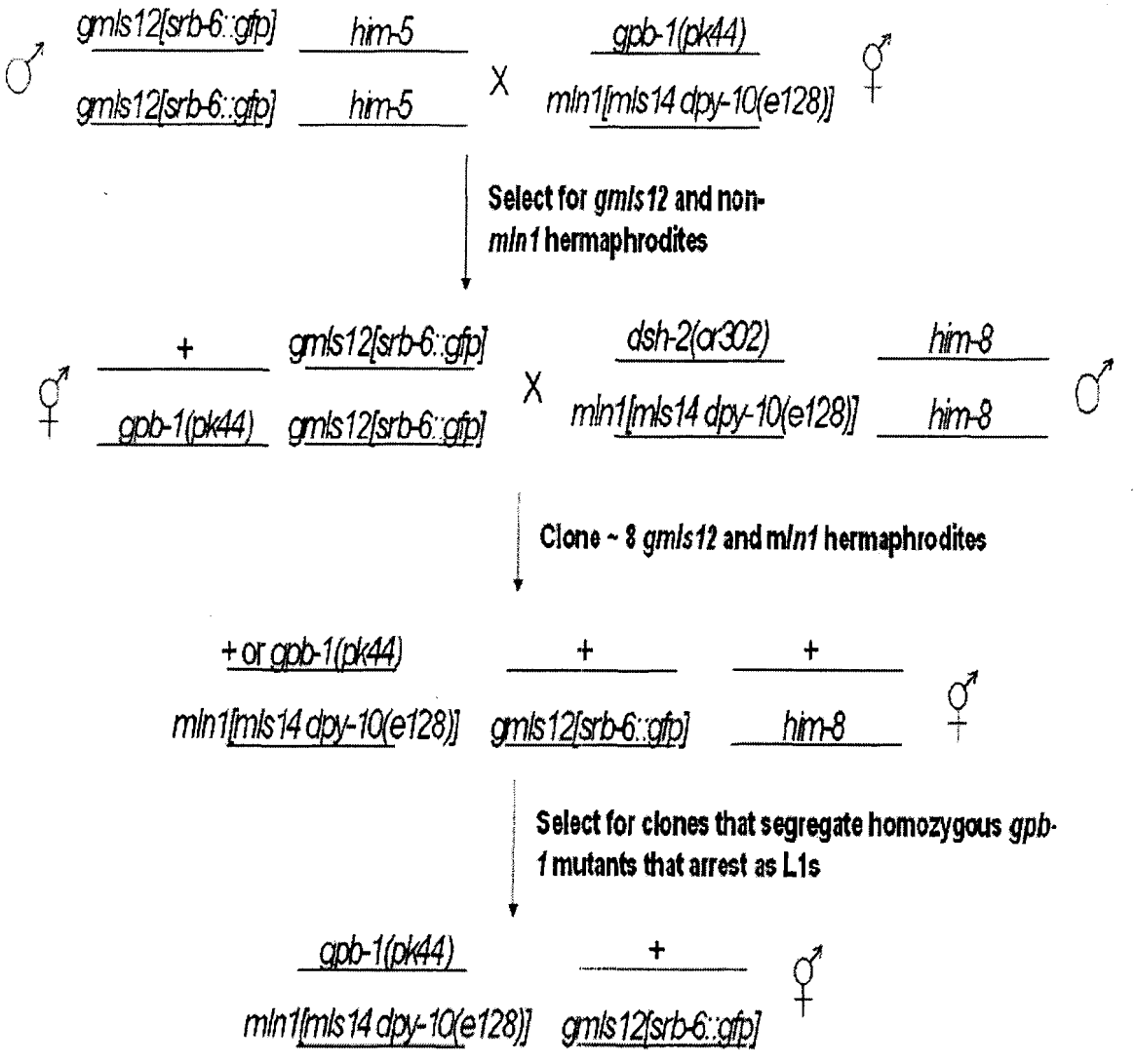

Appendix 14 Scheme for constructing strains with *ced-3(n717)* and *oyIs14[sra-6::gfp]*.

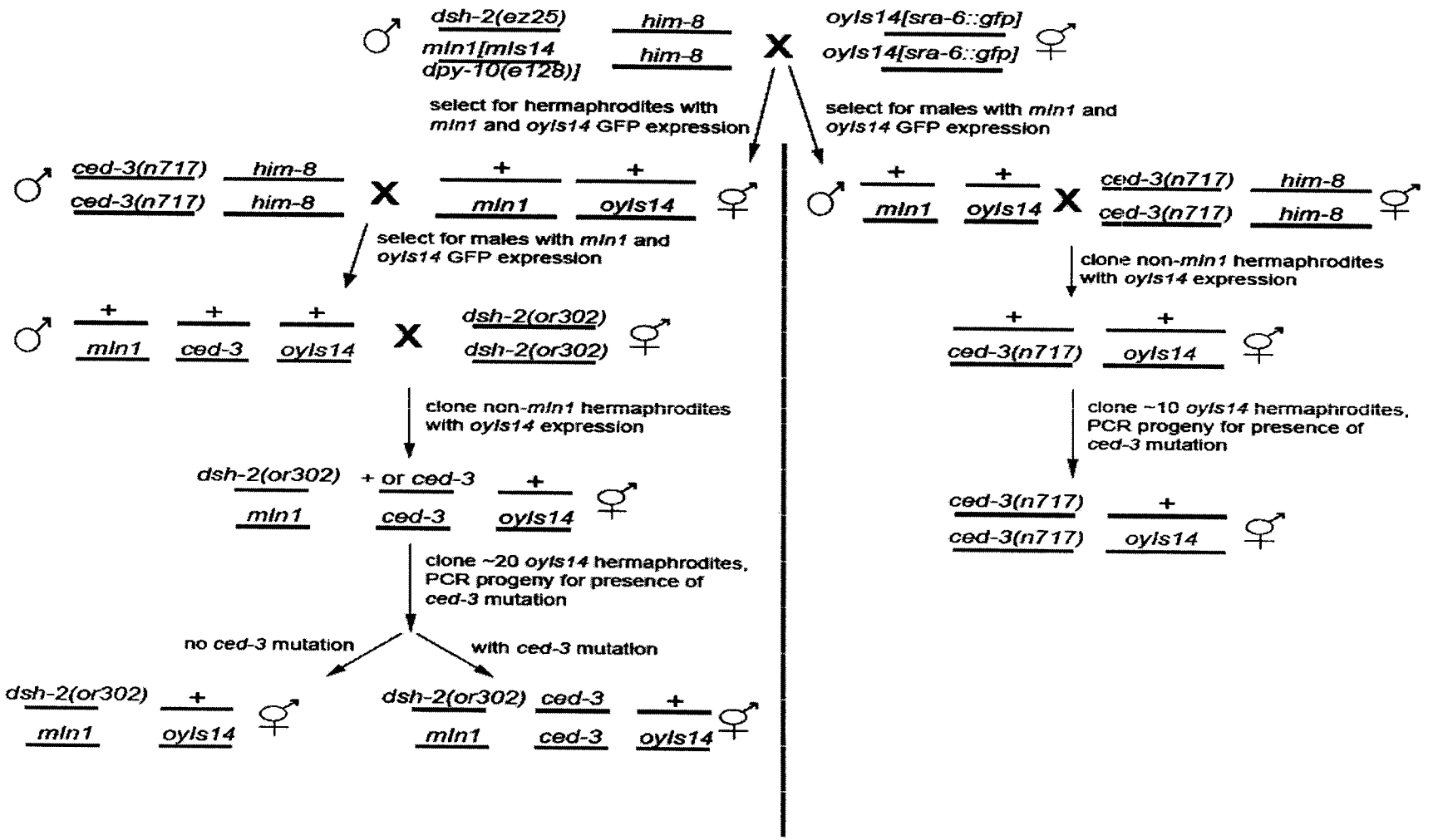

Appendix 15 Scheme for constructing the strain *gpa-16(it143); gmIs12.*

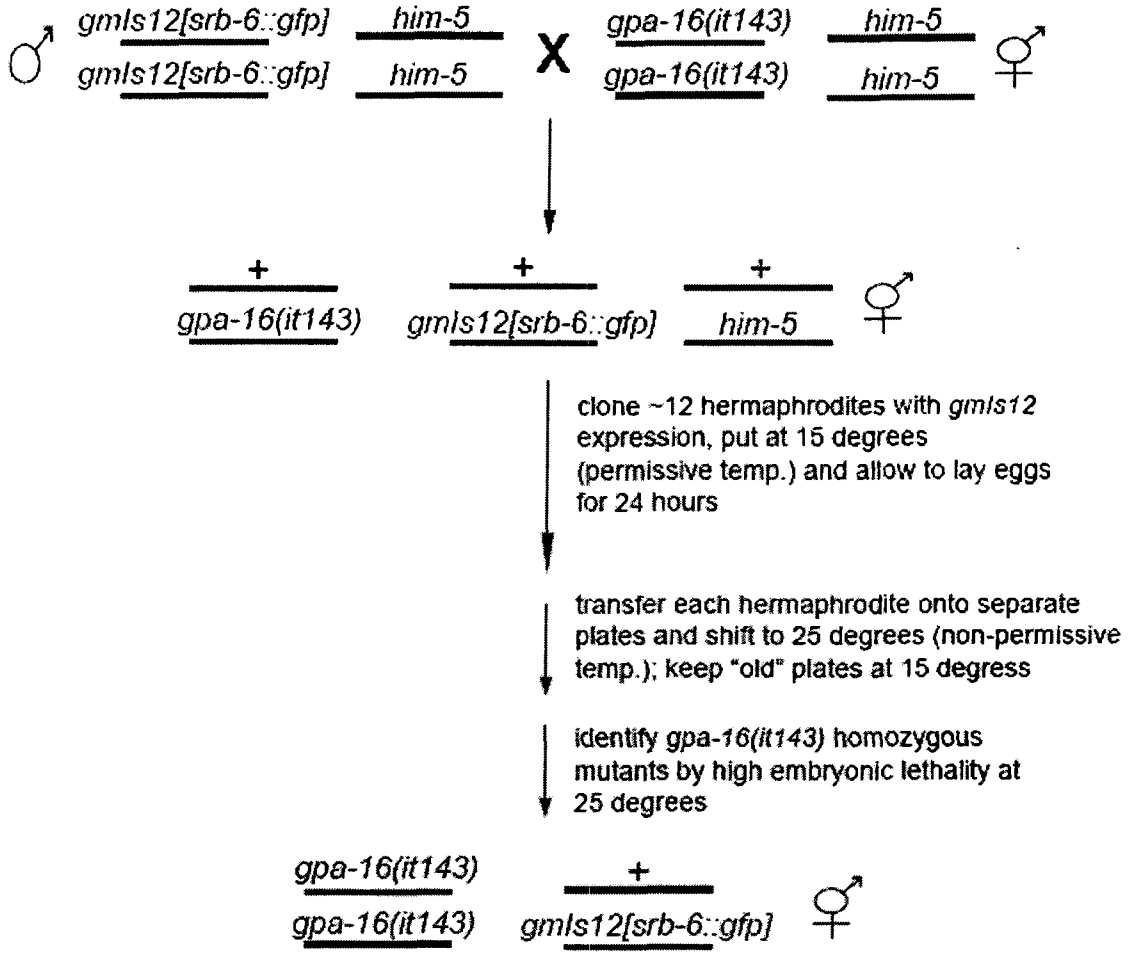

BIBLIOGRAPHY

Altun-Gultekin, Z., Y. Andachi, et al. (2001). "A regulatory cascade of three homeobox genes, ceh-10, ttx-3 and ceh-23, controls cell fate specification of a defined interneuron class in C. elegans." Development **128**(11): 1951-69.

Axelrod, J. D. (2001). "Unipolar membrane association of Dishevelled mediates Frizzled planar cell polarity signaling." Genes Dev **15**(10): 1182-7.

Axelrod, J. D., J. R. Miller, et al. (1998). "Differential recruitment of Dishevelled provides signaling specificity in the planar cell polarity and Wingless signaling pathways." Genes Dev **12**(16): 2610-22.

Bastock, R., H. Strutt, et al. (2003). "Strabismus is asymmetrically localised and binds to Prickle and Dishevelled during Drosophila planar polarity patterning." Development **130**(13): 3007-14.

Bergmann, D. C., M. Lee, et al. (2003). "Embryonic handedness choice in C. elegans involves the Galpha protein GPA-16." Development **130**(23): 5731-40.

Bei, Y., J. Hogan, et al. (2002). "SRC-1 and Wnt signaling act together to specify endoderm and to control cleavage orientation in early C. elegans embryos." Dev Cell **3**(1): 113-25.

Bellaiche, Y., O. Beaudoin-Massiani, et al. (2004). "The planar cell polarity protein Strabismus promotes Pins anterior localization during asymmetric division of sensory organ precursor cells in Drosophila." Development **131**(2): 469-78.

Bellaiche, Y., M. Gho, et al. (2001a). "Frizzled regulates localization of cell-fate determinants and mitotic spindle rotation during asymmetric cell division." Nat Cell Biol **3**(1): 50-7.

Bellaiche, Y., A. Radovic, et al. (2001b). "The Partner of Inscuteable/Discs-large complex is required to establish planar polarity during asymmetric cell division in Drosophila." Cell **106**(3): 355-66.

Bossinger, O., A. Klebes, et al. (2001). "Zonula adherens formation in Caenorhabditis elegans requires dlg-1, the homologue of the Drosophila gene discs large." Dev Biol **230**(1): 29-42.

Boutros, M., N. Paricio, et al. (1998). "Dishevelled activates JNK and discriminates between JNK pathways in planar polarity and wingless signaling." Cell **94**(1): 109-18.

Bowerman, B., M. K. Ingram, et al. (1997). "The maternal par genes and the segregation of cell fate specification activities in early Caenorhabditis elegans embryos." Development **124**(19): 3815-26.

Brenner, S. (1974). "The genetics of Caenorhabditis elegans." Genetics **77**(1): 71-94.

Brockie, P. J., D. M. Madsen, et al. (2001). "Differential expression of glutamate receptor subunits in the nervous system of Caenorhabditis elegans and their regulation by the homeodomain protein UNC-42." J Neurosci **21**(5): 1510-22.

Calvo, D., M. Victor, et al. (2001). "A POP-1 repressor complex restricts inappropriate cell type-specific gene transcription during Caenorhabditis elegans embryogenesis." Embo J **20**(24): 7197-208.

Capelluto, D. G., T. G. Kutateladze, et al. (2002). "The DIX domain targets dishevelled to actin stress fibres and vesicular membranes." Nature **419**(6908): 726-9.

Carreira-Barbosa, F., M. L. Concha, et al. (2003). "Prickle 1 regulates cell movements during gastrulation and neuronal migration in zebrafish." Development **130**(17): 4037-46.

Chang, W., C. E. Lloyd, et al. (2005). "DSH-2 regulates asymmetric cell division in the early C. elegans somatic gonad." Mech Dev **122**(6): 781-9.

Chin-Sang, I. D., S. L. Moseley, et al. (2002). "The divergent C. elegans ephrin EFN-4 functions inembryonic morphogenesis in a pathway independent of the VAB-1 Eph receptor." Development **129**(23): 5499-510.

Clark, S. G. and C. Chiu (2003). "C. elegans ZAG-1, a Zn-finger-homeodomain protein, regulates axonal development and neuronal differentiation." Development **130**(16): 3781-94.

Costa, M., W. Raich, et al. (1998). "A putative catenin-cadherin system mediates morphogenesis of the Caenorhabditis elegans embryo." J Cell Biol **141**(1): 297-308.

Darken, R. S., A. M. Scola, et al. (2002). "The planar polarity gene strabismus regulates convergent extension movements in Xenopus." Embo J **21**(5): 976-85.

Ebinu, J. O., D. A. Bottorff, et al. (1998). "RasGRP, a Ras guanyl nucleotide- releasing protein with calcium- and diacylglycerol-binding motifs." Science **280**(5366): 1082-6.

Edgley, M. L. and D. L. Riddle (2001). "LG II balancer chromosomes in Caenorhabditis elegans: mT1(II;III) and the mIn1 set of dominantly and recessively marked inversions." Mol Genet Genomics **266**(3): 385-95.

Ellis, H. M. and H. R. Horvitz (1986). "Genetic control of programmed cell death in the nematode C. elegans." Cell **44**(6): 817-29.

Ewald, A. J., S. M. Peyrot, et al. (2004). "Regional requirements for Dishevelled signaling during Xenopus gastrulation: separable effects on blastopore closure, mesendoderm internalization and archenteron formation." Development **131**(24): 6195-209.

Feiguin, F., M. Hannus, et al. (2001). "The ankyrin repeat protein Diego mediates Frizzled-dependent planar polarization." Dev Cell **1**(1): 93-101.

Francis, R. and R. H. Waterston (1991). "Muscle cell attachment in Caenorhabditis elegans." J Cell Biol **114**(3): 465-79.

George, S. E., K. Simokat, et al. (1998). "The VAB-1 Eph receptor tyrosine kinase functions in neural and epithelial morphogenesis in C. elegans." Cell **92**(5): 633-43.

Gho, M. and F. Schweisguth (1998). "Frizzled signalling controls orientation of asymmetric sense organ precursor cell divisions in Drosophila." Nature **393**(6681): 178-81.

Gilleard, J. S. and J. D. McGhee (2001). "Activation of hypodermal differentiation in the Caenorhabditis elegans embryo by GATA transcription factors ELT-1 and ELT-3." Mol Cell Biol **21**(7): 2533-44.

Goldstein, B. (1992). "Induction of gut in Caenorhabditis elegans embryos." Nature **357**(6375): 255-7.

Gotta, M. and J. Ahringer (2001). "Distinct roles for Galpha and Gbetagamma in regulating spindle position and orientation in Caenorhabditis elegans embryos." Nat Cell Biol **3**(3): 297-300.

Habas, R. and I. B. Dawid (2005). "Dishevelled and Wnt signaling: is the nucleus the final frontier?" J Biol **4**(1): 2.

Habas, R., Y. Kato, et al. (2001). "Wnt/Frizzled activation of Rho regulates vertebrate gastrulation and requires a novel Formin homology protein Daam1." Cell **107**(7): 843-54.

Hallam, S., E. Singer, et al. (2000). "The C. elegans NeuroD homolog cnd-1 functions in multiple aspects of motor neuron fate specification." Development **127**(19): 4239-52.

Harris, J., L. Honigberg, et al. (1996). "Neuronal cell migration in C. elegans: regulation of Hox gene expression and cell position." Development **122**(10): 3117-31.

Hawkins, N. and G. Garriga (1998). "Asymmetric cell division: from A to Z." Genes Dev **12**(23): 3625-38.

Hawkins, N. C., G. C. Ellis, et al. (2005). "MOM-5 frizzled regulates the distribution of DSH-2 to control C. elegans asymmetric neuroblast divisions." Dev Biol **284**(1): 246-59.

Hedgecock, E. M., J. G. Culotti, et al. (1987). "Genetics of cell and axon migrations in Caenorhabditis elegans." Development **100**(3): 365-82.

Heisenberg, C. P., M. Tada, et al. (2000). "Silberblick/Wnt11 mediates convergent extension movements during zebrafish gastrulation." Nature **405**(6782): 76-81.

Herman, M. (2001). "C. elegans POP-1/TCF functions in a canonical Wnt pathway that controls cell migration and in a noncanonical Wnt pathway that controls cell polarity." Development **128**(4): 581-90.

Hobert, O. (2002). "PCR fusion-based approach to create reporter gene constructs for expression analysis in transgenic C. elegans." Biotechniques **32**(4): 728-30.

Hoier, E. F., W. A. Mohler, et al. (2000). "The Caenorhabditis elegans APC-related gene apr-1 is required for epithelial cell migration and Hox gene expression." Genes Dev **14**(7): 874-86.

Hung, A. Y. and M. Sheng (2002). "PDZ domains: structural modules for protein complex assembly." J Biol Chem **277**(8): 5699-702.

Hung, T. J. and K. J. Kemphues (1999). "PAR-6 is a conserved PDZ domain-containing protein that colocalizes with PAR-3 in Caenorhabditis elegans embryos." Development **126**(1): 127-35.

Hutter, H. (2003). "Extracellular cues and pioneers act together to guide axons in the ventral cord of C. elegans." Development **130**(22): 5307-18.

Jansen, G., K. L. Thijssen, et al. (1999). "The complete family of genes encoding G proteins of Caenorhabditis elegans." Nat Genet **21**(4): 414-9.

Jessen, J. R., J. Topczewski, et al. (2002). "Zebrafish trilobite identifies new roles for Strabismus in gastrulation and neuronal movements." Nat Cell Biol **4**(8): 610-5.

Kelly, W. G., S. Xu, et al. (1997). "Distinct requirements for somatic and germline expression of a generally expressed Caernorhabditis elegans gene." Genetics **146**(1): 227-38.

Kidd, A. R., 3rd, J. A. Miskowski, et al. (2005). "A beta-catenin identified by functional rather than sequence criteria and its role in Wnt/MAPK signaling." Cell **121**(5): 761-72.

Kimble, J. (1981). "Alterations in cell lineage following laser ablation of cells in the somatic gonad of Caenorhabditis elegans." Dev Biol **87**(2): 286-300.

Knoblich, J. A. (2001). "Asymmetric cell division during animal development." Nat Rev Mol Cell Biol **2**(1): 11-20.

Krasnow, R. E., L. L. Wong, et al. (1995). "Dishevelled is a component of the frizzled signaling pathway in Drosophila." Development **121**(12): 4095-102.

Kuchinke, U., F. Grawe, et al. (1998). "Control of spindle orientation in Drosophila by the Par-3-related PDZ-domain protein Bazooka." Curr Biol **8**(25): 1357-65.

Kuhl, M., L. C. Sheldahl, et al. (2000). "The Wnt/Ca2+ pathway: a new vertebrate Wnt signaling pathway takes shape." Trends Genet **16**(7): 279-83.

Labouesse, M. (1997). "Deficiency screen based on the monoclonal antibody MH27 to identify genetic loci required for morphogenesis of the Caenorhabditis elegans embryo." Dev Dyn **210**(1): 19-32.

Labouesse, M., E. Hartwieg, et al. (1996). "The Caenorhabditis elegans LIN-26 protein is required to specify and/or maintain all non-neuronal ectodermal cell fates." Development **122**(9): 2579-88.

Landmann, F., S. Quintin, et al. (2004). "Multiple regulatory elements with spatially and temporally distinct activities control the expression of the epithelial differentiation gene lin-26 in C. elegans." Dev Biol **265**(2): 478-90.

Larabell, C. A., M. Torres, et al. (1997). "Establishment of the dorso-ventral axis in Xenopus embryos is presaged by early asymmetries in beta-catenin that are modulated by the Wnt signaling pathway." J Cell Biol **136**(5): 1123-36.

Li, C., K. Kim, et al. (1999). "FMRFamide-related neuropeptide gene family in Caenorhabditis elegans." Brain Res **848**(1-2): 26-34.

Lin, R., S. Thompson, et al. (1995). "pop-1 encodes an HMG box protein required for the specification of a mesoderm precursor in early C. elegans embryos." Cell **83**(4): 599-609.

Lo, M. C., F. Gay, et al. (2004). "Phosphorylation by the beta-catenin/MAPK complex promotes 14-3-3-mediated nuclear export of TCF/POP-1 in signal-responsive cells in C. elegans." Cell **117**(1): 95-106.

Lundquist, E. A., P. W. Reddien, et al. (2001). "Three C. elegans Rac proteins and several alternative Rac regulators control axon guidance, cell migration and apoptotic cell phagocytosis." Development **128**(22): 4475-88.

Maduro, M. and D. Pilgrim (1996). "Conservation of function and expression of unc-119 from two Caenorhabditis species despite divergence of non-coding DNA." Gene **183**(1-2): 77-85.

Maloof, J. N., J. Whangbo, et al. (1999). "A Wnt signaling pathway controls hox gene expression and neuroblast migration in C. elegans." Development **126**(1): 37-49.

Matsui, T., A. Raya, et al. (2005). "Noncanonical Wnt signaling regulates midline convergence of organ primordia during zebrafish development." Genes Dev **19**(1): 164-75.

Medina, A., W. Reintsch, et al. (2000). "Xenopus frizzled 7 can act in canonical and non-canonical Wnt signaling pathways: implications on early patterning and morphogenesis." Mech Dev **92**(2): 227-37.

Mello, C. C., J. M. Kramer, et al. (1991). "Efficient gene transfer in C.elegans: extrachromosomal maintenance and integration of transforming sequences." Embo J **10**(12): 3959-70.

Moon, R. T., J. D. Brown, et al. (1997). "WNTs modulate cell fate and behavior during vertebrate development." Trends Genet **13**(4): 157-62.

Nance, J. (2005). "PAR proteins and the establishment of cell polarity during C. elegans development." Bioessays **27**(2): 126-35.

Newman, A. P., J. G. White, et al. (1995). "The Caenorhabditis elegans lin-12 gene mediates induction of ventral uterine specialization by the anchor cell." Development **121**(2): 263-71.

Nusse, R. (2005). "Wnt signaling in disease and in development." Cell Res **15**(1): 28-32.

Oh, S. W., A. Mukhopadhyay, et al. (2005). "JNK regulates lifespan in Caenorhabditis elegans by modulating nuclear translocation of forkhead transcription factor/DAF-16." Proc Natl Acad Sci U S A **102**(12): 4494-9.

Page, B. D., W. Zhang, et al. (1997). "ELT-1, a GATA-like transcription factor, is required for epidermal cell fates in Caenorhabditis elegans embryos." Genes Dev **11**(13): 1651-61.

Park, T. J., R. S. Gray, et al. (2005). "Subcellular localization and signaling properties of dishevelled in developing vertebrate embryos." Curr Biol **15**(11): 1039-44.

Peckol, E. L., J. A. Zallen, et al. (1999). "Sensory activity affects sensory axon development in C. elegans." Development **126**(9): 1891-902.

Penton, A., A. Wodarz, et al. (2002). "A mutational analysis of dishevelled in Drosophila defines novel domains in the dishevelled protein as well as novel suppressing alleles of axin." Genetics **161**(2): 747-62.

Petronczki, M. and J. A. Knoblich (2001). "DmPAR-6 directs epithelial polarity and asymmetric cell division of neuroblasts in Drosophila." Nat Cell Biol **3**(1): 43-9.

Podbilewicz, B. and J. G. White (1994). "Cell fusions in the developing epithelial of C. elegans." Dev Biol **161**(2): 408-24.

Priess, J. R. and D. I. Hirsh (1986). "Caenorhabditis elegans morphogenesis: the role of the cytoskeleton in elongation of the embryo." Dev Biol **117**(1): 156-73.

Raich, W. B., C. Agbunag, et al. (1999). "Rapid epithelial-sheet sealing in the Caenorhabditis elegans embryo requires cadherin-dependent filopodial priming." Curr Biol **9**(20): 1139-46.

Rhyu, M. S., L. Y. Jan, et al. (1994). "Asymmetric distribution of numb protein during division of the sensory organ precursor cell confers distinct fates to daughter cells." Cell **76**(3): 477-91.

Rocheleau, C. E., W. D. Downs, et al. (1997). "Wnt signaling and an APC-related gene specify endoderm in early C. elegans embryos." Cell **90**(4): 707-16.

Rocheleau, C. E., J. Yasuda, et al. (1999). "WRM-1 activates the LIT-1 protein kinase to transduce anterior/posterior polarity signals in C. elegans." Cell **97**(6): 717-26.

Roegiers, F., S. Younger-Shepherd, et al. (2001). "Two types of asymmetric divisions in the Drosophila sensory organ precursor cell lineage." Nat Cell Biol **3**(1): 58-67.

Roh, M. (2004). Requirement for Wnt and Planar Cell Polarity for in asymmetric neuroblast division in *Caenorhabditis elegans*. Dept. of Molecular Biology and Biochemistry. Burnaby, Canada, Simon Fraser University.

Rose, L. S. and K. Kemphues (1998). "The let-99 gene is required for proper spindle orientation during cleavage of the C. elegans embryo." Development **125**(7): 1337-46.

Rothbacher, U., M. N. Laurent, et al. (2000). "Dishevelled phosphorylation, subcellular localization and multimerization regulate its role in early embryogenesis." Embo J **19**(5): 1010-22.

Sarafi-Reinach, T. R., T. Melkman, et al. (2001). "The lin-11 LIM homeobox gene specifies olfactory and chemosensory neuron fates in C. elegans." Development **128**(17): 3269-81.

Schlesinger, A., C. A. Shelton, et al. (1999). "Wnt pathway components orient a mitotic spindle in the early Caenorhabditis elegans embryo without requiring gene transcription in the responding cell." Genes Dev **13**(15): 2028-38.

Schubert, C. M., R. Lin, et al. (2000). "MEX-5 and MEX-6 function to establish soma/germline asymmetry in early C. elegans embryos." Mol Cell **5**(4): 671-82.

Seydoux, G. and I. Greenwald (1989). "Cell autonomy of lin-12 function in a cell fate decision in C. elegans." Cell **57**(7): 1237-45.

Sheldahl, L. C., D. C. Slusarski, et al. (2003). "Dishevelled activates Ca2+ flux, PKC, and CamKII in vertebrate embryos." J Cell Biol **161**(4): 769-77.

Shimada, Y., T. Usui, et al. (2001). "Asymmetric colocalization of Flamingo, a seven-pass transmembrane cadherin, and Dishevelled in planar cell polarization." Curr Biol **11**(11): 859-63.

Siegfried, E., T. B. Chou, et al. (1992). "wingless signaling acts through zeste-white 3, the Drosophila homolog of glycogen synthase kinase-3, to regulate engrailed and establish cell fate." Cell **71**(7): 1167-79.

Siegfried, E., E. L. Wilder, et al. (1994). "Components of wingless signalling in Drosophila." Nature **367**(6458): 76-80.

Siegfried, K. R., A. R. Kidd, 3rd, et al. (2004). "The sys-1 and sys-3 genes cooperate with Wnt signaling to establish the proximal-distal axis of the Caenorhabditis elegans gonad." Genetics **166**(1): 171-86.

Siegfried, K. R. and J. Kimble (2002). "POP-1 controls axis formation during early gonadogenesis in C. elegans." Development **129**(2): 443-53.

Simske, J. S. and J. Hardin (2001). "Getting into shape: epidermal morphogenesis in Caenorhabditis elegans embryos." Bioessays **23**(1): 12-23.

Sokol, S. Y. (1996). "Analysis of Dishevelled signalling pathways during Xenopus development." Curr Biol **6**(11): 1456-67.

Sternberg, P. W. and H. R. Horvitz (1988). "lin-17 mutations of Caenorhabditis elegans disrupt certain asymmetric cell divisions." Dev Biol **130**(1): 67-73.

Sulston, J. E. and H. R. Horvitz (1977). "Post-embryonic cell lineages of the nematode, Caenorhabditis elegans." Dev Biol **56**(1): 110-56.

Tada, M. and J. C. Smith (2000). "Xwnt11 is a target of Xenopus Brachyury: regulation of gastrulation movements via Dishevelled, but not through the canonical Wnt pathway." Development **127**(10): 2227-38.

Takeuchi, M., J. Nakabayashi, et al. (2003). "The prickle-related gene in vertebrates is essential for gastrulation cell movements." Curr Biol **13**(8): 674-9.

Thomas-Virnig, C. L., P. A. Sims, et al. (2004). "The inositol 1,4,5-trisphosphate receptor regulates epidermal cell migration in Caenorhabditis elegans." Curr Biol **14**(20): 1882-7.

Thorpe, C. J., A. Schlesinger, et al. (2000). "Wnt signalling in Caenorhabditis elegans: regulating repressors and polarizing the cytoskeleton." Trends Cell Biol **10**(1): 10-7.

Thorpe, C. J., A. Schlesinger, et al. (1997). "Wnt signaling polarizes an early C. elegans blastomere to distinguish endoderm from mesoderm." Cell **90**(4): 695-705.

Tree, D. R., J. M. Shulman, et al. (2002). "Prickle mediates feedback amplification to generate asymmetric planar cell polarity signaling." Cell **109**(3): 371-81.

Troemel, E. R., B. E. Kimmel, et al. (1997). "Reprogramming chemotaxis responses: sensory neurons define olfactory preferences in C. elegans." Cell **91**(2): 161-9.

Tsalik, E. L., T. Niacaris, et al. (2003). "LIM homeobox gene-dependent expression of biogenic amine receptors in restricted regions of the C. elegans nervous system." Dev Biol **263**(1): 81-102.

Tsou, M. F., A. Hayashi, et al. (2002). "LET-99 determines spindle position and is asymmetrically enriched in response to PAR polarity cues in C. elegans embryos." Development **129**(19): 4469-81.

van den Heuvel, M., R. Nusse, et al. (1989). "Distribution of the wingless gene product in Drosophila embryos: a protein involved in cell-cell communication." Cell **59**(4): 739-49.

Wallingford, J. B., S. E. Fraser, et al. (2002). "Convergent extension: the molecular control of polarized cell movement during embryonic development." Dev Cell **2**(6): 695-706.

Wallingford, J. B., B. A. Rowning, et al. (2000). "Dishevelled controls cell polarity during Xenopus gastrulation." Nature **405**(6782): 81-5.

Walston, T., C. Tuskey, et al. (2004). "Multiple Wnt signaling pathways converge to orient the mitotic spindle in early C. elegans embryos." Dev Cell **7**(6): 831-41.

Wang, X., P. J. Roy, et al. (1999). "Multiple ephrins control cell organization in C. elegans using kinase-dependent and -independent functions of the VAB-1 Eph receptor." Mol Cell **4**(6): 903-13.

Watts, J. L., B. Etemad-Moghadam, et al. (1996). "par-6, a gene involved in the establishment of asymmetry in early C. elegans embryos, mediates the asymmetric localization of PAR-3." Development **122**(10): 3133-40.

Whangbo, J. and C. Kenyon (1999). "A Wnt signaling system that specifies two patterns of cell migration in C. elegans." Mol Cell **4**(5): 851-8.

Wharton, K. A., Jr. (2003). "Runnin' with the Dvl: proteins that associate with Dsh/Dvl and their significance to Wnt signal transduction." Dev Biol **253**(1): 1-17.

Williams-Masson, E. M., P. J. Heid, et al. (1998). "The cellular mechanism of epithelial rearrangement during morphogenesis of the Caenorhabditis elegans dorsal hypodermis." Dev Biol **204**(1): 263-76.

Withee, J., B. Galligan, et al. (2004). "Caenorhabditis elegans WASP and Ena/VASP proteins play compensatory roles in morphogenesis and neuronal cell migration." Genetics **167**(3): 1165-76.

Wodarz, A., A. Ramrath, et al. (2000). "Drosophila atypical protein kinase C associates with Bazooka and controls polarity of epithelia and neuroblasts." J Cell Biol **150**(6): 1361-74.

Wong, H. C., A. Bourdelas, et al. (2003). "Direct binding of the PDZ domain of Dishevelled to a conserved internal sequence in the C-terminal region of Frizzled." Mol Cell **12**(5): 1251-60.

Wong, H. C., J. Mao, et al. (2000). "Structural basis of the recognition of the dishevelled DEP domain in the Wnt signaling pathway." Nat Struct Biol **7**(12): 1178-84.

Wong, L. L. and P. N. Adler (1993). "Tissue polarity genes of Drosophila regulate the subcellular location for prehair initiation in pupal wing cells." J Cell Biol **123**(1): 209-21.

Woods, D. F. and P. J. Bryant (1991). "The discs-large tumor suppressor gene of Drosophila encodes a guanylate kinase homolog localized at septate junctions." Cell **66**(3): 451-64.

Woods, D. F., C. Hough, et al. (1996). "Dlg protein is required for junction structure, cell polarity, and proliferation control in Drosophila epithelia." J Cell Biol **134**(6): 1469-82.

WormAtlas. 2005. http://www.wormatlas.org/handbook/hypodermis/IL.OLimagegallery.htm http://www.wormatlas.org/neurons.htm/oll.htm

Yamanaka, H., T. Moriguchi, et al. (2002). "JNK functions in the non-canonical Wnt pathway to regulate convergent extension movements in vertebrates." EMBO Rep **3**(1): 69-75.

Yanagawa, S., F. van Leeuwen, et al. (1995). "The dishevelled protein is modified by wingless signaling in Drosophila." Genes Dev **9**(9): 1087-97.

Yu, S., L. Avery, et al. (1997). "Guanylyl cyclase expression in specific sensory neurons: a new family of chemosensory receptors." Proc Natl Acad Sci U S A **94**(7): 3384-7.

Zipkin, I. D., R. M. Kindt, et al. (1997). "Role of a new Rho family member in cell migration and axon guidance in C. elegans." Cell **90**(5): 883-94.

Zwaal, R. R., J. Ahringer, et al. (1996). "G proteins are required for spatial orientation of early cell cleavages in C. elegans embryos." Cell **86**(4): 619-29.